Chapter 7

Biot's theory for porous media

In Acoustics, we have sometimes to consider the incidence of aerial waves upon porous bodies, in whose interstices some sort of aerial continuity is preserved...

The problem of propagation of sound in a circular tube, having regard to the influence of viscosity and heat-conduction, has been solved analytically by Kirchhoff, on the suppositions that the tangential velocity and the temperature-variation vanish at the walls. In discussing the solution, Kirchhoff takes the case in which the dimensions of the tube are such that the immediate effects of the dissipative forces are confined to a relatively thin stratum in the neighborhood of the walls. In the present application interest attaches rather to the opposite extreme, viz. when the diameter is so small that the frictional layer pretty well fills the tube. Nothing practically is lost by another simplification which it is convenient to make (following Kirchhoff) – that the velocity of propagation of viscous and thermal effects is negligible in comparison with that of sound.

John William Strutt (Lord Rayleigh) (Rayleigh, 1899b)

Biot's theory describes wave propagation in a porous saturated medium, i.e., a medium made of a solid matrix (skeleton or frame), fully saturated with a fluid. Biot (1956a,b) ignores the microscopic level and assumes that continuum mechanics can be applied to measurable macroscopic quantities. He postulates the Lagrangian and uses Hamilton's principle to derive the equations governing wave propagation. Rigorous approaches for obtaining the equations of motion are the homogenization theory (e.g., Burridge and Keller, 1985) and volume-averaging methods (e.g., Pride, Gangi and Morgan, 1994; Pride and Berryman, 1998), both of which relate the microscopic and macroscopic worlds. We follow Biot's approach, due to its simplicity.

Sound attenuation in air-filled porous media was investigated by Zwikker and Kosten (1949). They considered dilatational waves and described the physics of wave propagation by using the concept of impedance. Biot's theory and related theories of deformation and wave propagation in porous media are discussed in several reviews and books, notably, Rice and Cleary (1976), Johnson (1986), Bourbié, Coussy and Zinszner (1987), Cristescu (1986), Stoll (1989), Zimmermann (1991), Allard (1993), Coussy (1995), Corapcioglu and Tuncay (1996), Mavko, Mukerji and Dvorkin (1998), Wang (2000), Cederbaum, Li, and Schulgasser (2000), Santamarina, Klein and Fam (2001), and King (2005).

Extensions of Biot's theory, from first principles, are given by Brutsaert (1964) and Santos, Douglas and Corberó (1990) for partial saturation – one solid and two fluids – (see simulations in Carcione, Cavallini, Santos, Ravazzoli and Gauzellino (2004)); Leclaire,

Cohen-Ténoudji and Aguirre-Puente (1994) for frozen media; Carcione, Gurevich and Cavallini (2000) for shaley sandstones; Carcione and Seriani (2001) for frozen sediments – two solids and one fluid – (see simulations in Carcione, Santos, Ravazzoli and Helle (2003)); and Berryman and Wang (2000) for a double-porosity dual-permeability medium. The extension to non-isothermal conditions, to account for the effects of thermal expansion of both the pore fluid and the matrix, are given, for instance, in McTigue (1986). In a porous medium saturated with a fluid electrolyte, acoustic and electromagnetic waves are coupled (see Section 8.15). The extension of Biot's theory to describe this phenomenon is given in Pride (1994) and Pride and Haartsen (1996) (electro-seismic wave propagation). An important reference are the collected papers of M. A. Biot resulting from the conference held in his memory in Louvain-la Neuve (Thimus, Abousleiman, Cheng, Coussy and Detournay, 1998).

The main assumptions of the theory are:

1. Infinitesimal transformations occur between the reference and current states of deformation. Displacements, strains and particle velocities are small. Consequently, the Eulerian and Lagrangian formulations coincide up to the first-order. The constitutive equations, dissipation forces, and kinetic momenta are linear. (The strain energy, dissipation potential and kinetic energy are quadratic forms in the field variables.)

2. The principles of continuum mechanics can be applied to measurable macroscopic values. The macroscopic quantities used in Biot's theory are volume averages of the corresponding microscopic quantities of the constituents.

3. The wavelength is large compared with the dimensions of a macroscopic elementary volume. This volume has well defined properties, such as porosity, permeability and elastic moduli, which are representative of the medium. Scattering effects are thus neglected.

4. The conditions are isothermal.

5. The stress distribution in the fluid is hydrostatic. (It may be not completely hydrostatic, since the fluid is viscous.)

6. The liquid phase is continuous. The matrix consists of the solid phase and disconnected pores, which do not contribute to the porosity.

7. In most cases, the material of the frame is isotropic. Anisotropy is due to a preferential alignment of the pores (or cracks).

Our approach is based on energy considerations. We define the strain, kinetic and dissipated energies, and obtain the equation of motion by solving Lagrange's equations. In the following discussion, the solid matrix is indicated by the index "m", the solid by the index "s" and the fluid phase by the index "f".

7.1 Isotropic media. Strain energy and stress-strain relations

The displacement vectors and strain tensors of the frame and the fluid are macroscopic averages, well defined in the macroscopic elementary volume. The stresses are forces acting on the frame or the fluid per unit area of porous material. The stress components for the fluid are

$$\sigma_{ij}^{(f)} = -\phi p_f \delta_{ij}, \tag{7.1}$$

where p_f is the fluid pressure and ϕ is the porosity.

Taking into account equation (1.17), and since the fluid does not "support" shear stresses, we express the strain energy of the porous medium as

$$V = A\vartheta_m^2 + Bd_m^2 + C\vartheta_m\vartheta_f + D\vartheta_f^2, \tag{7.2}$$

where A, B, C and D are elasticity coefficients to be determined as a function of the solid and fluid properties, as well as by the microstructural properties of the medium. Note the coupling term between the solid and the fluid represented by the coefficient C. The stress components are given by

$$\sigma_{ij}^{(m)} = \frac{\partial V}{\partial e_{ij}^{(m)}}, \quad \text{and} \quad \sigma^{(f)} = \frac{\partial V}{\partial \vartheta_f}, \tag{7.3}$$

where $\sigma^{(f)} = -\phi p_f$. Using these equations, the stress-strain relations are

$$\sigma_{ij}^{(m)} = 2Bd_{ij}^{(m)} + (2A\vartheta_m + C\vartheta_f)\delta_{ij}, \tag{7.4}$$

and

$$\sigma^{(f)} = C\vartheta_m + 2D\vartheta_f. \tag{7.5}$$

In order to obtain the elasticity coefficients in terms of known properties, we consider three ideal experiments, under static conditions (Biot and Willis, 1957). First, the material is subjected to a pure shear deformation ($\vartheta_m = \vartheta_f = 0$). In this case, it is clear that B is the shear modulus of the frame, since the fluid does not contribute to the shearing force. Let us denote

$$B = \mu_m, \tag{7.6}$$

as the dry matrix shear modulus.

The other two experiments are described in the following sections.

7.1.1 Jacketed compressibility test

In the second ideal experiment, the material is enclosed in a thin, impermeable, flexible jacket and then subjected to an external hydrostatic pressure p. The pressure of the fluid inside the jacket remains constant, because the interior of the jacket is exposed to the atmosphere by a tube (see Figure 7.1). The pore pressure remains essentially constant and $\sigma^{(f)} = 0$. From equations (7.4) and (7.5), we obtain

$$-p = 2A\vartheta_m + C\vartheta_f, \tag{7.7}$$

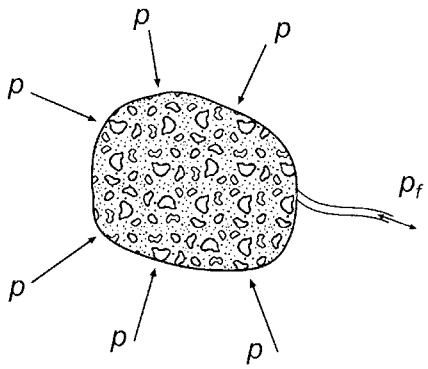

Figure 7.1: Porous material is enclosed in a thin impermeable jacket and then subjected to an external hydrostatic pressure p. The pressure of the fluid inside the jacket remains constant, because the inside of the jacket is exposed to the atmosphere by a tube of small cross-section.

and

$$0 = C\vartheta_m + 2D\vartheta_f. \tag{7.8}$$

In this test, the entire pressure is transmitted to the frame. Therefore,

$$K_m = -p/\vartheta_m, \tag{7.9}$$

where K_m is the bulk modulus of the frame, also called the drained modulus. Combining equations (7.7), (7.8) and (7.9), we obtain

$$2A - \frac{C^2}{2D} = K_m. \tag{7.10}$$

7.1.2 Unjacketed compressibility test

In the third ideal experiment, the sample is immersed in the saturating fluid to which a pressure p_f is applied. The pressure acts both on the frame part $1-\phi$, and the fluid part ϕ of the surfaces of the sample (see Figure 7.2).

Therefore, from equations (7.4) and (7.5)

$$-(1-\phi)p_f = 2A\vartheta_m + C\vartheta_f, \tag{7.11}$$

and

$$-\phi p_f = C\vartheta_m + 2D\vartheta_f. \tag{7.12}$$

In this experiment, the porosity does not change, since the deformation implies a change of scale. In this case,

$$K_s = -p_f/\vartheta_m, \quad \text{and} \quad K_f = -p_f/\vartheta_f, \tag{7.13}$$

where K_s is the bulk modulus of the elastic solid from which the frame is made, and K_f is the bulk modulus of the fluid. Since the solid frame is compressed from the inside also,

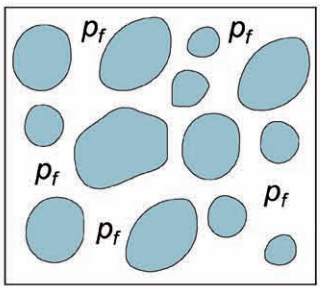

Figure 7.2: Configuration of the unjacketed experiment. The sample is immersed in a saturating fluid to which a pressure p_f is applied. The pressure acts both on the frame part and the fluid part.

in contrast to the jacketed experiment, the involved elastic modulus is that of the solid material.

Combining equations (7.11), (7.12) and (7.13), we get

$$1-\phi = \frac{2A}{K_s} + \frac{C}{K_f} \tag{7.14}$$

and

$$\phi = \frac{2D}{K_f} + \frac{C}{K_s}. \tag{7.15}$$

Solving equations (7.10), (7.14) and (7.15), we obtain

$$K \equiv 2A = \frac{(1-\phi)\left(1-\phi-\dfrac{K_m}{K_s}\right)K_s + \phi\dfrac{K_s}{K_f}K_m}{1-\phi-K_m/K_s+\phi K_s/K_f} = P - \frac{4}{3}N, \tag{7.16}$$

$$C = \frac{\left(1-\phi-\dfrac{K_m}{K_s}\right)\phi K_s}{1-\phi-K_m/K_s+\phi K_s/K_f} = Q, \tag{7.17}$$

and

$$2D = \frac{\phi^2 K_s}{1-\phi-K_m/K_s+\phi K_s/K_f} = R, \tag{7.18}$$

where P, N, Q, and R is Biot's notation[1] (Biot, 1956a; Biot and Willis, 1957).

We may recast the stress-strain relations (7.4) and (7.5) as

$$\sigma_{ij}^{(m)} = 2\mu_m d_{ij}^{(m)} + (K\vartheta_m + C\vartheta_f)\delta_{ij}, \tag{7.19}$$

and

$$\sigma^{(f)} = C\vartheta_m + R\vartheta_f. \tag{7.20}$$

[1]Readers should not confuse Q with the quality factor defined in previous chapters.

In deriving the preceding equations, we have assumed that the material of the frame is homogeneous. There are cases where the grains are cemented with a material of different properties, or where two different materials form two interpenetrating rock frames. On the basis of Biot's theory, those cases can be treated with different approaches (Brown and Korringa, 1975; Berryman and Milton, 1991; Gurevich and Carcione, 2000; Carcione, Gurevich and Cavallini, 2000).

7.2 The concept of effective stress

The stress-strain relations (7.19) and (7.20) can be interpreted as a relation between incremental fields, where stress and strain are increments with respect to a reference stress and strain – the case of wave propagation – or, as relations between the absolute fields. The last interpretation is used to illustrate the concept of effective stress.

Effective stress and effective pressure play an important role in rock physics. The use of this concept is motivated by the fact that pore pressure, p_f, and confining pressure, p_c, tend to have opposite effects on the acoustic and transport properties of the rock. Thus, it is convenient to characterize those properties with a single pressure, the effective pressure p_e. Terzaghi (1936) proposed $p_e = p_c - \phi p_f$, but his experiments, regarding the failure of geological materials, indicated that $p_e = p_c - p_f$. Let us analyze Biot's constitutive equations to obtain the effective-stress law predicted by this theory.

The total stress is decomposed into an effective stress, which acts on the frame, and into a hydrostatic stress, which acts on the fluid. In order to find this relation, we need to recast the constitutive equation in terms of the total stress

$$\sigma_{ij} = \sigma_{ij}^{(m)} + \sigma^{(f)}\delta_{ij}, \tag{7.21}$$

and the variation of fluid content

$$\zeta \equiv -\mathrm{div}[\phi(\mathbf{u}^{(f)} - \mathbf{u}^{(m)})] = -\phi(\vartheta_f - \vartheta_m), \tag{7.22}$$

where $\mathbf{u}^{(f)}$ and $\mathbf{u}^{(m)}$ are the displacement vectors of the fluid and solid matrix, respectively, and we have assumed that ϕ is constant in this derivation – this condition will be removed later. The variation of fluid content is a measure of the amount of fluid that has flowed in and out of a given volume of porous medium.

First, note that the modulus K defined in equation (7.16) can be written as

$$K = K_m + M(\alpha - \phi)^2, \tag{7.23}$$

where

$$M = \frac{K_s}{1 - \phi - K_m/K_s + \phi K_s/K_f}, \tag{7.24}$$

and[2]

$$\alpha = 1 - \frac{K_m}{K_s}. \tag{7.25}$$

[2]Readers should not confuse M and α with the complex modulus and attenuation factor defined in previous chapters.

Note the relation

$$\frac{1}{M} = \frac{\alpha - \phi}{K_s} + \frac{\phi}{K_f}. \tag{7.26}$$

Substituting equation (7.23) into equation (7.19) and using the expression of the deviatoric strain for the frame (see equation (1.15)), yields

$$\begin{aligned}\sigma_{ij}^{(m)} &= 2\mu_m d_{ij}^{(m)} + K_m \vartheta_m \delta_{ij} + [M(\alpha - \phi)^2 \vartheta_m + C\vartheta_f]\delta_{ij} \\ &= c_{ijkl}^{(m)} \epsilon_{kl}^{(m)} + [M(\alpha - \phi)^2 \vartheta_m + C\vartheta_f]\delta_{ij},\end{aligned} \tag{7.27}$$

where

$$c_{ijkl}^{(m)} = \left(K_m - \frac{2}{3}\mu_m\right)\delta_{ij}\delta_{kl} + \mu_m(\delta_{ik}\delta_{jl} + \delta_{il}\delta_{jk}) \tag{7.28}$$

is the elastic tensor of the frame. The total stress is then obtained by substituting (7.27) into equation (7.21), using (7.1), that is,

$$\sigma^{(f)} = -\phi p_f, \tag{7.29}$$

equation (7.20), and the relations $\alpha - \phi = C/R$ and $M = R/\phi^2$. We obtain

$$\sigma_{ij} = c_{ijkl}^{(m)} \epsilon_{kl}^{(m)} - \alpha p_f \delta_{ij} = 2\mu_m d_{ij}^{(m)} + K_m \vartheta_m \delta_{ij} - \alpha p_f \delta_{ij}. \tag{7.30}$$

Furthermore, using equations (7.29) and (7.22), and the relations

$$C = \phi M(\alpha - \phi), \qquad R = M\phi^2, \tag{7.31}$$

equation (7.20) can be written as

$$p_f = M(\zeta - \alpha \vartheta_m). \tag{7.32}$$

An alternative form of the total-stress components is obtained by substituting p_f into equation (7.30),

$$\sigma_{ij} = 2\mu_m d_{ij}^{(m)} + (K_m + \alpha^2 M)\vartheta_m \delta_{ij} - \alpha M \zeta \delta_{ij} = 2\mu_m d_{ij}^{(m)} + K_G \vartheta_m \delta_{ij} - \alpha M \zeta \delta_{ij}, \tag{7.33}$$

where

$$K_G = K_m + \alpha^2 M = \frac{K_s - K_m + \phi K_m\,(K_s/K_f - 1)}{1 - \phi - K_m/K_s + \phi K_s/K_f} \tag{7.34}$$

is a saturation (or undrained) modulus, obtained for $\zeta = 0$ ("closed system"). Equation (7.34) is known as Gassmann's equation (Gassmann, 1951), which, as shown in Section 7.7.1 (equation (7.286)), gives the low-frequency bulk modulus as a function of the frame and constituent properties. The dry-rock modulus expressed in terms of Gassmann's modulus is

$$K_m = \frac{(\phi K_s/K_f + 1 - \phi)K_G - K_s}{\phi K_s/K_f + K_G/K_s - 1 - \phi}. \tag{7.35}$$

A generalization of Gassmann's equation for two porous frames are given by Berryman and Milton (1991), Gurevich and Carcione (2000) and Carcione, Gurevich and Cavallini (2000). The case of n minerals is given in Carcione, Helle, Santos and Ravazzoli (2005).

The effective-stress concept means that the response of the saturated porous medium is described by the response of the dry porous medium with the applied stress replaced by the effective stress. Thus, we search for a modified stress σ'_{ij} which satisfies

$$\sigma'_{ij} = c^{(m)}_{ijkl}\epsilon^{(m)}_{kl}. \tag{7.36}$$

Comparison of equations (7.30) and (7.36) allows us to identify the Biot effective stress

$$\sigma'_{ij} = \sigma_{ij} + \alpha p_f \delta_{ij}. \tag{7.37}$$

The material constant α – defined in equation (7.25) – is referred to as the "Biot effective-stress coefficient". It is the proportion of fluid pressure which will produce the same strains as the total stress.

7.2.1 Effective stress in seismic exploration

Hydrocarbon reservoirs are generally overpressured. This situation can, in principle, be characterized by seismic waves. To this end, the dependence of the P-wave and S-wave velocities on effective stress plays an important role. It is well known from laboratory experiments that the acoustic and transport properties of rocks generally depend on "effective pressure", a combination of pore and confining pressures.

"Pore pressure" – in absolute terms – also known as formation pressure, is the "in situ pressure of the fluids in the pores. The pore pressure is equal to the "hydrostatic pressure" when the pore fluids only support the weight of the overlying pore fluids (mainly brine). In this case, there is communication from the reservoir to the surface. The "lithostatic" or "confining pressure" is due to the weight of overlying sediments, including the pore fluids[3]. A rock is said to be overpressured when its pore pressure is significantly greater than the hydrostatic pressure. The difference between confining pressure and pore pressure is called "differential pressure".

Figure 7.3 shows a typical pressure-depth relation, where the sediment of the transition zone is overpressured. Various physical processes cause anomalous pressures on an underground fluid. The most common causes of overpressure are disequilibrium compaction and "cracking", i.e., oil to gas conversion.

Let us assume a reservoir at depth z. The lithostatic pressure for an average sediment density $\bar{\rho}$ is equal to $p_c = \bar{\rho}gz$, where g is the acceleration of gravity. The hydrostatic pore pressure is approximately $p_H = \rho_w gz$, where ρ_w is the density of water. As stated above, $p_f = p_H$ if there are no permeability barriers between the reservoir and the surface, or when the pressure equilibration is fast – high overburden permeability. Taking the trace in equation (7.30), we get

$$\frac{1}{3}\sigma_{ii} = K_m\vartheta_m - \alpha p_f. \tag{7.38}$$

Identifying the left-hand side with minus the confining pressure and $K_m\vartheta_m$ with minus the effective pressure p_e, we obtain

$$p_e = p_c - \alpha p_f. \tag{7.39}$$

[3]Actually, a rock in the subsurface is subjected to a non-hydrostatic state of stress: in general, the vertical stress is greater than the horizontal stress, and this situation induces anisotropy in an otherwise isotropic rock.

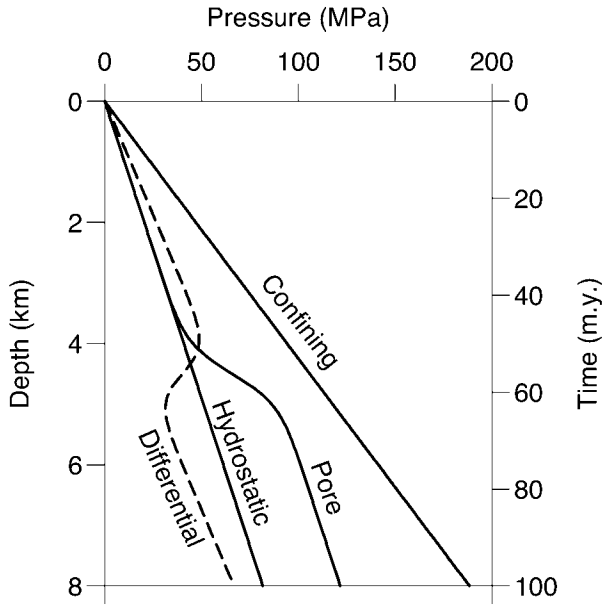

Figure 7.3: Typical pressure-depth plot, where the different pressure definitions are illustrated.

Terzaghi's equation (Terzaghi, 1925, 1943) is obtained for an incompressible solid material, $K_s \to \infty$. Then, from equation (7.25), $\alpha \to 1$, and the effective pressure, predicted by Biot's theory, is equal to the differential pressure.

Let us consider now an undrained test, that is, $\zeta = 0$. Then, the elimination of ϑ_m in equations (7.32) and (7.33) gives

$$p_f = B p_e, \tag{7.40}$$

where

$$B = \frac{\alpha M}{K_G} \tag{7.41}$$

is called the Skempton coefficient (Skempton, 1954). In this experiment, the fluid pressure depends linearly on the confining pressure. Measuring the Skempton coefficient allows us to calculate the two poroelasticity constants α and M,

$$\alpha = \frac{1}{B}\left(1 - \frac{K_m}{K_G}\right), \quad \text{and} \quad M = \frac{B^2 K_G^2}{K_G - K_m}. \tag{7.42}$$

Actually, each acoustic or transport property of the medium, such as wave velocity and permeability, has a different effective-stress coefficient. For instance, Gangi and Carlson (1996) show that the wave velocities depend on the effective pressure, which can be written as where

$$p_e = p_c - n_v p_f, \tag{7.43}$$

where n_v, the effective-stress coefficient, is a linear function of the differential pressure. This dependence of n_v versus differential pressure is in good agreement with the experimental values corresponding to the compressional velocity obtained by Prasad and Manghnani (1997). It is shown in Section 7.2.2 that the effective-stress coefficient for the porosity is 1.

Pore-volume balance

The case of disequilibrium compaction is that in which the sedimentation rate is so rapid that the pore fluids do not have a chance to "escape". Balancing mass and volume fractions in the pore space yields the pore pressure, the saturations and the porosity versus time and depth of burial. Thermal effects are also taken into account. The pore pressure, together with the confining pressure, determines the effective pressure which, in turn, determines the dry-rock moduli.

For a constant sediment burial rate, S, and a constant geothermal gradient, G, the temperature variation of a particular sediment volume is

$$T = T_0 + Gz, \quad z = St, \tag{7.44}$$

where t is here the deposition time and T_0 the surface temperature[4]. Typical values of G range from 10 to 30 °C/km, while S may range between 0.05 and 3 km/m.y. (m.y. = million years) (Mann and Mackenzie, 1990).

Assuming only liquid hydrocarbon and water in the pore space

$$\Omega_p = \Omega_o + \Omega_w, \tag{7.45}$$

where Ω_p is the pore volume, and Ω_o and Ω_w are the volumes of the hydrocarbon and water in the pore space, respectively. We have

$$d\Omega_p(p_e, T, M_p) = d\Omega_o(p_f, T, M_o) + d\Omega_w(p_f, T, M_w), \tag{7.46}$$

where M_o and M_w are the masses of the hydrocarbon and water phases and M_p is the total mass in the pore space.

If no mass (of the hydrocarbon or the water) leaves the pore space, (and there is no "phase" conversion), then $dM_p = 0 = dM_o = dM_w$ and we have

$$\begin{aligned} d\Omega_p &= \left(\frac{\partial \Omega_p}{\partial p_e}\right) dp_e + \left(\frac{\partial \Omega_p}{\partial T}\right) dT \\ &= \left(\frac{\partial \Omega_o}{\partial p_f} + \frac{\partial \Omega_w}{\partial p_f}\right) dp_f + \left(\frac{\partial \Omega_o}{\partial T} + \frac{\partial \Omega_w}{\partial T}\right) dT. \end{aligned} \tag{7.47}$$

We define

$$C_p = -\frac{1}{\Omega_p}\frac{d\Omega_p}{dp_e}, \quad C_o = -\frac{1}{\Omega_o}\frac{d\Omega_o}{dp_f}, \quad C_w = -\frac{1}{\Omega_w}\frac{d\Omega_w}{dp_f}, \tag{7.48}$$

the compressibilities for the pore space, hydrocarbon and water, and

$$\alpha_p = \frac{1}{\Omega_p}\frac{d\Omega_p}{dT}, \quad \alpha_o = \frac{1}{\Omega_o}\frac{d\Omega_o}{dT}, \quad \alpha_w = \frac{1}{\Omega_w}\frac{d\Omega_w}{dT}, \tag{7.49}$$

[4]Readers should not confuse T with the kinetic energy.

the corresponding thermal-expansion coefficients. Let us assume that the compressibilities of hydrocarbons and water are independent of pressure and temperature. That this is the case can be seen from the results given by Batzle and Wang (1992), in their Figures 5 and 13, where they show that the density is almost a linear function of temperature and pressure. This means that the mentioned properties are approximately constant (see also their Figure 7, where the oil compressibility remains almost constant when going from low temperature and low pressure to high temperature and high pressure). Moreover, let us assume that the rock compressibility C_p is independent of temperature but depends on pressure. We consider the following functional form for C_p as a function of effective pressure:

$$C_p = C_p^{\infty} + \beta \exp(-p_e/p^*), \tag{7.50}$$

where C_p^{∞}, β and p^* are coefficients obtained by fitting experimental data. Assume that at time t_i, corresponding to depth z_i, the volume of rock behaves as a closed system. That is, if the rock is a shale, its permeability is extremely low, and if the rock is a sandstone, the permeability of the sealing faults and surrounding layers is sufficiently low so that the rate of pressure increase greatly exceeds the dissipation of pressure by flow. Pore-pressure excess is measured relative to hydrostatic pressure.

Integration of (7.48) and (7.49) from p_{fi} (p_{ei}) to p_f (p_e) and T_i to $T_i + \Delta T$, where $\Delta T = T - T_i$, yields

$$\Omega_o(p_f, T) = \Omega_{oi}[\exp(-C_o \Delta p_f + \alpha_o \Delta T)], \tag{7.51}$$

$$\Omega_w(p_f, T) = \Omega_{wi}[\exp(-C_w \Delta p_f + \alpha_w \Delta T)], \tag{7.52}$$

and

$$\Omega_p(p_f, T) = \Omega_{pi}\{\exp[E(\Delta p_f) + \alpha_p \Delta T]\}, \tag{7.53}$$

where (see equation (7.50))

$$E(\Delta p_f) = -C_p^{\infty} \Delta p_e + \beta p^*[\exp(-p_e/p^*) - \exp(-p_{ei}/p^*)],$$

$\Delta p_e = p_e - p_{ei}$ and $\Delta p_f = p_f - p_{fi}$.

Assuming a linear dependence of the effective-stress coefficient, n, versus the differential pressure, $p_d = p_c - p_f$,

$$n = n_0 - n_1 p_d, \tag{7.54}$$

where n_0 and n_1 are constant coefficients, the effective pressure can be written as

$$p_e = p_c - (n_0 - n_1 p_c) p_f - n_1 p_f^2. \tag{7.55}$$

Using equation (7.47), the pore volume at pore pressure p_f and temperature T is given by

$$\begin{aligned} \Omega_p(p_f, T) = \Omega_{pi}\{\exp[E(\Delta p_f) + \alpha_p \Delta T]\} = \Omega_{wi}[\exp(-C_w \Delta p_f + \alpha_w \Delta T)] \\ + \Omega_{oi}[\exp(-C_o \Delta p_f + \alpha_o \Delta T)]. \end{aligned} \tag{7.56}$$

Since the initial saturations are

$$S_{wi} = \Omega_{wi}/\Omega_{pi}, \qquad S_{oi} = \Omega_{oi}/\Omega_{pi} = 1 - S_{wi}, \tag{7.57}$$

equation (7.56) becomes

$$\exp[E(\Delta p_f) + \alpha_p \Delta T] = S_{wi}[\exp(-C_w \Delta p_f + \alpha_w \Delta T)]$$

$$+(1 - S_{wi})[\exp(-C_o \Delta p_f + \alpha_o \Delta T)]. \tag{7.58}$$

The solution of equation (7.58) gives the pore pressure p_f as a function of depth and deposition time t, with $\Delta T = T - T_i = G(z - z_i) = GS(t - t_i)$ for a constant geothermal gradient and a constant sediment burial rate. The excess pore pressure is $p_f - p_H$.

Acoustic properties

In order to obtain the acoustic properties, such as wave velocity and attenuation factor, versus pore and confining pressures, the dry-rock bulk and rigidity moduli K_m and μ_m should be evaluated as a function of the effective pressure. Then, an appropriate model, like Biot's theory, can be used to obtain the properties of the saturated porous medium. Those moduli can be obtained from laboratory measurements in dry samples. If v_{P0} and v_{S0} are the experimental dry-rock compressional and shear velocities, the moduli are approximately given by

$$K_m(p_c) = (1 - \phi)\rho_s \left[v_{P0}^2(p_c) - \frac{4}{3} v_{S0}^2(p_c) \right], \qquad \mu_m(p_c) = (1 - \phi)\rho_s v_{S0}^2(p_c). \tag{7.59}$$

These are rock moduli at almost zero pore pressure, i.e., the case when the bulk modulus of the pore fluid is negligible compared with the frame bulk modulus, as, for example, air at room conditions.

The procedure is to fit the experimental data, say K_m, by functions of the form

$$K_m = K_m^{\infty} + a p_c + b \exp(-p_c/p^*), \tag{7.60}$$

where K_m^{∞}, a, b and p^* are fitting coefficients. Knowing the effective-stress coefficients for K_m and μ_m, it is possible to obtain the wave velocities for different combinations of the pore and confining pressures, since the property should be constant for a given value of the effective pressure. This is achieved by simply replacing the confining pressure by the effective pressure (7.55) in equations (7.60), where n corresponds either to K_m or to μ_m. An example of the application of this approach can be found in Carcione and Gangi (2000a,b), where the effects of disequilibrium compaction and oil to gas conversion on the seismic properties are investigated.

Use of high-frequency (laboratory) data to make predictions in the seismic – low-frequency – band should be considered with caution. The fluid effects on wave velocity and attenuation depend on the frequency range. At low frequencies, the fluid has enough time to achieve pressure equilibration (relaxed regime) and Gassmann's modulus properly describes the saturated bulk modulus. At high frequencies, the fluid cannot relax and this state of unrelaxation induces pore pressure gradients. Consequently, the bulk and shear moduli are stiffer than at low frequencies (White (1975), Mukerji and Mavko, 1994; Dvorkin, Mavko and Nur, 1995). This attenuation mechanism is discussed in Section 7.10.

7.2.2 Analysis in terms of compressibilities

The fact that there are two independent volumes and that two independent pressures can be applied to a porous medium implies four different compressibilities. Let us denote Ω_m,

Ω_p and Ω_b as the solid, pore and bulk volumes, respectively. The porosity and the void ratio are, respectively, defined by

$$\phi = \frac{\Omega_p}{\Omega_b}, \quad \text{and} \quad e = \frac{\Omega_p}{\Omega_m} = \frac{\Omega_p}{\Omega_b - \Omega_p} = \frac{\phi}{1-\phi}. \tag{7.61}$$

The two pressures are the confining and the pore-fluid pressures. Following the work of Zimmerman (1991, p. 3), the compressibilities are defined as

$$C_{bc} = -\frac{1}{\Omega_b}\frac{\partial \Omega_b}{\partial p_c}\Big)_{p_f} = \frac{1}{K_m}, \tag{7.62}$$

$$C_{bp} = \frac{1}{\Omega_b}\frac{\partial \Omega_b}{\partial p_f}\Big)_{p_c}, \tag{7.63}$$

$$C_{pc} = -\frac{1}{\Omega_p}\frac{\partial \Omega_p}{\partial p_c}\Big)_{p_f}, \tag{7.64}$$

and

$$C_{pp} = \frac{1}{\Omega_p}\frac{\partial \Omega_p}{\partial p_f}\Big)_{p_c} = C_p. \tag{7.65}$$

The first compressibility can be obtained with the jacketed compressibility test described in Section 7.1.1, and the last compressibility is the pore compressibility (see below). The different signs imply that all the compressibilities will be positive, because positive confining pressures decrease the volumes Ω_p and Ω_b, while positive pore pressures increase those volumes. The other, intrinsic, compressibilities are the solid material and fluid compressibilities,

$$C_s = K_s^{-1}, \quad \text{and} \quad C_f = K_f^{-1}, \tag{7.66}$$

respectively.

In order to obtain the relationships between the compressibilities, we need to perform a series of ideal experiments consisting of different pressure changes (dp_c, dp_f). The bulk volume changes due to the stress increment $(0, dp)$ are equal to the differences between the volume changes resulting from the stress increments (dp, dp) and $(dp, 0)$. The first of these experiments corresponds to that described by equation $(7.13)_1$, and the second to the jacketed experiment (Section 7.1.1). Since, in general, $d\Omega = \pm C\Omega dp$, with C being the corresponding compressibility, we have

$$C_{bp}\Omega_b dp = -C_s\Omega_b dp - (-C_{bc}\Omega_b dp) = (C_{bc} - C_s)\Omega_b dp, \tag{7.67}$$

then

$$C_{bp} = C_{bc} - C_s. \tag{7.68}$$

Let us consider now the pore volume changes and the same stress decomposition as before. The stress increment (dp, dp) generates a change of scale, implying that the change in pore volume is, in this case, given by $-C_s\Omega_p dp$. This can be interpreted as follows. The straining produced by (dp, dp) can be obtained by filling the pores with the solid material and applying a confining stress dp. Thus, a uniform straining in the solid results in the

same straining of the pore space, and the local dilatation is everywhere given by $-C_s dp$. We obtain

$$C_{pp}\Omega_p dp = -C_s\Omega_p dp - (-C_{pc}\Omega_p dp) = (C_{pc} - C_s)\Omega_p dp, \tag{7.69}$$

which implies

$$C_{pp} = C_{pc} - C_s. \tag{7.70}$$

A third relation can be obtained by invoking Bétti-Rayleigh's reciprocal theorem (Fung, 1965, p. 5): *in a linear elastic-solid, the work done by a set of forces acting through the corresponding displacements produced by a second set of forces is equal to the work done by the second set of forces acting through the corresponding displacements produced by the first set of forces.* Hence, if the two forces F_1 and F_2 act on an elastic body, the work done by F_1 acting upon the displacements due to F_2 is equal to the work done by F_2 acting upon the displacements due to F_1. Let F_1 and F_2 be the stress increments $(dp, 0)$ and $(0, dp)$, respectively. Then, the first work is

$$W_1 = -dp(C_{bp}\Omega_b dp) = -C_{bp}\Omega_b (dp)^2, \tag{7.71}$$

where the minus sign is due to the fact that the confining pressure decreases the bulk volume. The second work is

$$W_2 = dp(-C_{pc}\Omega_p dp) = -C_{pc}\Omega_p (dp)^2. \tag{7.72}$$

Here the sign is positive, since the pore pressure tends to increase the pore volume. Applying Bétti-Rayleigh's theorem and using equation $(7.61)_1$, we get

$$C_{bp} = \phi C_{pc} \tag{7.73}$$

(see also Mavko and Mukerji, 1995). Equations (7.68), (7.70) and (7.73) allow us to express three compressibilities in terms of ϕ, K_s and K_m,

$$C_{bp} = \frac{1}{K_m} - \frac{1}{K_s}, \tag{7.74}$$

$$C_{pc} = \frac{1}{\phi}\left(\frac{1}{K_m} - \frac{1}{K_s}\right), \tag{7.75}$$

and

$$C_{pp} = \frac{1}{\phi}\left(\frac{1}{K_m} - \frac{1+\phi}{K_s}\right). \tag{7.76}$$

Let us now obtain Gassmann's undrained modulus in terms of the above compressibilities. In an undrained compression, the fluid is not free to move into or out of the pore space. Such a situation is relevant to rapid processes such as wave propagation. The bulk and pore strains can be expressed in terms of the compressibilities as

$$d\epsilon_b = -C_{bc}dp_c + C_{bp}dp_f, \tag{7.77}$$

and

$$d\epsilon_p = -C_{pc}dp_c + C_{pp}dp_f, \tag{7.78}$$

The signs guarantee that decreasing confining pressure or increasing pore pressure imply positive strain increments. Now note that if the fluid completely fills the pore space and the mass of fluid is constant within the pore, we also have

$$d\epsilon_p = -C_f dp_f. \tag{7.79}$$

The ratio $-d\epsilon_b$ to dp_c is the undrained compressibility. Combining equations (7.77), (7.78) and (7.79), we get Gasmmann's compressibility,

$$C_u = -\frac{d\epsilon_b}{dp_c} = C_{bc} - \frac{C_{bp}C_{pc}}{C_{pp} + C_f} = \frac{1}{K_G}, \tag{7.80}$$

which, by virtue of equations (7.62), and (7.74)-(7.76) gives Gasmmann's compressibility, i.e., the inverse of Gasmmann's undrained modulus obtained in Section 7.2 (equation (7.34)) by setting the variation of fluid content ζ equal to zero.

Different effective-stress coefficients must be used for the various properties of the medium (Zimmerman, 1991, p. 32-40). Let us consider, for instance, the porosity. Equation (7.61) implies $\ln \phi = \ln \Omega_p - \ln \Omega_b$. Differentiating, we obtain

$$\frac{d\phi}{\phi} = \frac{d\Omega_p}{\Omega_p} - \frac{d\Omega_b}{\Omega_b} = d\epsilon_p - d\epsilon_b. \tag{7.81}$$

Using equations (7.77) and (7.78), we have

$$\frac{d\phi}{\phi} = (C_{bc} - C_{pc})dp_c - (C_{bp} - C_{pp})dp_f, \tag{7.82}$$

and substituting equations (7.74), (7.75) and (7.76), we note that the change in the porosity becomes

$$d\phi = -\left(\frac{1-\phi}{K_m} - \frac{1}{K_s}\right) d(p_c - p_f) = -\left(\frac{\alpha - \phi}{K_m}\right) d(p_c - p_f), \tag{7.83}$$

where α is given by equation (7.25). The incremental porosity depends on the differential pressure, since its effective-stress coefficient is equal to 1. The term in parentheses is always positive, and this implies that the porosity is a decreasing function of the differential pressure.

It is found experimentally that the effective-stress coefficients depend on pore and confining pressures. In principle, this may invalidate the whole concept of effective stress. However, if one assumes that the differentials $d\epsilon_b$ and $d\epsilon_p$ in equations (7.77) and (7.78) are exact differentials, the effective-stress coefficient for bulk deformations can be shown to depend on the differential pressure $p_d \equiv p_c - p_f$. The demonstration follows. If a differential is exact, the Euler condition states that the two mixed partial derivatives are equal; that is

$$\frac{\partial^2 \epsilon_b}{\partial p_f \partial p_c} = \frac{\partial}{\partial p_f}\left(\frac{\partial \epsilon_b}{\partial p_c}\right) = -\frac{\partial C_{bc}}{\partial p_f}, \tag{7.84}$$

$$\frac{\partial^2 \epsilon_b}{\partial p_c \partial p_f} = \frac{\partial}{\partial p_c}\left(\frac{\partial \epsilon_b}{\partial p_f}\right) = \frac{\partial C_{bp}}{\partial p_c} = \frac{\partial (C_{bc} - C_s)}{\partial p_c} = \frac{\partial C_{bc}}{\partial p_c}, \tag{7.85}$$

where equations (7.62), (7.63) and (7.68) have been used. Then

$$\frac{\partial C_{bc}}{\partial p_f} = -\frac{\partial C_{bc}}{\partial p_c}, \tag{7.86}$$

where we assumed that the solid compressibility C_s is independent of pressure. Similarly, the application of the Euler condition to ϵ_p yields

$$\frac{\partial C_{pc}}{\partial p_f} = -\frac{\partial C_{pc}}{\partial p_c}. \tag{7.87}$$

The form of the differential equations (7.86) and (7.87) for $C_{bc}(p_c, p_f)$ and $C_{pc}(p_c, p_f)$ implies that these compressibilities depend on the pressures only through the differential pressure,

$$C_{bc} = C_{bc}(p_d), \quad \text{and} \quad C_{pc} = C_{pc}(p_d). \tag{7.88}$$

Effective-stress coefficients for transport properties are obtained by Berryman (1992). For instance, the permeability effective-stress coefficient is found to be less than one, in contrast with experimental data for clay-rich sandstones. This is due to the assumption of microscopic homogeneity. Using a two-constituent porous medium, the theory predicts, in some cases, a coefficient greater than one.

7.3 Anisotropic media. Strain energy and stress-strain relations

Porous media are anisotropic due to bedding, compaction and the presence of aligned microcracks and fractures. In particular, in the exploration of oil and gas reservoirs, it is important to estimate the preferential directions of fluid flow. These are closely related to the permeability of the medium, and consequently to the geometrical characteristics of the skeleton. In other words, an anisotropic skeleton implies that permeability is anisotropic and vice versa. For instance, shales are naturally bedded and possess intrinsic anisotropy at the microscopic level. Similarly, compaction and the presence of microcracks and fractures make the skeleton anisotropic. Hence, it is reasonable to begin with the theory for the transversely isotropic case, which can be a good approximation for saturated compacted sediments. The extension to orthorhombic and lower-symmetry media is straightforward.

We assume that the solid constituent is isotropic and that the anisotropy is solely due to the arrangement of the grains (i.e., the skeleton is anisotropic). Generalizing the single-phase strain energy (1.8), we can write

$$\begin{aligned} 2V = {} & c_{11}(e_{11}^2 + e_{22}^2) + c_{33}e_{33}^2 + 2(c_{11} - 2c_{66})e_{11}e_{22} + 2c_{13}(e_{11} + e_{22})e_{33} \\ & + c_{44}(e_{23}^2 + e_{13}^2) + c_{66}e_{12}^2 + 2C_1(e_{11} + e_{22})\vartheta_f + 2C_3e_{33}\vartheta_f + 2F\vartheta_f^2 \end{aligned} \tag{7.89}$$

(Biot, 1955), where the strains e_{ij} correspond to the frame (The superscript (m) has been omitted for clarity). The last three terms are the coupling and the fluid terms, written in such a way as to exploit the invariance under rotations about the z-axis.

The stress-strain relations can be derived from equations (7.3). We get

$$\begin{aligned}
\sigma_{11}^{(m)} &= c_{11}\epsilon_{11}^{(m)} + (c_{11} - 2c_{66})\epsilon_{22}^{(m)} + c_{13}\epsilon_{33}^{(m)} + C_1\vartheta_f \\
\sigma_{22}^{(m)} &= c_{11}\epsilon_{22}^{(m)} + (c_{11} - 2c_{66})\epsilon_{11}^{(m)} + c_{13}\epsilon_{33}^{(m)} + C_1\vartheta_f \\
\sigma_{33}^{(m)} &= c_{33}\epsilon_{33}^{(m)} + c_{13}(\epsilon_{11}^{(m)} + \epsilon_{22}^{(m)}) + C_3\vartheta_f \\
\sigma_{23}^{(m)} &= 2c_{44}\epsilon_{23}^{(m)} \\
\sigma_{13}^{(m)} &= 2c_{44}\epsilon_{13}^{(m)} \\
\sigma_{12}^{(m)} &= 2c_{66}\epsilon_{12}^{(m)} \\
\sigma^{(f)} &= C_1(\epsilon_{11}^{(m)} + \epsilon_{22}^{(m)}) + C_3\epsilon_{33}^{(m)} + F\vartheta_f.
\end{aligned} \tag{7.90}$$

In order to obtain the elasticity coefficients in terms of known properties, we require eight experiments, since there are eight independent coefficients. Let us first recast the stress-strain relations in terms of the variation of fluid content, the total stress and the fluid pressure. Use of equation (7.22) implies $\vartheta_f = \vartheta_m - \zeta/\phi$, and equation $(7.90)_7$ can be expressed, in analogy with (7.32), as

$$p_f = M'(\zeta - \alpha_{ij}\epsilon_{ij}^{(m)}), \tag{7.91}$$

where

$$\boldsymbol{\alpha} = \begin{pmatrix} \alpha_1 & 0 & 0 \\ 0 & \alpha_1 & 0 \\ 0 & 0 & \alpha_3 \end{pmatrix}, \tag{7.92}$$

with

$$\alpha_1 = \phi\left(1 + \frac{C_1}{F}\right), \qquad \alpha_3 = \phi\left(1 + \frac{C_3}{F}\right) \tag{7.93}$$

and

$$M' = F/\phi^2. \tag{7.94}$$

Using the shortened matrix notation, we alternatively write[5]

$$\boldsymbol{\alpha} = (\alpha_1, \alpha_1, \alpha_3, 0, 0, 0)^\top, \tag{7.95}$$

where the components are denoted by α_I.

Let us consider equation $(7.90)_1$, and compute the total stress according to equation (7.21) to obtain a form similar to equation (7.30). Using equation (7.29), $\vartheta_f = \vartheta_m - \zeta/\phi$, and equations (7.91) and (7.93), we obtain

$$\sigma_{11} = c_{11}\epsilon_{11}^{(m)} + (c_{11} - 2c_{66})\epsilon_{22}^{(m)} + c_{13}\epsilon_{33}^{(m)} + C_1\vartheta_m - \frac{C_1}{\phi}\alpha_{ij}\epsilon_{ij}^{(m)} - \alpha_1 p_f. \tag{7.96}$$

Rearranging terms, we rewrite

$$\begin{aligned}
\sigma_{11} = (c_{11} + C_1 - C_1\alpha_1/\phi)\epsilon_{11}^{(m)} + (c_{12} + C_1 - C_1\alpha_1/\phi)\epsilon_{22}^{(m)} \\
+(c_{13} + C_1 - C_1\alpha_3/\phi)\epsilon_{33}^{(m)} - \alpha_1 p_f,
\end{aligned} \tag{7.97}$$

[5]Readers should not confuse $\boldsymbol{\alpha}$ with the attenuation vector.

where $c_{12} = c_{11} - 2c_{66}$. From (7.90), we obtain – using the shortened matrix notation (see equations (1.20) and (1.27)) – an equation of the form

$$\sigma_I = c_{IJ}^{(m)} e_J^{(m)} - \alpha_I p_f, \tag{7.98}$$

where

$$\begin{aligned}
c_{11}^{(m)} &= c_{22}^{(m)} = c_{11} + C_1(1 - \alpha_1/\phi) \\
c_{12}^{(m)} &= c_{12} + C_1(1 - \alpha_1/\phi) \\
c_{13}^{(m)} &= c_{13} + C_1(1 - \alpha_3/\phi) = c_{13} + C_3(1 - \alpha_1/\phi) \\
c_{33}^{(m)} &= c_{33} + C_3(1 - \alpha_3/\phi) \\
c_{44}^{(m)} &= c_{55}^{(m)} = c_{44} \\
c_{66}^{(m)} &= c_{66}.
\end{aligned} \tag{7.99}$$

For a drained condition (jacketed test), in which p_f is zero, we have

$$\sigma_I = c_{IJ}^{(m)} e_J^{(m)}. \tag{7.100}$$

Thus, the coefficients $c_{IJ}^{(m)}$ are identified as the components of the drained frame. Since there are five dry-rock moduli, five experiments are required to measure these moduli.

Three other experiments are required to obtain α_1, α_3 and M'. These experiments are unjacketed tests, where measurements in the plane of isotropy and in the axis of symmetry are performed. As in the isotropic case, the unjacketed compression test requires $\sigma_{ij}^{(m)} = -(1-\phi)p_f\delta_{ij}$, and $\sigma^{(f)} = -\phi p_f$ (see equations (7.11) and (7.12)). Then, from equation (7.21), the total stress is $\sigma_{ij} = -p_f\delta_{ij}$. The first three components of equation (7.98) become

$$\begin{aligned}
p_f(\alpha_1 - 1) &= c_{11}^{(m)}\epsilon_{11}^{(m)} + c_{12}^{(m)}\epsilon_{22}^{(m)} + c_{13}^{(m)}\epsilon_{33}^{(m)} \\
p_f(\alpha_1 - 1) &= c_{12}^{(m)}\epsilon_{11}^{(m)} + c_{11}^{(m)}\epsilon_{22}^{(m)} + c_{13}^{(m)}\epsilon_{33}^{(m)} \\
p_f(\alpha_3 - 1) &= c_{13}(\epsilon_{11}^{(m)} + \epsilon_{22}^{(m)}) + c_{33}\epsilon_{33}^{(m)}.
\end{aligned} \tag{7.101}$$

Because the loading corresponds to a change of scale for the porous medium, the resulting strain components are related to the bulk modulus of the solid by

$$\epsilon_{ij}^{(m)} = -\frac{p_f\delta_{ij}}{3K_s}, \tag{7.102}$$

assuming that the solid material is isotropic. Then, the effective-stress coefficients are given by

$$\begin{aligned}
\alpha_1 &= 1 - (c_{11}^{(m)} + c_{12}^{(m)} + c_{13}^{(m)})/(3K_s), \\
\alpha_3 &= 1 - (2c_{13}^{(m)} + c_{33}^{(m)})/(3K_s).
\end{aligned} \tag{7.103}$$

Similar expressions for α_1 and α_3 are given by Thompson and Willis (1991) in terms of Skempton coefficients (Skempton, 1954).

The last unjacketed test involves equation (7.91), and is expressed as

$$p_f = M'[\zeta - \alpha_1(\epsilon_{11}^{(m)} + \epsilon_{22}^{(m)}) - \alpha_3\epsilon_{33}^{(m)}], \tag{7.104}$$

with

$$\zeta = -\phi(\vartheta_f - \vartheta_m) = -\phi\left(\frac{p_f}{K_s} - \frac{p_f}{K_f}\right) = -\phi p_f\left(\frac{1}{K_s} - \frac{1}{K_f}\right), \tag{7.105}$$

according to equation (7.13). Substituting equations (7.102) and (7.105) into equation (7.104), we obtain

$$M' = K_s \left[\left(1 - \frac{K^*}{K_s} \right) - \phi \left(1 - \frac{K_s}{K_f} \right) \right]^{-1}, \tag{7.106}$$

where

$$K^* = c_{iijj}^{(m)} = \frac{1}{9}(2c_{11}^{(m)} + 2c_{12}^{(m)} + 4c_{13}^{(m)} + c_{33}^{(m)}) \tag{7.107}$$

is the generalized drained bulk modulus. Expression (7.106) is similar to (7.24), with K_m replaced by K^*.

The coefficients of the strain-energy density (7.89) can now be derived from equations (7.99). Using equation (7.93) and (7.94), we obtain

$$\begin{aligned}
c_{11} &= c_{11}^{(m)} + (\alpha_1 - \phi)^2 M' \\
c_{12} &= c_{12}^{(m)} + (\alpha_1 - \phi)^2 M' \\
c_{13} &= c_{13}^{(m)} + (\alpha_1 - \phi)(\alpha_3 - \phi) M' \\
c_{33} &= c_{33}^{(m)} + (\alpha_3 - \phi)^2 M' \\
c_{44} &= c_{44}^{(m)} \\
c_{66} &= c_{66}^{(m)} = (c_{11} - c_{12})/2 \\
C_1 &= \phi(\alpha_1 - \phi) M' \\
C_3 &= \phi(\alpha_3 - \phi) M' \\
F &= \phi^2 M'.
\end{aligned} \tag{7.108}$$

Furthermore, from equation (7.91) $p_f = M'(\zeta - \alpha_I e_I^{(m)})$, equation (7.98) becomes

$$\sigma_I = c_{IJ}^u e_J^{(m)} - M' \alpha_I \zeta, \tag{7.109}$$

where

$$c_{IJ}^u = c_{IJ}^{(m)} + M' \alpha_I \alpha_J \tag{7.110}$$

are the components of the undrained-modulus matrix $\mathbf{C}^u$, obtained for $\zeta = 0$, which is the equivalent of Gassmann's equation (7.34) (for instance, $c_{11}^u - 4c_{44}^u/3$ is equivalent to K_G).

As in equation (7.37), the effective stress can be expressed as

$$\sigma_I' = \sigma_I + \alpha_I p_f. \tag{7.111}$$

Unlike the isotropic case, an increase in pore pressure also induces shear stresses.

Skempton coefficients are obtained in an undrained test. Let us denote the undrained-compliance matrix by

$$\mathbf{S}^u = (\mathbf{C}^u)^{-1}, \tag{7.112}$$

and its components by s_{IJ}^u. When $\zeta = 0$, equation (7.109) gives

$$e_I^{(m)} = s_{IJ}^u \sigma_J^{(m)}. \tag{7.113}$$

Since, from equation (7.91), $p_f = -M' \alpha_I e_I^{(m)}$, we obtain

$$p_f = -B_I \sigma_I, \tag{7.114}$$

where

$$B_I = M' s^u_{IJ} \alpha_J \tag{7.115}$$

are the components of Skempton's 6×1 array. Unlike the isotropic case (see equation (7.40)), pore pressure can be generated by shear as well as normal stresses. The Skempton array for transversely isotropic media is

$$\mathbf{b} = (B_1, B_1, B_3, 0, 0, 0)^\top, \tag{7.116}$$

where

$$\begin{aligned} B_1 &= (s^u_{11} + s^u_{12})\alpha_1 + s^u_{13}\alpha_3, \\ B_3 &= 2s^u_{13}\alpha_1 + s^u_{33}\alpha_3. \end{aligned} \tag{7.117}$$

7.3.1 Effective-stress law for anisotropic media

We follow Carroll's demonstration (Carroll, 1979) to obtain the effective-stress law for general, anisotropic porous media. The stress-strain relation for a dry porous medium, obtained from equation (7.98) by setting $p_f = 0$, is

$$\sigma_{ij} = c^{(m)}_{ijkl} \epsilon^{(m)}_{kl}, \qquad \epsilon^{(m)}_{ij} = s^{(m)}_{ijkl} \sigma_{kl}, \tag{7.118}$$

where $s^{(m)}_{ijkl}$ denotes the compliance tensor, satisfying

$$c^{(m)}_{ijkl} s^{(m)}_{klrs} = \frac{1}{2}(\delta_{ir}\delta_{js} + \delta_{is}\delta_{jr}). \tag{7.119}$$

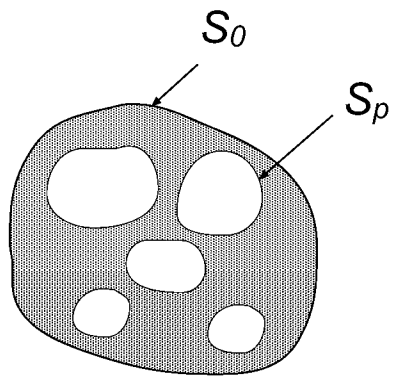

Figure 7.4: Sample of porous material, where S_0 and S_p are the outer boundaries of the sample and the pore boundaries, respectively.

Consider now a representative sample of a saturated porous medium (Figure 7.4). It is bounded by the outer surface S_0 and by the inner surface S_p (pore boundaries). Let us consider the loading

$$t_i = \sigma_{ij} n_j \quad \text{on} \quad S_0, \quad \text{and} \quad t_i = -p_f n_i \quad \text{on} \quad S_p, \tag{7.120}$$

where n_j are the components of a unit vector perpendicular to the respective bounding surfaces [6]. This loading can be treated as a superposition of two separate loadings

$$t_i = -p_f n_i \quad \text{on} \quad S_0, \quad \text{and} \quad t_i = -p_f n_i \quad \text{on} \quad S_p \tag{7.121}$$

and

$$t_i = \sigma_{ij} n_j + p_f n_i \quad \text{on} \quad S_0, \quad \text{and} \quad t_i = 0 \quad \text{on} \quad S_p. \tag{7.122}$$

The first loading gives rise to a hydrostatic pressure p_f in the solid material – it corresponds to a change of scale for the porous medium (see Figure 7.2).

The resulting strain is related to the compliance tensor of the solid $s^{(s)}_{ijkl}$,

$$\epsilon^{(1)}_{ij} = -p_f s^{(s)}_{ijkk}. \tag{7.123}$$

The second loading corresponds to the jacketed experiment (see Figure 7.1). It is related to the compliance tensor of the dry rock, since $p_f = 0$,

$$\epsilon^{(2)}_{ij} = s^{(m)}_{ijkl}(\sigma_{kl} + p_f \delta_{kl}). \tag{7.124}$$

The total strain is then given by

$$\epsilon^{(m)}_{ij} = \epsilon^{(1)}_{ij} + \epsilon^{(2)}_{ij} = s^{(m)}_{ijkl}\sigma_{kl} + p_f(s^{(m)}_{ijkk} - s^{(s)}_{ijkk}). \tag{7.125}$$

The effective-stress law is obtained by substituting equation (7.125) into equation (7.36), and written as

$$\sigma'_{ij} = c^{(m)}_{ijkl}[s^{(m)}_{klmn}\sigma_{mn} + p_f(s^{(m)}_{klmm} - s^{(s)}_{klmm})], \tag{7.126}$$

o, using (7.119),

$$\sigma'_{ij} = \sigma_{ij} + p_f(\delta_{ij} - c^{(m)}_{ijkl}s^{(s)}_{klmm}) \equiv \sigma_{ij} + p_f\alpha_{ij}. \tag{7.127}$$

This equation provides the effective-stress coefficients α_{ij} in the anisotropic case:

$$\alpha_{ij} = \delta_{ij} - c^{(m)}_{ijkl}s^{(s)}_{klmm}. \tag{7.128}$$

If the solid material is isotropic,

$$s^{(s)}_{klmm} = \frac{\delta_{kl}}{3K_s}, \tag{7.129}$$

and

$$\alpha_{ij} = \delta_{ij} - c^{(m)}_{ijkk}K_s^{-1}, \tag{7.130}$$

which is a generalization of equations (7.103).

7.3.2 Summary of equations

The stress-strain relations for a general anisotropic medium are (see also Cheng, 1997):

[6] As noted by Thompson and Willis (1991), such a load cannot be applied to the fluid parts of S_0, since the fluid can sustain only hydrostatic stress. Carroll's approach is, thus, strictly valid if none of the pores intersect the outer boundary.

Pore pressure

$$p_f = M(\zeta - \alpha_I e_I^{(m)}). \tag{7.131}$$

Total stress

$$\sigma_I = c_{IJ}^{(m)} e_J^{(m)} - \alpha_I p_f \quad (\sigma_{ij} = c_{ijkl}^{(m)} \epsilon_{kl}^{(m)} - \alpha_{ij} p_f), \tag{7.132}$$

$$\sigma_I = c_{IJ}^{u} e_J^{(m)} - M\alpha_I \zeta \quad (\sigma_{ij} = c_{ijkl}^{u} \epsilon_{kl}^{(m)} - M\alpha_{ij}\zeta). \tag{7.133}$$

Effective stress

$$\sigma_I' = \sigma_I + \alpha_I p_f. \tag{7.134}$$

Skempton relation

$$p_f = -B_I \sigma_I, \qquad B_I = M s_{IJ}^{u} \alpha_J. \tag{7.135}$$

Undrained-modulus matrix

$$c_{IJ}^{u} = c_{IJ}^{(m)} + M\alpha_I \alpha_J, \tag{7.136}$$

$$M = \frac{K_s}{(1 - K^*/K_s) - \phi\,(1 - K_s/K_f)}, \tag{7.137}$$

$$K^* = \frac{1}{9}\left[c_{11}^{(m)} + c_{22}^{(m)} + c_{33}^{(m)} + 2(c_{12}^{(m)} + c_{13}^{(m)} + c_{23}^{(m)})\right], \tag{7.138}$$

$$\begin{aligned}
\alpha_1 &= 1 - (c_{11}^{(m)} + c_{12}^{(m)} + c_{13}^{(m)})/(3K_s) \\
\alpha_2 &= 1 - (c_{12}^{(m)} + c_{22}^{(m)} + c_{23}^{(m)})/(3K_s) \\
\alpha_3 &= 1 - (c_{13}^{(m)} + c_{23}^{(m)} + c_{33}^{(m)})/(3K_s) \\
\alpha_4 &= -(c_{14}^{(m)} + c_{24}^{(m)} + c_{34}^{(m)})/(3K_s) \\
\alpha_5 &= -(c_{15}^{(m)} + c_{25}^{(m)} + c_{35}^{(m)})/(3K_s) \\
\alpha_6 &= -(c_{16}^{(m)} + c_{26}^{(m)} + c_{36}^{(m)})/(3K_s).
\end{aligned} \tag{7.139}$$

(Note that $J \geq I$ in the preceding equations).

7.3.3 Brown and Korringa's equations

An alternative derivation of the stress-strain relation for saturated porous anisotropic media is attributed to Brown and Korringa (1975), who obtained expressions for the components of the undrained-compliance tensor,

$$s_{ijkl}^{u} = s_{ijkl}^{(m)} - \frac{(s_{ijnn}^{(m)} - s_{ijnn}^{(s)})(s_{klnn}^{(m)} - s_{klnn}^{(s)})}{(s_{mmnn}^{(m)} - C_s) + \phi(C_f - C_s)}, \tag{7.140}$$

where the superscripts "u", "m" and "s" denote undrained (saturated), matrix (dry rock), and solid (solid material of the frame), and C_f and C_s are the compressibilities of the fluid and solid material, respectively (see equation (7.66))[7]. Equations (7.136) and (7.140) are equivalent. They are the anisotropic versions of Gassmann's undrained modulus.

Transversely isotropic medium

In order to illustrate how to obtain the compliance components from the stiffness components and vice versa, we consider a transversely isotropic medium. The relation between the stiffness and compliance components are

$$c_{11}+c_{12} = \frac{s_{33}}{s}, \quad c_{11}-c_{12} = \frac{1}{s_{11}-s_{12}}, \quad c_{13} = -\frac{s_{13}}{s}, \quad c_{33} = \frac{s_{11}+s_{12}}{s}, \quad c_{44} = \frac{1}{s_{44}}, \tag{7.141}$$

where

$$s = s_{33}(s_{11}+s_{12}) - 2s_{13}^2$$

(Auld, 1990a, p. 372). Moreover, $s_{66} = 2(s_{11}-s_{12})$. Equations for converting $\mathbf{C}$ to $\mathbf{S}$ are obtained by interchanging all c's and s's. The components of the corresponding undrained matrices transform in the same way. Let us consider the component $s^u_{1133} = s^u_{13}$. Then, the different quantities in equation (7.140) are given by

$$s^{(m)}_{11nn} = s^{(m)}_{11} + s^{(m)}_{12} + s^{(m)}_{13}, \quad s^{(m)}_{33nn} = s^{(m)}_{33} + 2s^{(m)}_{13}, \quad s^{(s)}_{11nn} = s^{(s)}_{33nn} = \frac{C_s}{3},$$

$$s^{(m)}_{mmnn} = 2s^{(m)}_{11} + 2s^{(m)}_{12} + 4s^{(m)}_{13} + s^{(m)}_{33}. \tag{7.142}$$

The value obtained for s^u_{13} by substituting these quantities into equation (7.140) should coincide with the value obtained from equations (7.136) and (7.141). That is,

$$s^u_{13} = \frac{c^u_{13}}{c}, \qquad c = c^u_{33}(c^u_{11}+c^u_{12}) - 2{c^u_{13}}^2. \tag{7.143}$$

7.4 Kinetic energy

Let us denote the macroscopic particle velocity by $v_i^{(p)} = \partial_t u_i^{(p)}$, $p = m$ or f, and the microscopic particle velocity by $w_i^{(p)}$. In the microscopic description, the kinetic energy is

$$T = \frac{1}{2}\int_{\Omega_m} \rho_s w_i^{(m)} w_i^{(m)} d\Omega + \frac{1}{2}\int_{\Omega_f} \rho_f w_i^{(f)} w_i^{(f)} d\Omega, \tag{7.144}$$

where ρ_f and ρ_s are the densities of the fluid and solid material, respectively, and $\Omega_m = (1-\phi)\Omega_b$, $\Omega_f = \phi\Omega_b$, with Ω_b being the volume of the elementary macroscopic and representative region of porous material. In the macroscopic description, the kinetic energy cannot be obtained by the summation of two terms, since the involved particle velocities are not the true (microscopic) velocities, but average velocities. We postulate a quadratic form with a coupling term, namely,

$$T = \frac{1}{2}\Omega_b(\rho_{11} v_i^{(m)} v_i^{(m)} + 2\rho_{12} v_i^{(m)} v_i^{(f)} + \rho_{22} v_i^{(f)} v_i^{(f)}). \tag{7.145}$$

[7]The solid material is isotropic. Note that in the isotropic case, $s^{(s)}_{mmnn} = C_s = 1/K_s$ and $c^{(s)}_{mmnn} = 9K_s$.

This hypothesis assumes statistical isotropy. (In the anisotropic case, terms of the form $v_i^{(p)} v_j^{(p')}$, $i \neq j$ contribute to the kinetic energy.)

We need to find expressions for the density coefficients as a function of the densities of the constituents and properties of the frame. Assuming that the density of the solid and fluid constituents are constant in region Ω_b, the kinetic energy (7.144) becomes

$$T = \frac{1}{2}\rho_s \Omega_m \langle w_i^{(m)} w_i^{(m)} \rangle_m + \frac{1}{2}\rho_f \Omega_f \langle w_i^{(f)} w_i^{(f)} \rangle_f, \tag{7.146}$$

where $\langle \ . \ \rangle$ denotes the average over the region occupied by the respective constituent. Equating the microscopic and macroscopic expressions for the kinetic energy, we obtain

$$\rho_{11} v_i^{(m)} v_i^{(m)} + 2\rho_{12} v_i^{(m)} v_i^{(f)} + \rho_{22} v_i^{(f)} v_i^{(f)} = (1-\phi)\rho_s \langle w_i^{(m)} w_i^{(m)} \rangle_m + \phi \rho_f \langle w_i^{(f)} w_i^{(f)} \rangle_f. \tag{7.147}$$

The linear momenta of the frame and the fluid are

$$\pi_i^{(m)} = \frac{\partial T}{\partial v_i^{(m)}} = \Omega_b (\rho_{11} v_i^{(m)} + \rho_{12} v_i^{(f)}), \tag{7.148}$$

and

$$\pi_i^{(f)} = \frac{\partial T}{\partial v_i^{(f)}} = \Omega_b (\rho_{22} v_i^{(f)} + \rho_{12} v_i^{(m)}), \tag{7.149}$$

respectively. The inertial forces acting on the frame and on the fluid are the rate of the respective linear momentum. An inertial interaction exists between the two phases. If, for instance, a sphere is moving in a fluid, the interaction creates an apparent increase in the mass of the sphere. In this case, the induced mass is ρ_{12}. When no relative motion between solid and fluid occurs, there is no interaction. The material moves as a whole ($v_i^{(m)} = v_i^{(f)}$) and the macroscopic velocity is identical to the microscopic velocity. In this case, we obtain the average density from equation (7.147) and write it as

$$\rho = (1-\phi)\rho_s + \phi\rho_f = \rho_{11} + 2\rho_{12} + \rho_{22}. \tag{7.150}$$

The linear momenta of the frame and the fluid, from equation (7.146), are

$$\pi_i^{(m)} = \frac{\partial T}{\partial w_i^{(m)}} = \Omega_b (1-\phi)\rho_s w_i^{(m)}, \tag{7.151}$$

and

$$\pi_i^{(f)} = \frac{\partial T}{\partial w_i^{(f)}} = \Omega_b \phi \rho_f w_i^{(f)}. \tag{7.152}$$

A comparison of equations (7.148) and (7.149) with (7.151) and (7.152) yields

$$\rho_{11} + \rho_{12} = (1-\phi)\rho_s, \tag{7.153}$$

and

$$\rho_{22} + \rho_{12} = \phi\rho_f. \tag{7.154}$$

Substituting ρ_{11} and ρ_{22} in terms of ρ_{12} into equation (7.147), we obtain the following expression for the induced mass:

$$\rho_{12} = -\frac{(1-\phi)\rho_s(\langle w_i^{(m)} w_i^{(m)} \rangle_m - v_i^{(m)} v_i^{(m)}) + \phi\rho_f(\langle w_i^{(f)} w_i^{(f)} \rangle_f - v_i^{(f)} v_i^{(f)})}{(v_i^{(f)} - v_i^{(m)})(v_i^{(f)} - v_i^{(m)})} \tag{7.155}$$

(Nelson, 1988). Thus, the induced mass is given by the difference between the mean square particle velocities and the square of the corresponding macroscopic particle velocities, weighted by the constituent densities. Since $0 \leq \phi \leq 1$, the induced mass is always negative.

Alternatively, rearranging terms in equation (7.155), we obtain

$$\rho_{12} = -(1-\phi)\rho_s \left[\frac{\langle (w_i^{(m)} - v_i^{(f)})(w_i^{(m)} - v_i^{(f)}) \rangle_m}{(v_i^{(f)} - v_i^{(m)})(v_i^{(f)} - v_i^{(m)})} - 1 \right]$$
$$-\phi\rho_f \left[\frac{\langle (w_i^{(f)} - v_i^{(m)})(w_i^{(f)} - v_i^{(m)}) \rangle_f}{(v_i^{(f)} - v_i^{(m)})(v_i^{(f)} - v_i^{(m)})} - 1 \right]. \tag{7.156}$$

We now define the tortuosities

$$\mathcal{T}_m = \frac{\langle (w_i^{(m)} - v_i^{(f)})(w_i^{(m)} - v_i^{(f)}) \rangle_m}{(v_i^{(f)} - v_i^{(m)})(v_i^{(f)} - v_i^{(m)})} \tag{7.157}$$

and

$$\mathcal{T} = \frac{\langle (w_i^{(f)} - v_i^{(m)})(w_i^{(f)} - v_i^{(m)}) \rangle_f}{(v_i^{(f)} - v_i^{(m)})(v_i^{(f)} - v_i^{(m)})}, \tag{7.158}$$

and the induced mass can be expressed as

$$\rho_{12} = -(1-\phi)\rho_s(\mathcal{T}_m - 1) - \phi\rho_f(\mathcal{T} - 1). \tag{7.159}$$

The tortuosity of the solid is the mean square deviation of the microscopic field of the solid from the fluid mean field, normalized by the square of the relative field between the fluid and solid constituents. The preceding statement is also true if "fluid" is substituted for "solid" in every instance, and vice versa. For a nearly rigid porous frame, the microscopic field is approximately equal to the macroscopic field, $\mathcal{T}_m \approx 1$, and

$$\rho_{12} = -\phi\rho_f(\mathcal{T} - 1), \tag{7.160}$$

which is the expression given by Biot (1956a). If the ratio $w_i^{(f)}/v_i^{(f)} = l/L$, where l is the tortuous path length between two points and L is the straight line distance between those points, the tortuosity (7.158) is simply

$$\mathcal{T} = \left(\frac{l}{L} \right)^2, \tag{7.161}$$

where we assumed that the frame is nearly rigid. This assumption implies that the tortuosity is related to the square of the relative path length.

A simple expression for the tortuosity can be obtained if we interpret ρ_{11} as the effective density of the solid moving in the fluid, namely,

$$\rho_{11} = (1-\phi)(\rho_s + r\rho_f), \tag{7.162}$$

where $r\rho_f$ is the induced mass due to the oscillations of the solid particles in the fluid. Using equations (7.153), (7.160), and (7.162), we obtain

$$\mathcal{T} = 1 + \left(\frac{1}{\phi} - 1 \right) r, \tag{7.163}$$

where $r = 1/2$ for spheres moving in a fluid (Berryman, 1980).

7.4.1 Anisotropic media

Let us consider two different approaches to obtain the kinetic energy in anisotropic media. In the first approach, the general form of the kinetic energy is assumed to be

$$T = \frac{1}{2}\Omega_b(q_{ij}v_i^{(m)}v_j^{(m)} + 2r_{ij}v_i^{(m)}v_j^{(f)} + t_{ij}v_i^{(f)}v_j^{(f)}), \tag{7.164}$$

where $\mathbf{Q}(q_{ij})$, $\bar{\mathbf{R}}(r_{ij})$ and $\mathbf{T}(t_{ij})$ are 3×3 mass matrices, with $\bar{\mathbf{R}}$ being the induced mass matrix. Let us assume that the three matrices can be diagonalized in the same coordinate system, so that

$$\begin{aligned} \mathbf{Q} &= \mathrm{diag}(q_1, q_2, q_3) \\ \bar{\mathbf{R}} &= \mathrm{diag}(r_1, r_2, r_3) \\ \mathbf{T} &= \mathrm{diag}(t_1, t_2, t_3). \end{aligned} \tag{7.165}$$

We shall see the implications of this assumption later. The kinetic energy in the microscopic description is given by equations (7.144) or (7.146). Equating the microscopic and macroscopic expressions of the kinetic energy, we obtain

$$q_i v_i^{(m)} v_i^{(m)} + 2r_i v_i^{(m)} v_i^{(f)} + t_i v_i^{(f)} v_i^{(f)} = (1-\phi)\rho_s \langle w_i^{(m)} w_i^{(m)} \rangle_m + \phi\rho_f \langle w_i^{(f)} w_i^{(f)} \rangle_f. \tag{7.166}$$

The linear momenta of the frame and the fluid are

$$\pi_i^{(m)} = \frac{\partial T}{\partial v_i^{(m)}} = \Omega_b(q_{(i)}v_i^{(m)} + r_{(i)}v_i^{(f)}), \tag{7.167}$$

and

$$\pi_i^{(f)} = \frac{\partial T}{\partial v_i^{(f)}} = \Omega_b(t_{(i)}v_i^{(f)} + r_{(i)}v_i^{(m)}), \tag{7.168}$$

where the subindex (i) means that there is no implicit summation. As in the isotropic case, to compute the relation between the different mass coefficients, we assume no relative motion between the frame and the fluid and equate the momenta (7.167) and (7.168) to the momenta (7.151) and (7.152). This gives

$$\begin{aligned} q_i + r_i &= (1-\phi)\rho_s, \\ r_i + t_i &= \phi\rho_f. \end{aligned} \tag{7.169}$$

Eliminating q_i and t_i in equation (7.166), we see that

$$r_i(v_i^{(f)} - v_i^{(m)})^2 = -(1-\phi)\rho_s(\langle w_i^{(m)} w_i^{(m)} \rangle_m - v_i^{(m)} v_i^{(m)}) - \phi\rho_f(\langle w_i^{(f)} w_i^{(f)} \rangle_f - v_i^{(f)} v_i^{(f)}), \tag{7.170}$$

which is the equivalent anisotropic relation of equation (7.155). With the use of equations (7.169), the kinetic energy (7.164) becomes

$$T = \frac{1}{2}\Omega_b[(1-\phi)\rho_s v_i^{(m)} v_i^{(m)} - r_i(v_i^{(m)} - v_i^{(f)})^2 + \phi\rho_f v_i^{(f)} v_i^{(f)}]. \tag{7.171}$$

Note that in the absence of relative motion, the average density (7.150) is obtained. The induced mass coefficients r_1, r_2 and r_3 are used as fitting parameters, as the tortuosity $\mathcal{T}$ in the isotropic case.

Let us define the displacement of the fluid relative to the solid frame,

$$\mathbf{w} = \phi(\mathbf{u}^{(f)} - \mathbf{u}^{(m)}), \tag{7.172}$$

such that the variation of fluid content (7.22) is

$$\zeta = -\text{div } \mathbf{w}. \tag{7.173}$$

The field variable

$$\dot{\mathbf{w}} = \partial_t \mathbf{w} = \phi(\mathbf{v}^{(f)} - \mathbf{v}^{(m)}) \tag{7.174}$$

is usually called the filtration velocity, which plays an important role in Darcy's law. In terms of vector $\mathbf{w}$, the kinetic energy (7.171) can be rewritten as

$$T = \frac{1}{2}\Omega_b(\rho v_i^{(m)} v_i^{(m)} + 2\rho_f v_i^{(m)} \partial_t w_i + m_i \partial_t w_i \partial_t w_i), \tag{7.175}$$

where

$$m_i = (\phi\rho_f - r_i)/\phi^2. \tag{7.176}$$

The second approach assumes that the relative microvelocity field of the fluid relative to the frame can be expressed as

$$v_i = a_{ij}\partial_t w_j \quad (\mathbf{v} = \mathbf{a} \cdot \dot{\mathbf{w}}), \tag{7.177}$$

where matrix $\mathbf{a}$ depends on the pore geometry (Biot, 1962).

The kinetic energy is

$$T = \frac{1}{2}\Omega_b(1-\phi)\rho_s v_i^{(m)} v_i^{(m)} + \frac{1}{2}\rho_f \int_{\Omega_f} (v_i^{(m)} + v_i)(v_i^{(m)} + v_i) d\Omega, \tag{7.178}$$

where the integration is taken on the fluid volume. The volume integral is

$$\int_{\Omega_f} (v_i^{(m)} + v_i)(v_i^{(m)} + v_i) d\Omega = \int_{\Omega_f} (v_i^{(m)} v_i^{(m)} + 2v_i^{(m)} v_i + v_i v_i) d\Omega. \tag{7.179}$$

We have

$$\int_{\Omega_f} (v_i^{(m)} v_i^{(m)} + 2v_i^{(m)} v_i + v_i v_i) d\Omega = \Omega_b(\phi v_i^{(m)} v_i^{(m)} + 2v_i^{(m)} \partial_t w_i) + \int_{\Omega_f} v_i v_i d\Omega. \tag{7.180}$$

From the relation (7.177), we obtain

$$\rho_f \int_{\Omega_f} v_i v_i d\Omega = m_{ij} \partial_t w_i \partial_t w_j, \qquad m_{ij} = \frac{\rho_f}{\Omega_b} \int_{\Omega_f} a_{ki} a_{kj} d\Omega. \tag{7.181}$$

After the substitution of equations (7.180) and (7.181), the kinetic energy (7.178) becomes

$$T = \frac{1}{2}\Omega_b(\rho v_i^{(m)} v_i^{(m)} + 2\rho_f v_i^{(m)} \partial_t w_i + m_{ij} \partial_t w_i \partial_t w_j), \tag{7.182}$$

Equations (7.175) and (7.182) are equivalent if

$$m_{ij} = m_i \delta_{ij}, \tag{7.183}$$

or

$$a_{ij} = a_i \delta_{ij}; \tag{7.184}$$

that is, if the three Cartesian components of the fluid motion are uncoupled, or a_{ij}, $i \neq j$ are small compared to the diagonal components. This is a strong restriction. Alternatively, we may consider an orthorhombic medium and choose the coordinate axes to lie in the planes of symmetry – recall that such a medium has three mutually orthogonal planes of mirror symmetry. In this case, the diagonalization is performed in the macroscopic domain (Biot, 1962).

7.5 Dissipation potential

Dissipation in mechanical models, consisting of springs and dashpots, is described by the constitutive equation of the dashpots, which relates the stress with the first time derivative of the strain. The strain energy is stored in the springs and a dissipation potential accounts for the dashpots. In Biot's theory, attenuation is caused by the relative motion between the frame and the fluid. Thus, the dissipation potential is written in terms of the particle velocities as

$$\Phi_D = \frac{1}{2} b (v_i^{(m)} - v_i^{(f)})(v_i^{(m)} - v_i^{(f)}), \tag{7.185}$$

where b is a friction coefficient. A potential formulation, such as equation (7.185), is only justified in the vicinity of thermodynamic equilibrium. It also assumes that the fluid flow is of the Poiseuille type, i.e., low Reynolds number and low frequencies.

The coefficient b is obtained by comparing the classical Darcy's law with the equation of the force derived from the dissipation potential. The dissipation forces are derived from a potential Ψ_D as

$$F_i = -\frac{\partial \Psi_D}{\partial u_i^{(f)}}, \tag{7.186}$$

such that

$$\frac{\partial \Psi_D}{\partial u_i^{(f)}} = \frac{\partial \Phi_D}{\partial v_i^{(f)}}. \tag{7.187}$$

Then,

$$F_i = -\frac{\partial \Psi_D}{\partial u_i^{(f)}} = b|v_i^{(f)} - v_i^{(m)}|. \tag{7.188}$$

Darcy's law (Darcy, 1856; Coussy, 1995, p. 71) relates the filtration velocity of the fluid, $\phi(v_i^{(f)} - v_i^{(m)})$ (see equation (7.174)) to the pressure gradient, $\partial_i p_f$, as

$$\phi(v_i^{(f)} - v_i^{(m)}) = \partial_t w_i = -\frac{\bar{\kappa}}{\eta} \partial_i p_f, \tag{7.189}$$

where $\bar{\kappa}$ is the global permeability and η is the viscosity of the fluid [8]. Since F_i is a force per unit volume of fluid material, $F_i = -\phi \partial_i p_f$. Comparing equations (7.188) and (7.189), we obtain the expression of the friction coefficient, namely

$$b = \phi^2 \frac{\eta}{\bar{\kappa}}. \tag{7.190}$$

[8] Note that permeability is defined by $\bar{\kappa}$ and the magnitude of the real wavenumber vector is denoted by κ.

7.5.1 Anisotropic media

The most general form of the dissipation potential in anisotropic media is

$$\Phi_D = \frac{1}{2} b_{ij} (v_i^{(m)} - v_i^{(f)})(v_j^{(m)} - v_j^{(f)}), \tag{7.191}$$

where b_{ij} are the components of a symmetric friction matrix $\bar{\mathbf{b}}$. Onsager's symmetry relations ensure the symmetry of $\bar{\mathbf{b}}$, and a positive-definite quadratic potential (Biot, 1954; de Groot and Mazur, 1963, p. 35; Nye, 1985, p. 207).

The potential (7.191) can be written in terms of the relative fluid displacement (7.172) as

$$\Phi_D = \frac{1}{2} \eta (\bar{\boldsymbol{\kappa}}^{-1})_{ij} \partial_t w_i \partial_t w_j, \tag{7.192}$$

where

$$\bar{\boldsymbol{\kappa}} = \phi^2 \eta \bar{\mathbf{b}}^{-1} \tag{7.193}$$

is the permeability matrix (see equation (7.189).

Darcy's law takes the form

$$\partial_t \mathbf{w} = \frac{1}{\eta} \bar{\boldsymbol{\kappa}} \cdot \operatorname{grad}(p_f). \tag{7.194}$$

For orthorhombic media, the friction matrix can be recast in diagonal form, in terms of three principal friction coefficients b_i, and, hence

$$\Phi_D = \frac{1}{2} b_i (v_i^{(m)} - v_i^{(f)})(v_i^{(m)} - v_i^{(f)}), \qquad b_i = \phi^2 \frac{\eta}{\bar{\kappa}_i}. \tag{7.195}$$

The dissipation forces are derived as

$$F_i = -\frac{\partial \Phi_D}{\partial v_i^{(f)}} = b_i |v_i^{(f)} - v_i^{(m)}|. \tag{7.196}$$

In terms of the three principal permeability components $\bar{\kappa}_i$ and the filtration velocity (7.174), we have

$$\Phi_D = \frac{1}{2} \frac{\eta}{\bar{\kappa}_i} \partial_t w_i \partial_t w_i = \frac{1}{2} \frac{\eta}{\bar{\kappa}_i} \dot{w}_i \dot{w}_i. \tag{7.197}$$

7.6 Lagrange's equations and equation of motion

The equation of motion can be obtained from Hamilton's principle. The Lagrangian density of a conservative system is defined as

$$L = T - V. \tag{7.198}$$

The motion of a conservative system can be described by Lagrange's equation, which is based on Hamilton's principle of least action (Achenbach, 1984, p. 61). The method can be extended to non-conservative systems if the dissipation forces can be derived

from a potential as in equation (7.186). Lagrange's equations, with the displacements as generalized coordinates, can be written as

$$\partial_t \left(\frac{\partial L}{\partial v_i^{(p)}} \right) + \partial_j \left[\frac{\partial L}{\partial (\partial_j u_i^{(p)})} \right] - \frac{\partial L}{\partial u_i^{(p)}} + \frac{\partial \Phi_D}{\partial v_i^{(p)}} = 0, \tag{7.199}$$

where $p = m$ for the frame and $p = f$ for the fluid. These equations are equivalent to Biot's classical approach

$$\partial_t \left(\frac{\partial T}{\partial v_i^{(p)}} \right) + \frac{\partial \Phi_D}{\partial v_i^{(p)}} = q_i^{(p)}, \tag{7.200}$$

where $q_i^{(p)}$ are the generalized elastic forces, given by

$$q_i^{(p)} = -\partial_j \left[\frac{\partial L}{\partial (\partial_j u_i^{(p)})} \right] = \partial_j \left[\frac{\partial V}{\partial (\partial_j u_i^{(p)})} \right], \tag{7.201}$$

because L does not depends explicitly on $u_i^{(p)}$ ($\partial L / \partial u_i^{(p)} = 0$) (Biot, 1956b). Note that from equations (1.2) and (7.3),

$$\frac{\partial V}{\partial (\partial_j u_i^{(m)})} = \frac{\partial V}{\partial e_{ij}^{(m)}} = \sigma_{ij}^{(m)}, \tag{7.202}$$

and

$$q_i^{(m)} = \partial_j \sigma_{ij}^{(m)} = \text{div } \boldsymbol{\sigma}^{(m)}. \tag{7.203}$$

According to equations (7.148)-(7.149), the generalized linear momenta per unit volume acting on the frame and on the fluid are

$$\pi_i^{(m)} = \frac{\partial T}{\partial v_i^{(m)}} = \rho_{11} v_i^{(m)} + \rho_{12} v_i^{(f)}, \tag{7.204}$$

and

$$\pi_i^{(f)} = \frac{\partial T}{\partial v_i^{(f)}} = \rho_{12} v_i^{(m)} + \rho_{22} v_i^{(f)}. \tag{7.205}$$

Then, the equation of motion, from (7.200), is

$$\partial_t \pi_i^{(p)} + F_i^{(p)} = \text{div } \boldsymbol{\sigma}^{(p)}, \tag{7.206}$$

where $F_i^{(p)} = -\partial \Phi_D / \partial v_i^{(p)}$ are the dissipation forces.

From the expression (7.185) for the dissipation potential, we have, for isotropic media,

$$\partial_j \sigma_{ij}^{(m)} = \rho_{11} \partial_{tt}^2 u_i^{(m)} + \rho_{12} \partial_{tt}^2 u_i^{(f)} + b(v_i^{(m)} - v_i^{(f)}) \tag{7.207}$$

and

$$-\phi \partial_i p_f = \rho_{12} \partial_{tt}^2 u_i^{(m)} + \rho_{22} \partial_{tt}^2 u_i^{(f)} - b(v_i^{(m)} - v_i^{(f)}), \tag{7.208}$$

where the sign of the friction terms are chosen to ensure attenuated propagating waves. Equations (7.207) and (7.208) hold for constant porosity (Biot, 1956a,b).

7.6.1 The viscodynamic operator

Adding equations (7.207) and (7.208) and using equations (7.21) and (7.29), we obtain

$$\partial_j \sigma_{ij} = (\rho_{11} + \rho_{12})\partial_{tt}^2 u_i^{(m)} + (\rho_{12} + \rho_{22})\partial_{tt}^2 u_i^{(f)}. \tag{7.209}$$

Using equations (7.153) and (7.154), substituting the relative fluid displacement (7.172) into equations (7.208) and (7.209), and considering equation (7.190), we obtain the low-frequency equations of motion

$$\partial_j \sigma_{ij} = \rho \partial_{tt}^2 u_i^{(m)} + \rho_f \partial_{tt}^2 w_i, \tag{7.210}$$

and

$$-\partial_i p_f = \rho_f \partial_{tt}^2 u_i^{(m)} + m\partial_{tt}^2 w_i + \frac{\eta}{\bar{\kappa}} \partial_t w_i, \tag{7.211}$$

where ρ is the average density (7.150), w_i are the components of vector $\mathbf{w}$, and

$$m = \rho_{22}/\phi^2 = \rho_f \mathcal{T}/\phi, \tag{7.212}$$

according to equations (7.154) and (7.160). Equations (7.210) and (7.211) hold for inhomogeneous porosity (Biot, 1962). The demonstration and the appropriate expression of the strain-energy density is obtained in Section 7.8.

Equation (7.211) can be rewritten as

$$-\partial_i p_f = \rho_f \partial_{tt}^2 u_i^{(m)} + Y * \partial_t w_i, \tag{7.213}$$

where

$$Y(t) = m\partial_t \delta(t) + \frac{\eta}{\bar{\kappa}} \delta(t), \tag{7.214}$$

is the low-frequency viscodynamic operator, with δ being Dirac's function.

In order to investigate the frequency range of validity of the viscodynamic operator (7.214) and find an approximate operator for the high-frequency range, we evaluate the friction force per unit volume in, say, the x-direction for a simple pore geometry. According to equations (7.186) and (7.187), the friction or dissipation force is given by

$$F_1^{(f)} = -\partial \Phi_D / \partial v_1^{(f)} = b(v_1^{(f)} - v_1^{(m)}) \equiv b\bar{v}_1, \tag{7.215}$$

where $\bar{v}_1 = v_1^{(f)} - v_1^{(m)}$ is the average macroscopic velocity of the fluid relative to the frame. Then, the friction coefficient is given by

$$b = F_1^{(f)}/\bar{v}_1, \tag{7.216}$$

i.e., it is the friction force per unit macroscopic velocity. To this end, we solve the problem of fluid flow between two parallel boundaries (see Figure 7.5).

7.6.2 Fluid flow in a plane slit

We consider that the fluid motion is in the x-direction and that the boundaries are located at $y = \pm a$, where a plays the role of the pore radius. The displacement only depends on

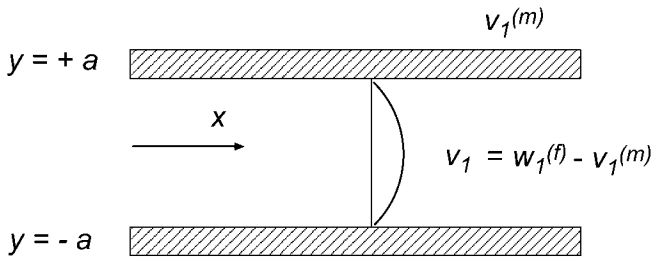

Figure 7.5: Two-dimensional flow between parallel walls.

the variable y, and we neglect pressure gradients and velocity components normal to the boundaries. The shear stress in the fluid is

$$\sigma_{12}^{(f)} = \eta \partial_t e_{12}^{(f)} = \eta \partial_2 \dot{w}_1^{(f)}, \tag{7.217}$$

where $\dot{w}_1^{(f)}$ is the microscopic particle velocity of the fluid. The viscous force is the divergence of the shear stress. Then, Euler's equation of motion for the viscous fluid is

$$-\partial_1 p_f + \eta \partial_2 \partial_2 \dot{w}_1^{(f)} = \rho_f \partial_t \dot{w}_1^{(f)}. \tag{7.218}$$

Defining the microscopic relative fluid velocity,

$$v_1 \equiv \dot{w}_1^{(f)} - v_1^{(m)}, \tag{7.219}$$

where $v_1^{(m)} = \partial_t u_1^{(m)}$ is the macroscopic particle velocity of the solid, we have

$$-\partial_1 p_f - \rho_f \partial_t v_1^{(m)} + \eta \partial_2 \partial_2 v_1 = \rho_f \partial_t v_1, \tag{7.220}$$

where we have neglected the term $\eta \partial_2 \partial_2 v_1^{(m)}$. If we consider that

$$-\partial_1 p_f - \rho_f \partial_t v_1^{(m)} \equiv \rho_f F \tag{7.221}$$

is equivalent to an external volume force, equation (7.220) becomes

$$\partial_t v_1 = \nu \partial_2 \partial_2 v_1 + F, \qquad \nu = \eta / \rho_f, \tag{7.222}$$

where ν is the dynamic viscosity. Assuming a harmonic wave with a time dependence $\exp(\mathrm{i}\omega t)$, the solution to this equation is

$$v_1 = \frac{F}{\mathrm{i}\omega} + c \cosh\left(\sqrt{\frac{\mathrm{i}\omega}{\nu}} y\right), \tag{7.223}$$

requiring that the function v_1 be symmetric in y. The condition $v_1 = 0$ at the boundaries allows us to determine the constant c. We obtain the solution

$$v_1 = \frac{F}{\mathrm{i}\omega}\left[1 - \frac{\cosh\left(\sqrt{\mathrm{i}\omega/\nu} y\right)}{\cosh\left(\sqrt{\mathrm{i}\omega/\nu} a\right)}\right]. \tag{7.224}$$

When $\omega \to 0$, equation (7.224) becomes

$$v_1 = \frac{F}{2\nu}(a^2 - y^2), \tag{7.225}$$

and the velocity profile is parabolic, corresponding to the Poiseuille flow.

The average (filtration) velocity $\dot{w}_1$ (see equation (7.174)) is

$$\dot{w}_1 = \frac{1}{2a}\int_{-a}^{+a} v_1 dy = \frac{F}{\mathrm{i}\omega}\left[1 - \frac{1}{a}\sqrt{\frac{\nu}{\mathrm{i}\omega}}\tanh\left(a\sqrt{\frac{\mathrm{i}\omega}{\nu}}\right)\right], \tag{7.226}$$

since the averaging is performed in the fluid section (i.e., an effective porosity equal to 1).

Defining the dimensionless variable as

$$q = a\sqrt{\frac{\mathrm{i}\omega}{\nu}}, \tag{7.227}$$

the average velocity becomes

$$\dot{w}_1 = \frac{\rho_f F a^2}{\eta q^2}\left[1 - \frac{1}{q}\tanh(q)\right]. \tag{7.228}$$

The combination of equations (7.221) and (7.228) yields

$$-\partial_1 p_f - \rho_f \partial_t v_1^{(m)} = \frac{\eta}{a^2}\left[\frac{q^2}{1 - (1/q)\tanh(q)}\right]\dot{w}_1. \tag{7.229}$$

A comparison of equations (7.213) and (7.229) reveals that the viscodynamic operator of the plane slit for harmonic waves is

$$\tilde{Y} \equiv \mathcal{F}[Y(q)] = \frac{\eta}{a^2}\left[\frac{q^2}{1 - (1/q)\tanh(q)}\right]. \tag{7.230}$$

Using equation (7.224), the viscous stress at the walls is

$$\tau = \eta\partial_2 v_1(y = +a) + \eta\partial_2 v_1(y = -a) = 2\eta\partial_2 v_1(y = -a) = \left(\frac{2\eta F}{\mathrm{i}\omega a}\right) q\,\tanh(q). \tag{7.231}$$

A generalized $\bar{b}$ proportional to the viscous stress can be obtained. Since $\bar{b}$ should be equal to the total friction force per unit average relative velocity and unit volume of bulk material (i.e., the porosity ϕ), the friction force per unit area of the fluid is obtained by multiplying the stress τ by $\phi/2a$. Then

$$\bar{b} = \frac{\phi\tau}{2a\dot{w}_1} \equiv \left(\frac{3\eta\phi}{a^2}\right) F_1 \equiv bF_1, \tag{7.232}$$

where

$$F_1(q) = \frac{1}{3}\left[\frac{q\,\tanh(q)}{1 - (1/q)\tanh(q)}\right] \tag{7.233}$$

$(F_1(0) = 1)$[9]. At high frequencies, $F_1 \to q/3$; that is,

$$F_1(\infty) = \frac{a}{3}\sqrt{\frac{\mathrm{i}\omega}{\nu}}, \tag{7.234}$$

and the friction force increases as the square root of the frequency.

Consider the case of low frequencies. Expanding the expression (7.230) in powers of q^2, and limiting the expansion to the first term in q^2 gives

$$\tilde{Y} = \frac{3\eta}{a^2}\left(\frac{2}{5}q^2 + 1\right). \tag{7.235}$$

Comparing the time Fourier transform of equation (7.214) with equation (7.235), we find that at low frequencies,

$$m = (6/5)\rho_f. \tag{7.236}$$

Now note that $\tilde{Y}/q^2 \to \eta/a^2$ in equation (7.230) at the high-frequency limit, i.e., when $q \to \infty$. In this limit, the viscous contribution should vanish and the result should give the expression of the inertial term $\mathrm{i}\omega m/q^2$. Since $\mathrm{i}\omega/q^2 = \nu/a^2$, we obtain

$$m = \rho_f \tag{7.237}$$

at high frequencies (Biot, 1962).

The operator (7.230) can be recast as the sum of an inertial term $\mathrm{i}\omega m$ and a viscous term $\bar{\eta}/\bar{\kappa}$ as

$$\tilde{Y}(\omega) = \mathrm{i}\omega m(\omega) + \frac{\bar{\eta}(\omega)}{\bar{\kappa}}, \tag{7.238}$$

where

$$\bar{\eta}(\omega) = \eta F_1(\omega), \tag{7.239}$$

and m depends on frequency.

It turns out that the viscodynamic operator for pores of a circular cross-section can be obtained from F_1 by substituting a by $3r/4$, where r is the radius of the tubes:

$$F_1(a) \to F_1\left(\frac{3r}{4}\right). \tag{7.240}$$

Alternatively, this is equivalent to a scaling in the frequency $\omega \to 9\omega/16$. Thus, for a general porous medium, we may write

$$F_1 = F_1(\beta\omega), \tag{7.241}$$

where β is a structural factor that depends on the geometry of the pores; $\beta = 1$ for slit-like pores, and $\beta = 9/16$ for a tube of a circular cross-section. The best value of β is obtained by fitting experimental data.

Johnson, Koplik and Dashen (1987) obtain an expression for the dynamic tortuosity $\bar{\mathcal{T}}(\omega)$, which provides a good description of both the magnitude and phase of the exact

[9] F_1 should not be confused with the dissipation forces defined in (7.186). The notation is consistent with Biot (1956b).

dynamic tortuosity of large networks formed from a distribution of random radii. The dynamic tortuosity and dynamic permeability are

$$\bar{\mathcal{T}}(\omega) = \mathcal{T} + \mathrm{i}xF \quad \text{and} \quad \bar{\kappa}(\omega) = \frac{\mathrm{i}\eta\phi}{\bar{\mathcal{T}}\omega\rho_f} = \kappa_0 \left(F - \frac{\mathrm{i}\mathcal{T}}{x} \right)^{-1}, \tag{7.242}$$

respectively, where

$$F(\omega) = \sqrt{1 - \frac{4\mathrm{i}\mathcal{T}^2\bar{\kappa}_0}{x\Lambda^2\phi}}, \quad x = \frac{\eta\phi}{\omega\bar{\kappa}_0\rho_f}. \tag{7.243}$$

In equation (7.243), $\bar{\kappa}_0$ is the global permeability, $\mathcal{T}$ is the tortuosity defined in (7.158) and Λ is a geometrical parameter, with $2/\Lambda$ being the surface-to-pore volume ratio of the pore-solid interface. The following relation between $\mathcal{T}$, $\bar{\kappa}_0$, and Λ can be used:

$$\frac{\xi\mathcal{T}\bar{\kappa}_0}{\phi\Lambda^2} = 1, \tag{7.244}$$

where $\xi = 12$ for a set of canted slabs of fluid, and $\xi = 8$ for a set of non-intersecting canted tubes. Function F plays the role of function F_1 in the previous analysis. Figure 7.6 compares the real (a) and imaginary (b) parts of F and F_1 (solid and dashed lines, respectively) versus the frequency f, for $\bar{\kappa}_0 = 1$ Darcy (10^{-12} m^2), $\eta = 1$ cP, $\rho_f = 1040$ kg/m^3, $\phi = 0.23$, $\mathcal{T} = 2$, $a = 20$ μm, $\xi = 2$ and $\beta = 0.6$. Since Johnson, Koplik and Dashen (1987) use the opposite convention for the sign of the Fourier transform, we represent $F(-\omega)$.

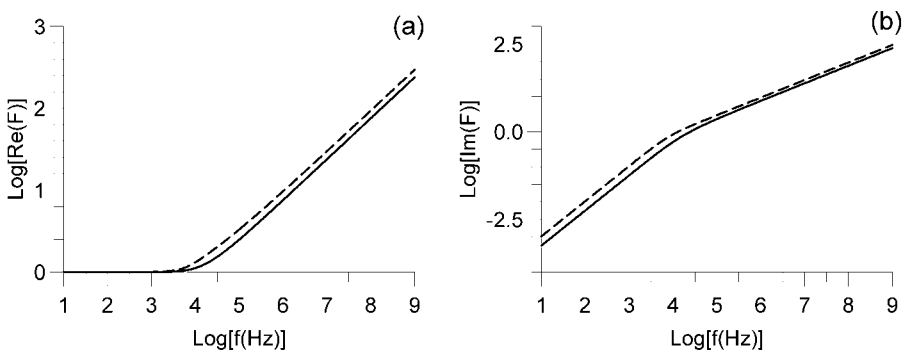

Figure 7.6: A comparison of function F_1 for a plane slit (with $\beta = 0.6$) and function F proposed by Johnson, Koplik and Dashen (1987) to model the dynamic tortuosity.

The viscodynamic operator (7.214) derived from the Lagrangian approach is valid up to frequencies where the Poiseuille flow breaks down. According to equation (7.224) the complex wavenumber of the oscillations is

$$k = \sqrt{\frac{\mathrm{i}\omega}{\nu}} = (1 + \mathrm{i})\sqrt{\frac{\omega}{2\nu}}. \tag{7.245}$$

The quarter wavelength of the boundary layer is

$$\lambda_4 = \frac{1}{4}\frac{2\pi}{\mathrm{Re}(k)} = \pi\sqrt{\frac{\nu}{2\omega}}. \tag{7.246}$$

If we assume that the Poiseuille flow breaks down when λ_4 is of the order of the pore size $2a$, the limit frequency is

$$\omega_l = \frac{\pi^2\nu}{8a^2}. \tag{7.247}$$

If we consider that the permeability of slit-like pores is

$$\bar{\kappa} = \frac{\phi a^2}{3}, \tag{7.248}$$

in agreement with equations (7.190), (7.232) and (7.238), the limit frequency can be expressed as

$$\omega_l = \left(\frac{\pi^2}{24}\right)\frac{\eta\phi}{\bar{\kappa}\rho_f}. \tag{7.249}$$

In a general porous medium, we may assume that the transition occurs when inertial and viscous forces are of the same order, i.e., when $\mathrm{i}\omega m = \eta/\bar{\kappa}$ (see equation (7.238)). This relation defines another criterion, based on the limit frequency

$$\omega_l' = \frac{\eta}{m\bar{\kappa}}. \tag{7.250}$$

Using equation (7.212), we rewrite equation (7.250) as

$$\omega_l' = \frac{\eta\phi}{\mathcal{T}\bar{\kappa}\rho_f}. \tag{7.251}$$

These frequencies define the limit of validity of the low-frequency Biot's theory.

7.6.3 Anisotropic media

The equation of motion for anisotropic media has the form (7.206)

$$\partial_t \pi_i^{(p)} + F_i^{(p)} = \mathrm{div}\ \boldsymbol{\sigma}^{(p)}, \tag{7.252}$$

considering the pore pressure and stress components (7.131) and (7.133), the linear momenta (7.167) and (7.168), and the dissipation forces (7.196). We assume for simplicity, an orthorhombic medium, and that the elasticity, permeability and induced mass matrices are diagonal in the same coordinate system.

Explicitly, we obtain

$$\partial_j \sigma_{ij}^{(m)} = [(1-\phi)\rho_s - r_{(i)}]\partial_{tt}^2 u_i^{(m)} + r_{(i)}\partial_{tt}^2 u_i^{(f)} + b_i(v_i^{(m)} - v_i^{(f)}) \tag{7.253}$$

and

$$-\partial_i(\phi p_f) = r_{(i)}\partial_{tt}^2 u_i^{(m)} + (\phi\rho_f - r_{(i)})\partial_{tt}^2 u_i^{(f)} - b_i(v_i^{(m)} - v_i^{(f)}). \tag{7.254}$$

In terms of the relative fluid displacement, these equations are similar in form to equations (7.210) and (7.211), namely,

$$\partial_j \sigma_{ij} = \rho \partial_{tt}^2 u_i^{(m)} + \rho_f \partial_{tt}^2 w_i, \tag{7.255}$$

and

$$-\partial_i p_f = \rho_f \partial_{tt}^2 u_i^{(m)} + m_i \partial_{tt}^2 w_i + \frac{\eta}{\bar{\kappa}_i} \partial_t w_i, \tag{7.256}$$

where m_i is given in equation (7.176). Introducing the viscodynamic matrix

$$\mathbf{Y} = \begin{pmatrix} Y_1 & 0 & 0 \\ 0 & Y_2 & 0 \\ 0 & 0 & Y_3 \end{pmatrix}, \tag{7.257}$$

with components $Y_i = Y_{(i)(j)}\delta_{ij}$, we see that equation (7.256) becomes

$$-\partial_i p_f = \rho_f \partial_{tt}^2 u_i^{(m)} + Y_i * \partial_t w_i, \tag{7.258}$$

where

$$Y_i = m_i \partial_t \delta + \frac{\eta}{\bar{\kappa}_i} \delta. \tag{7.259}$$

Equations (7.255) and (7.256) hold for inhomogeneous porosity.

7.7 Plane-wave analysis

The characteristics of waves propagating in a porous medium can be obtained by "probing" the medium with plane waves. Because, in isotropic media, the compressional waves are decoupled from the shear waves, the respective equations of motion can be obtained by taking divergence and curl in equations (7.207) and (7.208).

7.7.1 Compressional waves

Let us consider first the lossless case ($b = 0$ in equation (7.207) and (7.208)). Firstly, applying the divergence operation to equation (7.207), and assuming constant material properties, we obtain

$$\partial_i \partial_j \sigma_{ij}^{(m)} = \rho_{11} \partial_{tt}^2 \vartheta_m + \rho_{12} \partial_{tt}^2 \vartheta_f, \tag{7.260}$$

where $\vartheta_m = \partial_i u_i^{(m)}$ and $\vartheta_f = \partial_i u_i^{(f)}$. From equation (7.19) and using (1.15), we have

$$\partial_i \partial_j \sigma_{ij}^{(m)} = 2\mu_m \partial_i \partial_j \epsilon_{ij}^{(m)} + \left(K - \frac{2}{3}\mu_m \right) \partial_i \partial_i \vartheta_m + C \partial_i \partial_i \vartheta_f. \tag{7.261}$$

Because $2\partial_i \partial_j \epsilon_{ij}^{(m)} = \partial_i \partial_j \partial_j u_i^{(m)} + \partial_i \partial_j \partial_i u_j^{(m)} = 2\partial_i \partial_j \partial_j u_i^{(m)} = 2\partial_i \partial_i \vartheta_m$, we obtain from (7.260),

$$\left(K + \frac{4}{3}\mu_m \right) \partial_i \partial_i \vartheta_m + C \partial_i \partial_i \vartheta_f = \rho_{11} \partial_{tt}^2 \vartheta_m + \rho_{12} \partial_{tt}^2 \vartheta_f. \tag{7.262}$$

Secondly, the divergence of equation (7.208) and the use of (7.20) gives

$$C \partial_i \partial_i \vartheta_m + R \partial_i \partial_i \vartheta_f = \rho_{12} \partial_{tt}^2 \vartheta_m + \rho_{22} \partial_{tt}^2 \vartheta_f. \tag{7.263}$$

Let us consider, without loss of generality – because the medium is isotropic – propagation in the x-direction, and assume the plane waves

$$\vartheta_m = \vartheta_{m0} \exp[\mathrm{i}(\omega t - \kappa x)], \tag{7.264}$$

$$\vartheta_f = \vartheta_{f0} \exp[\mathrm{i}(\omega t - \kappa x)], \tag{7.265}$$

where κ is the real wavenumber. Substituting these expressions into equations (7.262) and (7.263), we find that

$$\mathbf{B} \cdot \boldsymbol{\vartheta} = v_p^2 \, \mathbf{D} \cdot \boldsymbol{\vartheta}, \tag{7.266}$$

where

$$v_p = \frac{\omega}{\kappa} \tag{7.267}$$

is the phase velocity, and

$$\boldsymbol{\vartheta} = \begin{pmatrix} \vartheta_{m0} \\ \vartheta_{f0} \end{pmatrix}, \quad \mathbf{B} = \begin{pmatrix} K + 4\mu_m/3 & C \\ C & R \end{pmatrix}, \quad \mathbf{D} = \begin{pmatrix} \rho_{11} & \rho_{12} \\ \rho_{12} & \rho_{22} \end{pmatrix}. \tag{7.268}$$

Equation (7.266) constitutes an eigenvalue/eigenvector problem whose characteristic equation is

$$\det(\mathbf{D}^{-1} \cdot \mathbf{B} - v_p^2 \, \mathbf{I}_2) = 0. \tag{7.269}$$

The solution of this second-order equation in v_p^2 has two roots, corresponding to two compressional waves. Let us denote the respective velocities by $v_{p\pm}$, where the signs correspond to the signs of the square root resulting from the solution of equation (7.269). Now, let us consider the two eigenvectors $\boldsymbol{\vartheta}_+$ and $\boldsymbol{\vartheta}_-$ and the respective equations resulting from (7.266),

$$\mathbf{B} \cdot \boldsymbol{\vartheta}_+ = v_{p+}^2 \, \mathbf{D} \cdot \boldsymbol{\vartheta}_+, \quad \mathbf{B} \cdot \boldsymbol{\vartheta}_- = v_{p-}^2 \, \mathbf{D} \cdot \boldsymbol{\vartheta}_-. \tag{7.270}$$

Multiplying the first by $\boldsymbol{\vartheta}_-$ and the second by $\boldsymbol{\vartheta}_+$ from the left-hand side, we get

$$\boldsymbol{\vartheta}_- \cdot \mathbf{B} \cdot \boldsymbol{\vartheta}_+ = v_{p+}^2 \boldsymbol{\vartheta}_- \cdot \mathbf{D} \cdot \boldsymbol{\vartheta}_+, \quad \boldsymbol{\vartheta}_+ \cdot \mathbf{B} \cdot \boldsymbol{\vartheta}_- = v_{p-}^2 \boldsymbol{\vartheta}_+ \cdot \mathbf{D} \cdot \boldsymbol{\vartheta}_-. \tag{7.271}$$

Since matrices $\mathbf{B}$ and $\mathbf{D}$ are symmetric and $v_{p+} \neq v_{p-}$, we obtain two orthogonality conditions, namely,

$$\boldsymbol{\vartheta}_- \cdot \mathbf{B} \cdot \boldsymbol{\vartheta}_+ = 0, \quad \boldsymbol{\vartheta}_- \cdot \mathbf{D} \cdot \boldsymbol{\vartheta}_+ = 0. \tag{7.272}$$

In explicit form, the first condition is

$$(K + 4\mu_m/3)\vartheta_{m0-}\vartheta_{m0+} + C(\vartheta_{m0-}\vartheta_{f0+} + \vartheta_{f0-}\vartheta_{m0+}) + R\vartheta_{f0-}\vartheta_{f0+} = 0. \tag{7.273}$$

Because the elasticity constants are positive, this relation shows that if the amplitudes for one mode, say ϑ_{m0+} and ϑ_{f0+} have the same sign, ϑ_{m0-} and ϑ_{f0-} have opposite signs. This means that there is a wave for which the solid and the fluid move in phase and another in which they are in counterphase. Moreover, the following relation holds

$$\boldsymbol{\vartheta}_+ \cdot \mathbf{B} \cdot \boldsymbol{\vartheta}_+ = v_{p+}^2 \boldsymbol{\vartheta}_+ \cdot \mathbf{D} \cdot \boldsymbol{\vartheta}_+, \quad \boldsymbol{\vartheta}_- \cdot \mathbf{B} \cdot \boldsymbol{\vartheta}_- = v_{p-}^2 \boldsymbol{\vartheta}_- \cdot \mathbf{D} \cdot \boldsymbol{\vartheta}_-, \tag{7.274}$$

implying

$$v_{p\pm}^2 = \frac{(K + 4\mu_m/3)\vartheta_{m0\pm}^2 + 2C\vartheta_{m0\pm}\vartheta_{f0\pm} + R\vartheta_{f0\pm}^2}{\rho_{11}\vartheta_{m0\pm}^2 + 2\rho_{12}\vartheta_{m0\pm}\vartheta_{f0\pm} + \rho_{22}\vartheta_{f0\pm}^2}. \tag{7.275}$$

Considering the relative signs between the components and that ρ_{12} is the only negative coefficient (see equation (7.160)), we deduce that the higher velocity has amplitudes in phase and the lower velocity has amplitudes in opposite phase. The last wave is called the slow wave or the wave of the second kind (Biot, 1956a).

Let us consider now the lossy case, starting from equations (7.210) and (7.213), where the last equation is intended in general, i.e., describing both the high and the low-frequency ranges. Applying the divergence operation to equation (7.210), using (7.172), and assuming constant material properties, we obtain

$$\partial_i\partial_j\sigma_{ij} = \rho\partial^2_{tt}\vartheta_m - \phi\rho_f(\partial^2_{tt}\vartheta_m - \partial^2_{tt}\vartheta_f). \tag{7.276}$$

From equation (7.33) and using (1.15), we have

$$\partial_i\partial_j\sigma_{ij} = 2\mu_m\partial_i\partial_j\epsilon^{(m)}_{ij} + \left(K_G - \frac{2}{3}\mu_m - \phi\alpha M\right)\partial_i\partial_i\vartheta_m + \phi\alpha M\partial_i\partial_i\vartheta_f, \tag{7.277}$$

and (7.276) becomes

$$\left(K_G + \frac{4}{3}\mu_m - \phi\alpha M\right)\partial_i\partial_i\vartheta_m + \phi\alpha M\partial_i\partial_i\vartheta_f = (1-\phi)\rho_s\partial^2_{tt}\vartheta_m + \phi\rho_f\partial^2_{tt}\vartheta_f, \tag{7.278}$$

where we used the relation $2\partial_i\partial_j\epsilon^{(m)}_{ij} = 2\partial_i\partial_i\vartheta_m$ and equation (7.150).

Now consider equation (7.213). The divergence of this equation and the use of (7.22) and (7.32) gives

$$\partial_i\partial_i p_f = M(\alpha-\phi)\partial_i\partial_i\vartheta_m + M\phi\partial_i\partial_i\vartheta_f = \rho_f\partial^2_{tt}\vartheta_m - \phi Y * \partial_t\vartheta_m + \phi Y * \partial_t\vartheta_f. \tag{7.279}$$

Let us consider, without loss of generality, the plane waves

$$\vartheta_m = \vartheta_{m0}\exp[\mathrm{i}(\omega t - kx)], \tag{7.280}$$

$$\vartheta_f = \vartheta_{f0}\exp[\mathrm{i}(\omega t - kx)], \tag{7.281}$$

where k is the complex wavenumber. Substituting the expressions (7.280) and (7.281) into equations (7.278) and (7.279), we obtain

$$\left[K_G + \frac{4}{3}\mu_m - \phi\alpha M - v_c^2(1-\phi)\rho_s\right]\vartheta_{m0} + \phi(\alpha M - \rho_f v_c^2)\vartheta_{f0} = 0, \tag{7.282}$$

$$\left[M(\alpha-\phi) - v_c^2\left(\rho_f + \frac{\mathrm{i}}{\omega}\phi\tilde{Y}\right)\right]\vartheta_{m0} + \phi\left(M + \frac{\mathrm{i}}{\omega}\tilde{Y}v_c^2\right)\vartheta_{f0} = 0, \tag{7.283}$$

where $\tilde{Y}$ is given by equation (7.238) and

$$v_c = \frac{\omega}{k} \tag{7.284}$$

is the complex velocity. The dispersion relation is obtained by taking the determinant of the system of equations (7.282) and (7.283) equal to zero; that is

$$\left[K_G + \frac{4}{3}\mu_m - \phi\alpha M - v_c^2(1-\phi)\rho_s\right]\left(M + \frac{\mathrm{i}}{\omega}v_c^2\tilde{Y}\right)$$

$$-(\alpha M - \rho_f v_c^2)\left[M(\alpha-\phi) - v_c^2\left(\rho_f + \frac{\mathrm{i}}{\omega}\phi\tilde{Y}\right)\right] = 0. \tag{7.285}$$

Multiplying this equation by ω and taking the limit $\omega \to 0$, we get Gassmann's velocity, regardless of the value of the viscodynamic operator,

$$v_G = \sqrt{\frac{1}{\rho}\left(K_G + \frac{4}{3}\mu_m\right)}. \tag{7.286}$$

Reordering terms in equation (7.285), we obtain

$$-\left(\rho_f^2 + \frac{\mathrm{i}}{\omega}\tilde{Y}\rho\right)v_c^4 + \left[\frac{\mathrm{i}}{\omega}\tilde{Y}\left(K_G + \frac{4}{3}\mu_m\right) + M(2\alpha\rho_f - \rho)\right]v_c^2 + M\left(K_m + \frac{4}{3}\mu_m\right) = 0, \tag{7.287}$$

where equation (7.34) has been used. The solution of this second-order equation in v_c^2 has two roots, corresponding to the fast and slow compressional waves obtained earlier. Let us denote the respective complex velocities by $v_{c\pm}$, where the signs correspond to the signs of the square root resulting from the solution of equation (7.287). The phase velocity v_p is equal to the angular frequency ω divided by the real part of the complex wavenumber k; that is,

$$v_{p\pm} = [\mathrm{Re}(v_{c\pm}^{-1})]^{-1}, \tag{7.288}$$

and the attenuation factor α is equal to minus the imaginary part of the complex wavenumber; that is

$$\alpha_\pm = -\omega[\mathrm{Im}(v_{c\pm}^{-1})]. \tag{7.289}$$

The high-frequency velocity, say v_∞, of the low-frequency theory is obtained by taking the limit $\mathrm{i}\tilde{Y}/\omega \to -m$ in equation (7.238) – this is equivalent to considering $\eta = 0$, since the inertial effects dominate over the viscosity effects. Equation (7.287) then becomes

$$(m\rho - \rho_f^2)v_\infty^4 - \left[m\left(K_G + \frac{4}{3}\mu_m\right) - M(2\alpha\rho_f - \rho)\right]v_\infty^2 + M\left(K_m + \frac{4}{3}\mu_m\right) = 0, \tag{7.290}$$

where v_∞ is real-valued. Using (7.34) and defining the dry-rock P-wave modulus as

$$E_m = K_m + \frac{4}{3}\mu_m, \tag{7.291}$$

we note that equation (7.290) becomes

$$(m\rho - \rho_f^2)v_\infty^4 - [m(E_m + \alpha^2 M) - M(2\alpha\rho_f - \rho)]v_\infty^2 + ME_m = 0. \tag{7.292}$$

It can be verified that $v_{\infty+} > v_G$.

Relation with Terzaghi's law and the second P wave

Terzaghi's law, used in geotechnics (Terzaghi, 1925), can be obtained from Biot's theory if $\alpha = \phi$, $K_f \ll K_m$ and $\mathcal{T} \to 1$. The result is a decoupling of the solid and fluid phases (Bourbié, Coussy and Zinszner, 1987, p. 81). Let us consider the first two conditions.

Then, $M = K_f/\phi$ from equation (7.26), $E_m + \alpha^2 M \simeq E_m$, $M(2\rho_f\alpha - \rho) \ll E_m$, and the solution of equation (7.292) is

$$v_\infty^2 = \frac{mE_m \pm \sqrt{m^2E_m^2 - 4(m\rho - \rho_f^2)ME_m}}{2(m\rho - \rho_f^2)}. \tag{7.293}$$

Due to the second condition, $M \ll K_m$, and the second term inside the square root is much smaller than the first term. The fast-wave velocity is

$$v_{\infty+} = \sqrt{\frac{E_m}{\rho - \phi\rho_f/\mathcal{T}}}, \tag{7.294}$$

and a Taylor expansion of the square root in (7.292) gives

$$v_{\infty-} = \sqrt{\frac{K_f}{\rho_f\mathcal{T}}}, \tag{7.295}$$

where equation (7.212) has been used. Note that Therzaghi's law requires $\mathcal{T} \to 1$, which implies $v_{\infty+} = \{E_m/[(1-\phi)\rho_s]\}^{-1/2}$ and $v_{\infty-} = \sqrt{K_f/\rho_f}$. Thus, the fast wave travels in the skeleton and the slow wave in the fluid. The latter has the fluid velocity divided by the factor $\sqrt{\mathcal{T}} \geq 1$, because of the tortuous nature of the pore space. Use of the superfluid ^{4}He, which is two orders of magnitude more compressible than water, makes equation (7.295) very accurate (Johnson, 1986). In this case, the slow wave is identified with the fourth-sound phenomenon. Measurements of the fourth-sound velocity give us the tortuosity $\mathcal{T}$.

To our knowledge, the first observation of the second (slow) P wave is attributed to Plona (1980). He used water-saturated sintered glass beads (see Bourbié, Coussy and Zinszner (1987, p. 88)). However, Oura (1952a,b) measured the slow-wave velocity in snow, and seems to have grasped its nature before Biot's theoretical prediction in 1956 (Biot, 1956a). Oura states "... the sound wave is propagated mainly by air in snow and its icy structure only interferes with the propagation." (See Johnson (1982) for an interpretation using Biot's theory.) Observations of the slow wave in natural media are reported by Nakagawa, Soga and Mitchell (1997) for granular soils and Kelder and Smeulders (1997) for Nivelsteiner sandstone (see Section 7.13).

Actually, the slow wave has been predicted by Biot before 1956. Biot (1952) obtained the velocity of the tube wave (Scholte wave) in a fluid-filled circular borehole. This velocity in the low-frequency limit is given by

$$v_{\infty-} = \frac{v_f}{\sqrt{1 + K_f/\mu_s}}, \tag{7.296}$$

where K_f is the fluid bulk modulus, $v_f = \sqrt{K_f/\rho_f}$ is the fluid sound velocity, ρ_f is the fluid density, and μ_s is the formation shear modulus. Norris (1987) shows that the tube wave is a limiting case of the slow wave when the bore is considered as an isolated pore in a homogeneous porous medium. A typical borehole radius is 10 cm, and considering an acoustic logging frequency of 1 kHz and water, the viscous skin depth is on the order of 100 μm. If the borehole is considered to be a pore, the case of zero viscosity has to be

considered, i.e., the viscosity effects are negligible compared to the intertial effects. The tube wave follows from Biot's theory, by taking the limit of vanishing porosity, using a tortuosity $\mathcal{T} = 1$ and a dry-rock modulus $K_m = \mu_s$, where μ_s is the grain shear modulus in Biot's theory.

The diffusive slow mode

Let us consider equations (7.278) and (7.279) at very low frequencies, when terms proportional to ω^2 can be neglected (i.e., terms containing second-order time derivatives). Using equation (7.214) and denoting the Laplacian $\partial_i \partial_i$ by Δ, we can rewrite those equations as

$$\left(K_G + \frac{4}{3}\mu_m - \phi\alpha M\right) \Delta\vartheta_m + \phi\alpha M \Delta\vartheta_f = 0 \tag{7.297}$$

and

$$\Delta p_f = M(\alpha - \phi)\Delta\vartheta_m + M\phi\Delta\vartheta_f = -\frac{\phi\eta}{\bar{\kappa}}(\partial_t\vartheta_m - \partial_t\vartheta_f). \tag{7.298}$$

Eliminating ϑ_m and ϑ_f, and defining $\mathcal{P} = \Delta p$, we obtain the diffusion equation

$$d\ \Delta\mathcal{P} = \partial_t\mathcal{P}, \tag{7.299}$$

where, using equation (7.34),

$$d = M\left(\frac{\bar{\kappa}}{\eta}\right)\left(\frac{K_m + 4\mu_m/3}{K_G + 4\mu_m/3}\right) \tag{7.300}$$

is the corresponding hydraulic diffusivity constant. Because we have neglected the acceleration terms, we have obtained the differential equation corresponding to the diffusive slow mode (Chandler and Johnson, 1981). Shapiro, Audigane and Royer (1999) apply the anisotropic version of this theory for estimating the permeability tensor from induced microseismic experiments in a borehole.

7.7.2 The shear wave

Before deriving the shear-wave properties, let us recall that the curl operation requires a vector product between the Cartesian unit vectors; that is, $\hat{\mathbf{e}}_i \times \hat{\mathbf{e}}_j = \epsilon_{ijk}\ \hat{\mathbf{e}}_k$, where ϵ_{ijk} is the Levi-Civita tensor. Then, the curl of a vector $\mathbf{u}$ is $\hat{\mathbf{e}}_i\ \partial_i \times \hat{\mathbf{e}}_j\ u_j = \epsilon_{ijk}\partial_i u_j\ \hat{\mathbf{e}}_k$. We define

$$\mathbf{\Omega}^{(m)} = \text{curl}\ \mathbf{u}^{(m)}, \qquad \mathbf{\Omega}^{(f)} = \text{curl}\ \mathbf{u}^{(f)}. \tag{7.301}$$

Applying the curl operator first to equation (7.210), using equation (7.172), and assuming constant material properties, we obtain

$$\epsilon_{lik}\partial_l\partial_j\sigma_{ij}\ \hat{\mathbf{e}}_k = \rho\partial_{tt}^2\mathbf{\Omega}^{(m)} - \phi\rho_f(\partial_{tt}^2\mathbf{\Omega}^{(m)} - \partial_{tt}^2\mathbf{\Omega}^{(f)}). \tag{7.302}$$

Using equations (7.33) and (1.15), we have

$$2\mu_m\epsilon_{lik}\partial_l\partial_j\epsilon_{ij}^{(m)}\ \hat{\mathbf{e}}_k = \rho\partial_{tt}^2\mathbf{\Omega}^{(m)} - \phi\rho_f(\partial_{tt}^2\mathbf{\Omega}^{(m)} - \partial_{tt}^2\mathbf{\Omega}^{(f)}), \tag{7.303}$$

where the terms containing the dilatations ϑ_m and ϑ_f disappear, because the curl of the gradient of a function is zero. Because $2\epsilon_{lik}\partial_l\partial_j\epsilon_{ij}^{(m)}\,\hat{\mathbf{e}}_k = \epsilon_{lik}\partial_l\partial_j(\partial_i u_j^{(m)} + \partial_j u_i^{(m)})\,\hat{\mathbf{e}}_k = \epsilon_{lik}\partial_l\partial_i\vartheta_j^{(m)}\hat{\mathbf{e}}_k + \partial_j\partial_j(\epsilon_{lik}\partial_l u_i^{(m)})\,\hat{\mathbf{e}}_k = \partial_j\partial_j\boldsymbol{\Omega}^{(m)}$, we finally obtain

$$\mu_m\partial_j\partial_j\boldsymbol{\Omega}^{(m)} = (1-\phi)\rho_s\partial_{tt}^2\boldsymbol{\Omega}^{(m)} + \phi\rho_f\partial_{tt}^2\boldsymbol{\Omega}^{(f)}, \tag{7.304}$$

where we used equation (7.150).

Consider now equation (7.213). The curl of this equation gives

$$0 = \rho_f\partial_{tt}^2\boldsymbol{\Omega}^{(m)} - \phi Y * \partial_t\boldsymbol{\Omega}^{(m)} + \phi Y * \partial_t\boldsymbol{\Omega}^{(f)}. \tag{7.305}$$

Let us consider, without loss of generality, plane waves traveling in the x-direction and polarized in the y-direction; that is $\boldsymbol{\Omega}^{(p)} = (0, 0, \partial_1 u_2^{(p)})$ ($p = m$ or f). Let us define $\Omega^{(m)} = \partial_1 u_2^{(m)}$ and $\Omega^{(f)} = \partial_1 u_2^{(f)}$. Then

$$\Omega^{(m)} = \Omega_{m0}\exp[\mathrm{i}(\omega t - kx)], \tag{7.306}$$

$$\Omega^{(f)} = \Omega_{f0}\exp[\mathrm{i}(\omega t - kx)], \tag{7.307}$$

where k is the complex wavenumber. Substituting these plane-wave expressions into equations (7.304) and (7.305), we obtain

$$\left[\mu_m - v_c^2(1-\phi)\rho_s\right]\Omega_{m0} - \phi\rho_f v_c^2\Omega_{f0} = 0, \tag{7.308}$$

$$-\left(\rho_f + \frac{\mathrm{i}}{\omega}\tilde{Y}\phi\right)\Omega_{m0} + \left(\frac{\mathrm{i}}{\omega}\tilde{Y}\phi\right)\Omega_{f0} = 0, \tag{7.309}$$

where $v_c = \omega/k$ is the complex shear-wave velocity. The solution is easily obtained as

$$v_c = \sqrt{\frac{\mu_m}{\rho - \mathrm{i}\omega\rho_f^2\tilde{Y}^{-1}}}. \tag{7.310}$$

The phase velocity v_p is equal to the angular frequency ω divided by the real part of the complex wavenumber k; that is,

$$v_p = [\mathrm{Re}(v_c^{-1})]^{-1}, \tag{7.311}$$

and the attenuation factor is equal to the imaginary part of the complex wavenumber; that is,

$$\alpha = \omega[\mathrm{Im}(v_c^{-1})]. \tag{7.312}$$

At low frequencies, $\tilde{Y} = \mathrm{i}\omega m + \eta/\bar{\kappa}$ (see equation (7.214)) and equation (7.310) becomes

$$v_c = \sqrt{\frac{\mu_m}{\rho - \rho_f^2[m - \mathrm{i}\eta/(\omega\bar{\kappa})]^{-1}}}. \tag{7.313}$$

In the absence of dissipation ($\eta/\bar{\kappa} = 0$) or when $\omega \to \infty$,

$$v_c = \sqrt{\frac{\mu_m}{\rho - \rho_f^2 m^{-1}}} = \sqrt{\frac{\mu_m}{\rho - \rho_f\phi\mathcal{T}^{-1}}}, \tag{7.314}$$

and

$$\Omega_{f0} = \left(1 - \frac{\rho_f}{\phi m}\right)\Omega_{m0} = \left(1 - \frac{1}{\mathcal{T}}\right)\Omega_{m0}, \tag{7.315}$$

from equations (7.212) and (7.309). Since the quantity in parentheses is positive, because $\mathcal{T} \geq 1$, the rotation of the solid and the fluid are in the same direction. At zero frequency ($\omega \to 0$), $v_c \to \sqrt{\mu_m/\rho}$ and, from equation (7.309), $\Omega_{m0} = \Omega_{f0}$, and there is no relative motion between the solid and the fluid. Note that because $m \geq 0$, the velocity (7.314) is higher than the average velocity $\sqrt{\mu_m/\rho}$.

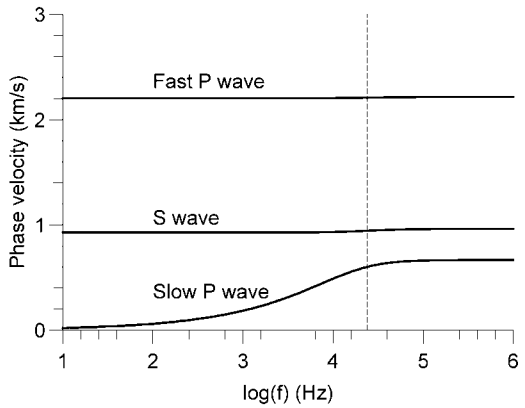

Figure 7.7: Phase velocities versus frequency of the fast P wave, shear wave and slow P wave in water saturated sandstone. The medium properties are $K_s = 35$ GPa, $\rho_s = 2650$ kg/m^3, $K_m = 1.7$ GPa, $\mu_m = 1.855$ GPa, $\phi = 0.3$, $\bar{\kappa} = 1$ Darcy, $\mathcal{T} = 2$, $K_f = 2.4$ GPa, $\rho_f = 1000$ kg/m^3, and $\eta = 1$ cP (Carcione, 1998).

Figure 7.7 shows the phase velocities of the different wave modes (equations (7.288) and (7.311) as a function of frequency). The medium is water-saturated sandstone and the curves correspond to the low-frequency theory (i.e, $\tilde{Y} = \mathrm{i}\omega m + (\eta/\bar{\kappa})$). The vertical dashed line is the frequency $f_l' = \omega_l'/(2\pi)$ (equation (7.251)), which indicates the upper limit for the validity of low-frequency Biot's theory. The slow wave has a quasi-static character at low frequencies and becomes overdamped due to the fluid viscosity. If we replace water by oil (say, $\eta = 260$ cP), this behavior then corresponds to higher frequencies. This phenomenon precludes the observation of the slow wave at seismic frequencies. The presence of clay particles in the pores is an additional cause of attenuation of the slow wave (Klimentos and McCann, 1988).

7.8 Strain energy for inhomogeneous porosity

The Lagrangian formulation developed by Biot in his 1956 paper (Biot, 1956a) holds for constant porosity. He uses the average displacements of the solid and the fluid as Lagrangian coordinates, $u_i^{(m)}$ and $u_i^{(f)}$, and the respective stress components, $\sigma_{ij}^{(m)}$ and $\sigma^{(f)}$, as conjugate variables. The equations for variable porosity are developed in Biot

(1962) and compared in detail to the 1956 equations. In his 1962 work, he proposes, as generalized coordinates, the displacements of the solid matrix and the variation of fluid content ζ defined in equation (7.22). In this case, the corresponding conjugate variables are the total-stress components, σ_{ij}, and the fluid pressure, p_f. It is shown in this section that the 1962 equations are the correct ones for describing propagation in an inhomogeneous porous medium. They are consistent with Darcy's law and the boundary conditions at interfaces separating media with different properties. Two approaches are developed in the following sections. The first is based on the complementary energy theorem under small variations of stress, and the second is based on volume-averaging methods. An alternative demonstration, not given here, has been developed by Rudnicki (2000, personal communication), in terms of thermodynamic potentials.

7.8.1 Complementary energy theorem

Let us consider an elementary volume Ω_b of porous material bounded by surface S. Assume that Ω_b is initially in static equilibrium under the action of surface forces

$$f_i^{(m)} = \sigma_{ij}^{(m)} n_j, \quad f_i^{(f)} = -\phi p_f n_i, \tag{7.316}$$

where n_i are the components of the outward unit vector perpendicular to S. Assume that the system is perturbed by $\delta f_i^{(m)}$ and $\delta f_i^{(f)}$ and let $V(\delta f_i^{(m)}, \delta f_i^{(f)})$ be the strain-energy density, and

$$V^* = \int_{\Omega_b} V d\Omega - \int_S (f_i^{(m)} u_i^{(m)} + f_i^{(f)} u_i^{(f)}) dS \tag{7.317}$$

be the complementary energy. Strictly, V should be the complementary strain-energy density; however, for linear stress-strain relations, V is equal to the strain-energy density (Fung, 1965, p. 293 and 295). The complementary energy theorem states that *of all sets of forces that satisfy the equations of equilibrium and boundary conditions, the actual one that is consistent with the prescribed displacements is obtained by minimizing the complementary energy* (Fung, 1965, p. 294). Then

$$\delta V^* = 0 = \int_{\Omega_b} \delta V d\Omega - \int_S (\delta f_i^{(m)} u_i^{(m)} + \delta f_i^{(f)} u_i^{(f)}) dS \tag{7.318}$$

or

$$\int_{\Omega_b} \delta V d\Omega = \int_S (\delta f_i^{(m)} u_i^{(m)} + \delta f_i^{(f)} u_i^{(f)}) dS. \tag{7.319}$$

We have

$$\delta f_i^{(m)} = (\delta \sigma_{ij} + \phi \delta_{ij} \delta p_f) n_j \quad \text{and} \quad \delta f_i^{(f)} = -\phi \delta p_f n_i, \tag{7.320}$$

where we have used equations (7.21) and (7.29). Equation (7.318) becomes

$$\delta V^* = 0 = \int_{\Omega_b} \delta V d\Omega - \int_S (u_i^{(m)} \delta \sigma_{ij} n_j - w_i \delta p_f n_i) dS, \tag{7.321}$$

where w_i are the components of vector $\mathbf{w}$ defined in equation (7.172). Applying Green's theorem to the surface integral, we obtain

$$\delta V^* = 0 = \int_{\Omega_b} \delta V d\Omega - \int_{\Omega_b} [\partial_j (u_i^{(m)} \delta \sigma_{ij}) - \partial_i (w_i \delta p_f)] d\Omega. \tag{7.322}$$

Because the system is in equilibrium before and after the perturbation, and the fluid pressure is constant in Ω_b, the stress increments must satisfy

$$\partial_j(\delta\sigma_{ij}) = 0, \quad \text{and} \quad \partial_i(\delta p_f) = 0, \tag{7.323}$$

and we can write

$$\delta V^* = 0 = \int_{\Omega_b} \delta V d\Omega - \int_{\Omega_b} (\epsilon_{ij}^{(m)}\delta\sigma_{ij} + \zeta\delta p_f) d\Omega, \tag{7.324}$$

where $\zeta = -\partial_i w_i$ is the variation of fluid content (equation (7.22)), and $\epsilon_{ij}^{(m)}$ is of the form defined in equation (1.3). To obtain the fluid term $\zeta\delta p_f$, we used the fact that the porosity is locally constant, i.e., it is constant in the elementary volume Ω_b, but it may vary point to point in the porous medium. Moreover, the symmetry of the stress tensor has been used to obtain the relation $\partial_j u_i^{(m)}\delta\sigma_{ij} = \epsilon_{ij}^{(m)}\delta\sigma_{ij}$.

We finally deduce from equation (7.324) that

$$\delta V = \epsilon_{ij}^{(m)}\delta\sigma_{ij} + \zeta\ \delta p_f, \tag{7.325}$$

where evidently V has the functional dependence $V(\sigma_{ij}, p_f)$, because upon taking the total derivative, we obtain

$$dV = \frac{\partial V}{\partial\sigma_{ij}} d\sigma_{ij} + \frac{\partial V}{\partial p_f} dp_f. \tag{7.326}$$

Comparing the last two equations, we can identify the strain-stress relations

$$\frac{\partial V}{\partial\sigma_{ij}} = \epsilon_{ij}^{(m)}, \qquad \frac{\partial V}{\partial p_f} = \zeta. \tag{7.327}$$

For linear stress-strain relations, we have

$$2V = \epsilon_{ij}^{(m)}\sigma_{ij} + \zeta\ p_f. \tag{7.328}$$

Similarly, under small variations of displacements $V = V(\epsilon_{ij}^{(m)}, \zeta)$ and

$$\delta V = \delta\epsilon_{ij}^{(m)}\sigma_{ij} + \delta\zeta\ p_f. \tag{7.329}$$

The stress-strain relations are

$$\sigma_{ij} = \partial V/\partial\epsilon_{ij}^{(m)}, \qquad p_f = \partial V/\partial\zeta. \tag{7.330}$$

These stress-strain relations, valid for non-uniform porosity, are given in equations (7.131) and (7.133); see Biot (1962) for an equivalent demonstration of equation (7.329) for small variations of displacements.

7.8.2 Volume-averaging method

We follow Pride and Berryman's approach (Pride and Berryman, 1998) to find the appropriate strain-energy density. Consider a volume $\Omega_b = \Omega_s + \Omega_f$ ($\Omega_s = \Omega_m$) of porous medium – $\Omega_p = \Omega_f$ for a fully saturated medium – and the weight function $W(\mathbf{r} - \mathbf{r}') = 1$

for $\mathbf{r}'$ inside Ω_b and $W(\mathbf{r}-\mathbf{r}')=0$ for $\mathbf{r}'$ outside Ω_b, where $\mathbf{r}$ is the position vector. The averages of a generic field ψ for points in the solid material and in the fluid are defined as

$$\bar{\psi}_s = \frac{1}{\Omega_s}\int_{\Omega_s} W(\mathbf{r}-\mathbf{r}')\psi_s d\Omega', \tag{7.331}$$

and

$$\bar{\psi}_f = \frac{1}{\Omega_f}\int_{\Omega_f} W(\mathbf{r}-\mathbf{r}')\psi_f d\Omega', \tag{7.332}$$

respectively. We define the microscopic stress tensor in the solid material by $\tau_{ij}^{(s)}$, and the microscopic fluid pressure by τ_f. The equilibrium conditions imply that the respective perturbations satisfy

$$\partial_j(\delta\tau_{ij}^{(s)}) = 0, \quad \text{and} \quad \partial_i(\delta\tau_f) = 0. \tag{7.333}$$

Then, $\delta\tau_f = \delta\bar{\tau}_f = \delta p_f$ in the fluid region. The region defined by Ω_b is bounded by surface S of which S_s corresponds to the solid material and S_f to the fluid part. Moreover, denote S_i as the solid material/fluid interface contained inside Ω_b. Since $\partial_i' r_j' = \delta_{ij}$ and $\delta\tau_{ij}^{(s)}(\mathbf{r})$ does not depend on $\mathbf{r}'$,

$$\partial_k'(\tau_{ki}^{(s)} r_j') = \tau_{ij}^{(s)}, \tag{7.334}$$

where, for brevity, we omit, hereafter, the increment symbol δ on the stresses. Integrating this quantity over the region Ω_s, we obtain

$$\frac{1}{\Omega_b}\int_{\Omega_s}\partial_k'(\tau_{ki}^{(s)} r_j')d\Omega' = \frac{1}{\Omega_b}\int_{\Omega_s}\tau_{ij}^{(s)}d\Omega' = (1-\phi)\bar{\tau}_{ij}^{(s)} \equiv (1-\phi)\,\sigma_{ij}^{(s)}, \tag{7.335}$$

because $\Omega_s = (1-\phi)\Omega_b$.

On the other hand, the same quantity can be expressed in terms of surface integrals by using Green's theorem,

$$\frac{1}{\Omega_b}\int_{\Omega_s}\partial_k'(\tau_{ki}^{(s)} r_j')d\Omega' = \frac{1}{\Omega_b}\int_{S_s} n_k^{(s)}\tau_{ki}^{(s)} r_j' dS' + \frac{1}{\Omega_b}\int_{S_i} n_k^{(s)}\tau_{ki}^{(s)} r_j' dS', \tag{7.336}$$

where $n_k^{(s)}$ is the outward unit vector normal to the surfaces S_s and S_i. Now, in S_i, we have the boundary condition $n_k^{(s)}\,\tau_{ki}^{(s)} = -\,p_f n_i^{(s)}$. Using this fact and equation (7.335), we get

$$(1-\phi)\sigma_{ij}^{(s)} = \frac{1}{\Omega_b}\int_{S_s} n_k^{(s)}\tau_{ki}^{(s)} r_j' dS' - \frac{p_f}{\Omega_b}\int_{S_i} n_i^{(s)} r_j' dS'. \tag{7.337}$$

The equivalent relation for the fluid is

$$-\phi p_f\delta_{ij} = -\frac{p_f}{\Omega_b}\int_{S_f} n_i^{(f)} r_j' dS' + \frac{p_f}{\Omega_b}\int_{S_i} n_i^{(s)} r_j' dS', \tag{7.338}$$

where we used the fact that $n_i^{(f)} = -n_i^{(s)}$ on S_i. Adding equations (7.337) and (7.338), we get the total average stress σ_{ij},

$$\sigma_{ij} \equiv (1-\phi)\sigma_{ij}^{(s)} - \phi p_f\delta_{ij} = \frac{1}{\Omega_b}\int_{S_s} n_k^{(s)}\tau_{ki}^{(s)} r_j' dS' - \frac{p_f}{\Omega_b}\int_{S_f} n_i^{(f)} r_j' dS'. \tag{7.339}$$

To obtain the macroscopic strain energy, we will consider the jacketed experiment, in which a porous sample is sealed in a very thin and flexible jacket and immersed in a reservoir providing a spatially uniform confining stress $\boldsymbol{\tau}^{(c)}$. As in the jacketed test illustrated in Figure 7.1, a small tube connects the interior of the sample with an external fluid reservoir at pressure p_f; Ω_b is the volume of the sample, $S = S_s + S_f$ is the external surface with S_s and S_f denoting the solid and fluid parts of the sample's exterior surface, and S_T is the surface of the small tube (S_f includes S_T). Because the cross-section of the tube is negligible compared to S, we may assume that $\boldsymbol{\tau}^{(c)}$ is equal to the macroscopic stress $\boldsymbol{\sigma}$. The variation of fluid content is the volume of fluid that enters (or leaves) the sample through the tube. Since the tube is moving with the jacket, the variation of fluid content is given by

$$\zeta = -\frac{1}{\Omega_b}\int_{S_T} n_i^{(T)} w_i^{(f)} dS', \tag{7.340}$$

where $n_i^{(T)}$ is the outward normal to the tube cross-section and $w_i^{(f)}$ is the microscopic fluid displacement[10]. Note that, in principle, the application of Green's theorem leads to the more familiar equation (7.22). However, the identification $\zeta = -\text{div}\ \mathbf{w}$, according to equations (7.22) and (7.172) requires certain conditions. Pride and Berryman (1998) demonstrate that equation (7.22) holds if the center of the grain distribution in the averaging volume coincides with the center of this volume. Biot (1956a) assumes that the surface porosity across an arbitrary cross-section of a sample and the volume porosity ϕ are the same. This assumption is almost equivalent to Pride and Berryman's condition. For highly heterogeneous or highly anisotropic materials, it is possible that the above relation needs to be modified and an additional parameter, modeling the surface porosity, should be introduced (Pride and Berryman, 1998).

The strain-tensor components of the frame are given by

$$E_{ij}^{(m)} = \frac{1}{\Omega_b}\int_S n_i^{(J)} w_j^{(J)} dS', \tag{7.341}$$

where $n_i^{(J)}$ is the outward normal to the jacket surface and $w_j^{(J)}$ is the microscopic displacement of the jacket surface. Note that

$$\epsilon_{ij}^{(m)} = \frac{1}{2\Omega_b}\int_S (n_i^{(J)} w_j^{(J)} + w_i^{(J)} n_j^{(J)}) dS'. \tag{7.342}$$

The strain-energy density is the sum of the average solid-material and fluid energy densities. We can express these densities by

$$2V_{\text{solid}} = \frac{1}{\Omega_b}\int_{\Omega_s} \tau_{ij}^{(s)} \partial_i' w_j^{(m)} d\Omega' \tag{7.343}$$

and

$$2V_{\text{fluid}} = -\frac{1}{\Omega_b}\int_{\Omega_f} \tau_f \partial_i' w_i^{(f)} d\Omega', \tag{7.344}$$

with

$$V = V_{\text{solid}} + V_{\text{fluid}}. \tag{7.345}$$

[10]This notation is consistent with that used in Section 7.4. The microscopic displacement $w_i^{(f)}$ should not be confused with the macroscopic displacement of the fluid relative to the solid, defined in (7.172).

Since the fluid pressure is uniform inside the jacket, this implies $\tau_f = p_f$, and using the boundary conditions $n_i^{(f)} w_i^{(f)} = -n_i^{(s)} w_i^{(m)}$ on S_i, we have

$$2V_{\text{fluid}} = -\frac{p_f}{\Omega_b}\left(\int_{S_f} n_i^{(f)} w_i^{(f)} dS' - \int_{S_i} n_i^{(s)} w_i^{(m)} dS'\right). \tag{7.346}$$

In the case of the solid, due to the equilibrium condition (7.333), $\tau_{ij}^{(s)} \partial_i' w_j^{(m)} = \partial_i'(\tau_{ij}^{(s)} w_i^{(m)})$ we have

$$2V_{\text{solid}} = \frac{1}{\Omega_b}\int_{S_s} n_i^{(s)} \tau_{ij}^{(s)} w_j^{(m)} dS' - \frac{p_f}{\Omega_b}\int_{S_i} n_i^{(s)} w_i^{(m)} dS', \tag{7.347}$$

where the boundary condition $n_i^{(s)} \tau_{ij}^{(s)} = -n_i^{(s)} p_f$ was used on S_i. Adding equations (7.346) and (7.347) gives

$$2V = \frac{1}{\Omega_b}\left(\int_{S_s} n_i^{(s)} \tau_{ij}^{(s)} w_j^{(m)} dS' - p_f \int_{S_f} n_i^{(f)} w_i^{(f)} dS'\right). \tag{7.348}$$

In light of the jacketed experiment, the second integral can be partitioned between an integral on the fluid surface plus an integral on the tube cross-section. Then, using equation (7.340), we have

$$2V = \frac{1}{\Omega_b}\left(\int_{S_s} n_i^{(s)} \tau_{ij}^{(s)} w_j^{(m)} dS' - p_f \int_{S_{fJ}} n_i^{(f)} w_i^{(f)} dS'\right) + \zeta\, p_f, \tag{7.349}$$

where S_{fJ} is the surface of fluid in contact with the jacket. The energy balance on the surface of the jacket implies that the first term of the right-hand side can be expressed as

$$\frac{1}{\Omega_b}\left(\int_{S_s} n_i^{(s)} \tau_{ij}^{(s)} w_j^{(m)} dS' - p_f \int_{S_{fJ}} n_i^{(f)} w_i^{(f)} dS'\right) = \frac{1}{\Omega_b}\int_S n_i^{(J)} \tau_{ij}^{(c)} w_j^{(J)} dS'$$

$$= \frac{\tau_{ij}^{(c)}}{\Omega_b}\int_S n_i^{(J)} w_j^{(J)} dS', \tag{7.350}$$

because $\tau_{ij}^{(c)}$ is spatially uniform. Using the fact that $\tau_{ij}^{(c)} = \sigma_{ij}$ and equation (7.341), we find that the strain energy (7.349) becomes

$$2V = E_{ij}^{(m)} \sigma_{ij} + \zeta\, p_f, \tag{7.351}$$

which can be conducted to equation (7.328) if we consider that the rotational part of the strain tensor $\mathbf{E}^{(m)}$, namely,

$$\frac{1}{2\Omega_b}\int_S (n_i^{(J)} w_j^{(J)} - w_i^{(J)} n_j^{(J)}) dS' \tag{7.352}$$

does not contribute to the work required to deform the sample, since no stress moments are applied.

7.9 Boundary conditions

The phenomena describing the reflection, refraction and diffraction of waves are related to the presence of inhomogeneities and interfaces. Knowledge of the corresponding boundary conditions is essential to correctly describe these phenomena. In fluid/fluid contacts in porous materials, we should expect fluid flow across the interface when a wave passes, and as we have mode conversion from P to S energy in single-phase media, we may expect mode conversion between the three waves propagating in a porous medium. In the developments that follow, we derive the appropriate boundary conditions for the different cases:

1. Porous medium/porous medium.
2. Porous medium/viscoelastic (single-phase) medium.
3. Porous medium/viscoacoustic medium (lossy fluid).
4. Free surface of a porous medium.

7.9.1 Interface between two porous media

We consider two different approaches used to derive the appropriate boundary conditions for an interface between two porous media. The first follows in part the demonstration of Deresiewicz and Skalak (1963) and the second is that developed by Gurevich and Schoenberg (1999), based on a method used to obtained the interface conditions in electromagnetism. The conditions, as given here, also hold for the anisotropic case.

Deresiewicz and Skalak's derivation

Let us consider a volume Ω_b of porous material bounded by surface S, and let us calculate the rate of change of the sum of the kinetic- and strain-energy densities, and dissipation potential; that is, $\partial_t T + \partial_t V + \Phi_D \equiv P$, where P is the power input. First, note that the substitution of equations (7.131) and (7.133) into equation (7.328) gives

$$2V = c^u_{ijkl}\epsilon^{(m)}_{ij}\epsilon^{(m)}_{kl} - 2M\alpha_{ij}\epsilon^{(m)}_{ij}\zeta + M\zeta^2, \tag{7.353}$$

and that

$$2\partial_t V = 2(c^u_{ijkl}\epsilon^{(m)}_{kl} - M\alpha_{ij}\zeta)\partial_t\epsilon^{(m)}_{ij} + 2M(\zeta - \alpha_{ij}\epsilon^{(m)}_{ij})\partial_t\zeta = 2(\sigma_{ij}\partial_t\epsilon^{(m)}_{ij} + p_f\ \partial_t\zeta), \tag{7.354}$$

where we have used $c^u_{ijkl} = c^u_{klij}$. Using these equations and the expressions for the kinetic and dissipated energies (7.175) and (7.197) (per unit volume) and integrating these energy densities on Ω_b, we obtain

$$P = \partial_t T + \partial_t V + \Phi_D = \int_{\Omega_b} [(\rho\partial_t v^{(m)}_i + \rho_f\partial^2_{tt}w_i)v^{(m)}_i$$

$$+(\rho_f\partial_t v^{(m)}_i + m_i\partial^2_{tt}w_i + (\eta/\bar{\kappa}_i)\partial_t w_i)\partial_t w_i + (\sigma_{ij}\partial_j v^{(m)}_i - p_f\partial_i\partial_t w_i)]d\Omega, \tag{7.355}$$

where we have used the relation $\sigma_{ij}\partial_t\epsilon_{ij}^{(m)} = \sigma_{ij}\partial_j v_i^{(m)}$. Since $\sigma_{ij}\partial_j v_i^{(m)} = \partial_j(\sigma_{ij}v_i^{(m)}) - \partial_j\sigma_{ij}v_i^{(m)}$ and $p_f\partial_i\partial_t w_i = \partial_i(p_f\partial_t w_i) - \partial_i p_f\partial_t w_i$, we apply the divergence theorem to the terms in the last parentheses on the right and get

$$P = \int_\Omega [(\rho\partial_t v_i^{(m)} + \rho_f\partial_{tt}^2 w_i - \partial_j\sigma_{ij})v_i^{(m)}$$

$$+(\rho_f\partial_t v_i^{(m)} + m_i\partial_{tt}^2 w_i + (\eta/\bar{\kappa}_i)\partial_t w_i + \partial_i p_f)\partial_t w_i]d\Omega + \int_S (\sigma_{ij}v_i^{(m)} - p_f\delta_{ij}\partial_t w_i)n_j dS, \quad (7.356)$$

where n_j are the components of the outer normal to S. In this equation, we can identify the differential equations of motion (7.255) and (7.256), such that the volume integral vanishes, and

$$P = \int_S (\sigma_{ij}v_i^{(m)} - p_f\delta_{ij}\partial_t w_i)n_j dS \quad (7.357)$$

quantifies the rate of work done on the material by the forces acting on its surface.

We now consider two different porous media in contact with volumes Ω_1 and Ω_2 and bounding surfaces S_1 and S_2, respectively, with a common boundary S_c, as shown in Figure 7.8. Let us define the power per unit area as

$$p_k = (\sigma_{ij}^{(k)}v_i^{(m)(k)} - p_f^{(k)}\delta_{ij}\partial_t w_i^{(k)})n_j^{(k)}, \quad k = 1, 2. \quad (7.358)$$

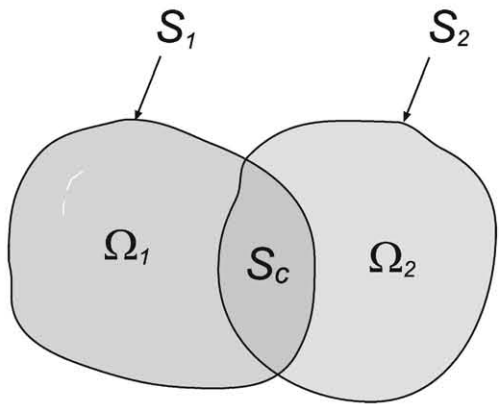

Figure 7.8: Two different porous media in contact with volumes Ω_1 and Ω_2 and bounding surfaces S_1 and S_2, respectively, with a common boundary S_c.

The respective power inputs are

$$P_1 = \int_{S_1} p_1 dS + \int_{S_c} p_1 dS, \qquad P_2 = \int_{S_2} p_2 dS + \int_{S_c} p_2 dS. \quad (7.359)$$

The power input of the combined system should satisfy

$$P = \int_{S_1} p_1 dS + \int_{S_2} p_2 dS. \quad (7.360)$$

Conservation of energy implies $P = P_1 + P_2$, and, therefore,

$$\int_{S_c} p_1 dS + \int_{S_c} p_2 dS = 0, \tag{7.361}$$

or, using the fact that in the common boundary $n_j^{(1)} = -n_j^{(2)} = n_j$,

$$\int_{S_c} [(\sigma_{ij}^{(1)} v_i^{(m)(1)} - p_f^{(1)} \delta_{ij} \partial_t w_i^{(1)}) - (\sigma_{ij}^{(2)} v_i^{(m)(2)} - p_f^{(2)} \delta_{ij} \partial_t w_i^{(2)})] n_j dS = 0, \tag{7.362}$$

which can be satisfied if we require the continuity across the interface of the power input per unit area, namely,

$$(\sigma_{ij} v_i^{(m)} - p_f \delta_{ij} \partial_t w_i) n_j. \tag{7.363}$$

This condition can be fulfilled by requiring the continuity of

$$v_i^{(m)}, \quad \partial_t w_i n_i, \quad \sigma_{ij} n_j, \quad p_f; \tag{7.364}$$

that is, eight boundary conditions.

The first condition requires that the two frames remain in contact at the interface. Note that continuity of $u_i^{(f)} n_i$ instead of $w_i n_i$ also guarantees the continuity of the power input per unit area. However, this is in contradiction with the conservation of fluid mass through the interface. The second condition (7.364) implies perfect fluid flow across the interface. If the interface is perpendicular to the z-axis, equation (7.364) implies continuity of

$$v_i^{(m)}, \quad \partial_t w_3, \quad \sigma_{i3}, \quad p_f. \tag{7.365}$$

If there is not perfect communication between the two media, fluid flow results in a pressure drop through the interface according to Darcy's law

$$p_f^{(2)} - p_f^{(1)} = \frac{1}{\bar{\kappa}_s} \partial_t w_i n_i, \tag{7.366}$$

where $\bar{\kappa}_s$ is the hydraulic permeability (per unit length) of the interface, or

$$p_f^{(2)} - p_f^{(1)} = \frac{1}{\bar{\kappa}_s} \partial_t w_3, \tag{7.367}$$

for $n_i = \delta_{i3}$.

The second condition (7.364) is obtained for $\bar{\kappa}_s \to \infty$. The choice $\bar{\kappa}_s = 0$ corresponds to a sealed interface ($\partial_t w_i n_i = 0$). A rigorous justification of equation (7.366) can be obtained by invoking Hamilton's principle (Bourbié, Coussy and Zinszner, 1987, p. 246).

Gurevich and Schoenberg's derivation

Gurevich and Schoenberg (1999) derive the boundary conditions directly from Biot's equation of poroelasticity by replacing the discontinuity surface with a thin transition layer – in which the properties of the medium change rapidly but continuously – and then taking the limit as the layer thickness tends to zero. The method considers the inhomogeneous equations of motion and assumes that the interface is described by a jump in the material properties of the porous medium. Let A be a point on the discontinuity surface, and

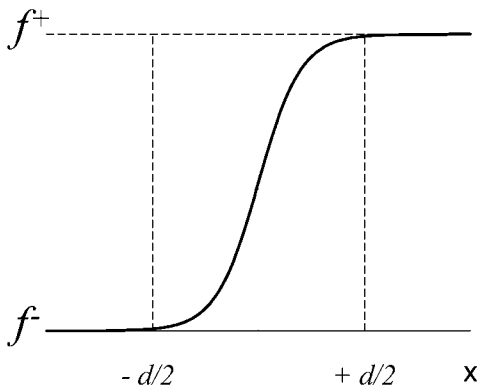

Figure 7.9: Transition zone at the interface between two porous media.

consider a Cartesian system with its origin at point A and its x-axis perpendicular to the discontinuity surface (Figure 7.9).

Following Feynman, Leighton and Sands (1964, p. 33-4 to 33-7), we substitute the discontinuity by a thin transition layer of thickness d, in which the material properties change rapidly but continuously. The thickness d is small enough to ensure that the derivatives with respect to x of the material properties are much larger than the derivatives with respect to y and z.

According to the arguments discussed in Section 7.8, Biot's differential equation for an inhomogeneous anisotropic poroelastic medium are given by equations (7.131), (7.133), (7.255) and (7.258). Denoting the particle velocities by $v_i^{(m)}$ and $\dot{w}_i = \partial_t w_i$, and using equations (7.172) and (7.173), the equations of motion can be expressed in a particle-velocity/stress form as

$$\begin{aligned} \partial_j \sigma_{ij} &= \rho \partial_t v_i^{(m)} + \rho_f \partial_t \dot{w}_i \\ -\partial_i p_f &= \rho_f \partial_t v_i^{(m)} + Y_i * \dot{w}_i \\ -\partial_i p_f &= M(\partial_i \dot{w}_i + \alpha_I \dot{e}_I^{(m)}) \\ \partial_t \sigma_I &= c_{IJ}^u \dot{e}_J^{(m)} + M \alpha_I \partial_i \dot{w}_i, \end{aligned} \tag{7.368}$$

where

$$\begin{aligned} \dot{e}_1^{(m)} &= \partial_1 v_1^{(m)} \\ \dot{e}_2^{(m)} &= \partial_2 v_2^{(m)} \\ \dot{e}_3^{(m)} &= \partial_3 v_3^{(m)} \\ \dot{e}_4^{(m)} &= \partial_2 v_3^{(m)} + \partial_3 v_2^{(m)} \\ \dot{e}_5^{(m)} &= \partial_1 v_3^{(m)} + \partial_3 v_1^{(m)} \\ \dot{e}_6^{(m)} &= \partial_1 v_2^{(m)} + \partial_2 v_1^{(m)}. \end{aligned} \tag{7.369}$$

We take the limit $d \to 0$ and neglect all the terms containing the derivatives ∂_2 and ∂_3.

We obtain the following eleven equations:

$$\begin{aligned}
&\partial_1\sigma_{1i} = \mathcal{O}(1), \quad i = 1,2,3,\\
&-\partial_1 p_f = \mathcal{O}(1),\\
&M\partial_1\dot{w}_1 + \alpha_1\partial_1 v_1^{(m)} + \alpha_5\partial_1 v_3^{(m)} + \alpha_6\partial_1 v_2^{(m)} = \mathcal{O}(1),\\
&c_{1I}\partial_1 v_1^{(m)} + c_{5I}\partial_1 v_3^{(m)} + c_{6I}\partial_1 v_2^{(m)} + M\alpha_I\partial_1\dot{w}_1 = \mathcal{O}(1), \quad I = 1,\ldots,6.
\end{aligned} \tag{7.370}$$

Equations $(7.370)_3$ and $(7.370)_4$ are satisfied if and only if

$$\partial_1 v_i^{(m)} = \mathcal{O}(1), \quad \partial_1\dot{w}_i = \mathcal{O}(1). \tag{7.371}$$

As indicated in Figure 7.9, the jump at the interface of a material property and field variable denoted by f is $f^+ - f^-$. Substituting each derivative $\partial_1 f$ by the corresponding finite-difference value $(f^+ - f^-)/d$, multiplying both sides of each of the equations $(7.370)_1$, $(7.370)_2$ and (7.371) by d, and taking the limit $d \to 0$, yields

$$\begin{aligned}
&\sigma_{i1}^+ - \sigma_{i1}^- = 0, \quad i = 1,2,3,\\
&p_f^+ - p_f^- = 0,\\
&v_i^{(m)^+} - v_i^{(m)^-} = 0, \quad i = 1,2,3,\\
&w_1^+ - w_1^- = 0;
\end{aligned} \tag{7.372}$$

that is, eight independent boundary conditions. These conditions are equivalent to the open-pore boundary conditions (7.364) of Deresiewicz and Skalak (1963). This means that Deresiewicz and Skalak's model of partially permeable contact when the pores of the two media do not match at the interface is highly unlikely to occur. A different interpretation is provided by Gurevich and Schoenberg (1999). They consider a thin poroelastic layer of thickness d with permeability proportional to d, and open-pore boundary conditions at both sides of the layer. They show that the boundary condition (7.366) holds for low frequencies, but for high frequencies the hydraulic permeability $\bar{\kappa}_s$ should be frequency dependent. The solution of the reflection-transmission problem of plane waves for this boundary condition is given by Deresiewicz and Rice (1964), Dutta and Odé (1983), Santos, Corberó, Ravazzoli and Hensley (1992), Denneman, Drijkoningen, and Wapenaar (2002) and Sharma (2004).

de la Cruz and Spanos (1989) obtain an alternative set of boundary conditions, based on volume-average arguments. They interpret the contact between the porous media as a transition region. An interesting discussion regarding these boundary conditions and those of Deresiewicz and Skalak (1963) is provided by Gurevich (1993).

7.9.2 Interface between a porous medium and a viscoelastic medium

In this case, the viscoelastic medium, say, medium 2, is impermeable ($\partial_t w_3 = 0$), and its porosity should be set equal to zero. These conditions require

$$\partial_t w_3^{(1)} = 0, \quad \text{or} \quad v_3^{(m)(1)} = v_3^{(f)(1)} \tag{7.373}$$

and the continuity of

$$v_i^{(m)}, \quad \sigma_{i3}, \qquad i = 1,2,3. \tag{7.374}$$

The solution of the reflection-transmission problem of plane waves for this boundary condition is given by Sharma, Kaushik and Gogna (1990).

7.9.3 Interface between a porous medium and a viscoacoustic medium

The viscoacoustic medium, say, medium 2, is a fluid, and therefore has porosity equal to 1. Hence there is free flow across the interface ($\bar{\kappa}_s = \infty$), and the filtration velocity of the fluid is $\partial_t w_i^{(2)} = v_i^{(2)} - v_i^{(m)(1)}$. This requires

$$\phi_1(v_3^{(f)(1)} - v_3^{(m)(1)}) = v_3^{(2)} - v_3^{(m)(1)}, \quad p_f^{(1)} = p_f^{(2)}, \quad \sigma_{33}^{(1)} = -p_f^{(2)}, \quad \sigma_{13}^{(1)} = \sigma_{23}^{(1)} = 0. \tag{7.375}$$

An example is given in Santos, Corberó, Ravazzoli and Hensley (1992).

7.9.4 Free surface of a porous medium

There are no constraints on the displacements since the medium is free to move. For this reason, the stress components and pore pressure vanish. The natural conditions are

$$\sigma_{33}^{(1)} = \sigma_{13}^{(1)} = \sigma_{23}^{(1)} = 0, \quad p_f^{(1)} = 0. \tag{7.376}$$

The solution of the reflection-transmission problem of plane waves for this boundary condition is given by Deresiewicz and Rice (1962).

7.10 The mesoscopic loss mechanism. White model

A major cause of attenuation in porous media is wave-induced fluid flow, which occurs at different spatial scales. The flow can be classified as macroscopic, mesoscopic and microscopic. The attenuation mechanism predicted by Biot's theory has a macroscopic nature. It is the wavelength-scale equilibration between the peaks and troughts of the P wave. Geertsma and Smit (1961) showed that the dissipation factor $1/Q$ of the fast P wave, obtained as $\mathrm{Im}(v_c^2)/\mathrm{Re}(v_c^2)$ in analogy with viscoelasticity (see equation (3.128)), can be approximated by that of a Zener model for $Q \gtrsim 5$. They obtain the expression (2.175):

$$Q^{-1}(\omega) = \frac{\omega(\tau_\epsilon - \tau_\sigma)}{1 + \omega^2 \tau_\epsilon \tau_\sigma}, \qquad \tau_\sigma = \left(\frac{v_G}{v_{\infty+}}\right)^2 \tau_\epsilon, \qquad \tau_\epsilon = \frac{\mathcal{X}\bar{\kappa}\rho}{\eta}, \tag{7.377}$$

where $v_{\infty+}$ is the P-wave velocity at the high-frequency limit (see equation (7.292)), v_G is given by equation (7.286) and $\mathcal{X} = \rho_f \mathcal{T}/(\rho\phi) - (\rho_f/\rho)^2$. We have seen in Section 2.4.3 that the location of the Zener relaxation peak is $\omega_B = 1/\sqrt{\tau_\sigma \tau_\epsilon}$ (see equation (2.176)). Then, $f_B = \omega_B/2\pi$ and using (7.377) we get

$$f_B = \left(\frac{v_{\infty+}}{v_G}\right) \frac{\eta}{2\pi \mathcal{X} \bar{\kappa} \rho} \approx \frac{\eta}{2\pi \mathcal{X} \bar{\kappa} \rho} = \frac{\phi \eta \rho}{2\pi \bar{\kappa} \rho_f (\rho \mathcal{T} - \phi \rho_f)}. \tag{7.378}$$

This equation shows that the relaxation peak moves towards the high frequencies with increasing viscosity and decreasing permeability. This means that, at low frequencies, attenuation decreases with increasing viscosity (or decreasing permeability). This is in contradiction with experimental data (e.g., Jones, 1986). Another apparent drawback of Biot's theory is that the macroscopic-flow mechanism underestimates the velocity dispersion and attenuation in rocks (e.g., Mochizuki, 1982; Dvorkin, Mavko and Nur, 1995; Arntsen and Carcione, 2001).

It is common to invoke "non-Biot" attenuation mechanisms to explain low-frequency (seismic and sonic) attenuation in rocks. These mechanisms are the so-called local fluid flow, or "squirt" flow absorption mechanisms, which have been extensively discussed in the literature (O'Connell and Budiansky, 1974; Dvorkin, Mavko and Nur, 1995; Mavko, Mukerji and Dvorkin, 1998). In this mechanism, fluid-filled microcracks respond with greater fluid-pressure changes than the main pore space. The resulting flow at this microscopic level is the responsible for the energy loss. These models have the proper dependence on viscosity with the center frequency of the attenuation peak inversely proportional to fluid viscosity. However, it has been shown that this mechanism is incapable of describing the measured levels of dissipation at seismic frequencies (Diallo, Prasad and Appel, 2003). Pride, Berryman and Harris (2004) have shown that attenuation and velocity dispersion measurements can be explained by the combined effect of mesoscopic-scale inhomogeneities and energy transfer between wave modes. We refer to this mechanism as mesoscopic loss. The mesoscopic-scale length is intended to be much larger than the grain sizes but much smaller than the wavelength of the pulse. For instance, if the fluid compressibility varies significantly from point to point, diffusion of pore fluid between different regions constitutes a mechanism that can be important at seismic frequencies. White (1975) and White, Mikhaylova and Lyakhovitskiy (1975) were the first to introduce the mesoscopic loss mechanism based on approximations in the framework of Biot's theory. They considered gas pockets in a water-saturated porous medium and porous layers alternately saturated with water and gas, respectively. These are the first so-called "patchy saturation" models. Dutta and Odé (1979a,b) and Dutta and Seriff (1979) solved the problem exactly by using Biot's theory and confirmed the accuracy of White's results.[11]

To illustrate the mesoscopic loss mechanism, we compute the P-wave complex modulus of a layered medium in the direction perpendicular to the layering. We follow the demonstration by White (1975) and White, Mikhaylova and Lyakhovitskiy (1975) and, in this case, the result is exact.

Figure 7.10 shows alternating layers composed of two fluid-saturated porous media, where, by symmetry, the elementary volume is enclosed by no-flow boundaries. In order to obtain the P-wave complex modulus, we apply a tension $\sigma_0 \exp(\mathrm{i}\omega t)$ on the top and bottom of the elementary volume and compute the resulting strain $\epsilon \exp(\mathrm{i}\omega t)$. Then, the complex modulus is given by the ratio

$$\mathcal{E} = \frac{\sigma_0}{\epsilon}. \tag{7.379}$$

The strain ϵ is obtained in two steps by computing the strains ϵ_0 and ϵ_f without and with fluid flow across the interfaces separating the two media.

If there is no fluid flow, the strain is

$$\epsilon_0 = \frac{\sigma_0}{\mathcal{E}_0}, \tag{7.380}$$

where the composite modulus is given by equation $(1.179)_4$ as

$$\mathcal{E}_0 = \left(\frac{p_1}{E_{G_1}} + \frac{p_2}{E_{G_2}} \right)^{-1}, \tag{7.381}$$

[11] Dutta and Seriff (1979) point out a mistake in White (1975), where White uses the P-wave modulus instead of the bulk modulus to derive the complex bulk modulus.

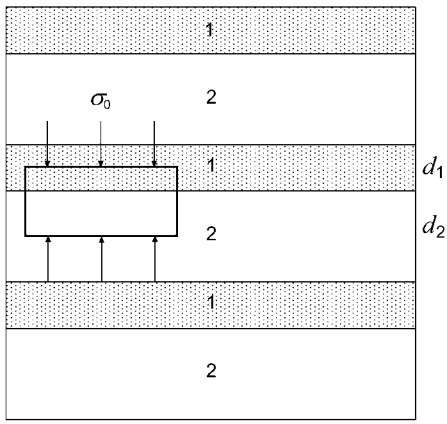

Figure 7.10: Alternating layers composed of two fluid-saturated porous media.

(see also equation $(1.188)_2$), with $p_l = d_l/(d_1 + d_2)$, $l = 1, 2$,

$$E_{G_l} = K_{G_l} + \frac{4}{3}\mu_{m_l}, \quad l = 1, 2, \tag{7.382}$$

where K_{G_l} are the Gassmann moduli of the porous media (equation (7.34)) and μ_{m_l} are the respective dry-rock shear moduli.

The displacements in the x- and y-directions are zero under the application of the normal stress σ_0, and $\epsilon_{11}^{(m)} = \epsilon_{22}^{(m)} = 0$. Moreover, at low frequencies, fluid and solid move together and $\zeta = 0$ in equation (7.33). Under these conditions and using equation (1.15) we have at each medium

$$\sigma_0 = \left(K_G + \frac{4}{3}\mu_m\right)\epsilon_{33}^{(m)} = E_G\epsilon_{33}^{(m)}. \tag{7.383}$$

On the other hand, equation (7.32) implies $-p_f = \alpha M\theta_m = \alpha M\epsilon_{33}^{(m)}$, which combined with (7.383) gives

$$\frac{-p_f}{\sigma_0} = \frac{\alpha M}{E_G} \equiv r, \tag{7.384}$$

where M and α are given by equations (7.24) and (7.25), respectively. Then, for each medium, it is

$$-p_{f_l}^{+} = r_l\sigma_0, \quad l = 1, 2, \tag{7.385}$$

where the plus sign indicates that the fluid pressure is that of the fast compressional wave. According to this equation, there is a fluid-pressure difference at the interfaces, and this difference generates fluid flow and slow (diffusion) waves traveling into each medium. As fluid flows, the matrix expands in the z-direction and $\sigma_{33} = 0$. In this case, ζ does not vanish and equation (7.33) implies

$$0 = E_G\epsilon_{33}^{(m)} - \alpha M\zeta. \tag{7.386}$$

Combining this equation with (7.32) gives the effective bulk modulus

$$\frac{p_f}{\zeta} = M\left(1 - \frac{\alpha^2 M}{E_G}\right) = \frac{ME_m}{E_G} \equiv K_E, \tag{7.387}$$

where we have used equations (7.34) and (7.291). Another result from equation (7.386) is the expansion coefficient

$$\frac{\epsilon_{33}^{(m)}}{\zeta} = \frac{\alpha M}{E_G} = r. \tag{7.388}$$

At low frequencies, when the acceleration terms can be neglected, equations (7.213) and (7.214) give Darcy's law

$$\dot{w}_3 = -\frac{\bar{\kappa}}{\eta}\partial_3 p_f, \quad \text{or} \quad \partial_3 \dot{w}_3 = -\frac{\bar{\kappa}}{\eta}\partial_3^2 p_f. \tag{7.389}$$

On the other hand, equations (7.173), (7.174) and (7.387) imply

$$\partial_3 \dot{w}_3 = -\frac{1}{K_E}\partial_t p_f. \tag{7.390}$$

The two preceding equations yield

$$\partial_3^2 p_f = -\frac{\eta}{\bar{\kappa} K_E}\partial_t p_f. \tag{7.391}$$

The solution is

$$p_f = [A\exp(az) + B\exp(-az)]\exp(\mathrm{i}\omega t), \tag{7.392}$$

where

$$a^2 = \frac{\mathrm{i}\omega\eta}{\bar{\kappa} K_E}, \tag{7.393}$$

and, from equation (7.389),

$$\dot{w}_3 = -\frac{\bar{\kappa} a}{\eta}[A\exp(az) - B\exp(-az)]\exp(\mathrm{i}\omega t). \tag{7.394}$$

Since, by symmetry, there is no fluid flow across the center of any layer, $\dot{w}_3 = 0$ at $z = d_1/2$ ($z = -d_2/2$) requires that $B = A\exp(ad_1)$ ($B = A\exp(-ad_2)$). Then, the relation between the fluid pressure p_f (equation (7.392)) and the filtration velocity $\dot{w}_3$ (equation (7.394)) at $z = 0$ is

$$p_{f_1}^- = I_1 \dot{w}_3)_1, \quad \text{and} \quad p_{f_2}^- = -I_2 \dot{w}_3)_2, \tag{7.395}$$

where

$$I_l = \frac{\eta_l}{\bar{\kappa}_l a_l}\coth\left(\frac{a_l d_l}{2}\right), \quad l = 1, 2, \tag{7.396}$$

are the impedances looking into medium 1 and medium 2 from the interface (with a_l given by (7.393)), and the superscript minus sign indicates that the fluid pressure corresponds to the diffusive mode.

According to equation (7.385), there is a fluid-pressure difference between the porous media, but the total pressure $p_f^+ + p_f^-$ and $\dot{w}_3$ should be continuous at the interface.

Continuity of pore pressure is achieved by the generation of a slow P wave which diffuses away from the interface. These conditions, together with equations (7.385) and (7.395), imply that the fluid particle velocity at the interface is

$$v \equiv \dot{w}_3 = \left(\frac{r_2 - r_1}{I_1 + I_2}\right)\sigma_0, \qquad r_l = \frac{\alpha_l M_l}{E_{Gl}}, \quad l = 1, 2. \tag{7.397}$$

As fluid flows out of medium 1, for instance, the thickness of layer 1 decreases while that of medium 2 increases. According to equation (7.388), the matrix displacement due to the fluid flow is $u_3^{(m)} = -r[\dot{w}_3/(\mathrm{i}\omega)]$. Therefore, the displacement fields related to this "unloading" and "loading" motions are

$$u_1 \equiv u_3^{(m)})_1 = -\frac{r_1 v}{\mathrm{i}\omega} \quad \text{and} \quad u_2 \equiv u_3^{(m)})_2 = \frac{r_2 v}{\mathrm{i}\omega}, \tag{7.398}$$

respectively. The sum of the displacements divided by the thickness of the elementary volume is the strain due to the fluid flow

$$\epsilon_f = 2\left(\frac{u_1 + u_2}{d_1 + d_2}\right) = \frac{2(r_2 - r_1)^2\sigma_0}{\mathrm{i}\omega(d_1 + d_2)(I_1 + I_2)}, \tag{7.399}$$

where we have used equations (7.385), (7.397) and (7.398). The total strain is $\epsilon = \epsilon_0 + \epsilon_f$ and equations (7.379), (7.380) and (7.399) yield the P-wave complex modulus

$$\mathcal{E} = \left[\frac{1}{\mathcal{E}_0} + \frac{2(r_2 - r_1)^2}{\mathrm{i}\omega(d_1 + d_2)(I_1 + I_2)}\right]^{-1}. \tag{7.400}$$

The approximate transition frequency separating the relaxed and unrelaxed states (i.e., the approximate location of the relaxation peak) is

$$f_m = \frac{8\bar{\kappa}_1 K_{E1}}{\pi\eta_1 d_1^2} \tag{7.401}$$

(Dutta and Seriff, 1979), where the subindex 1 refers to water for a layered medium alternately saturated with water and gas. At this reference frequency, the Biot slow-wave attenuation length equals the mean layer thickness or characteristic length of the inhomogeneities (Gurevich and Lopatnikov, 1995) (see next paragraph). Equation (7.401) indicates that the mesoscopic loss mechanism moves towards the low frequencies with increasing viscosity and decreasing permeability, i.e., the opposite behaviour of the Biot relaxation mechanism whose peak frequency is given by equation (7.378).

The mesoscopic loss mechanism is due to the presence of the Biot slow wave and the diffusivity constant is $d = \bar{\kappa}K_E/\eta$, according to equation (7.391). Note that the same result has been obtained in Section 7.7.1 (equation 7.300)). The critical fluid-diffusion relaxation length L is obtained by setting $|az| = |aL| = 1$ in equation (7.394). It gives $L = \sqrt{d/\omega}$. The fluid pressures will be equilibrated if L is comparable to the period of the stratification. For smaller diffusion lengths (e.g., higher frequencies) the pressures will not be equilibrated, causing attenuation and velocity dispersion. Notice that the reference frequency (7.401) is obtained when for a diffusion length $L = d_1/4$.

Let us assume that the properties of the frame are the same in media 1 and 2. At enough low frequencies, the fluid pressure is uniform (isostress state) and the effective modulus of the pore fluid is given by Wood's equation (Wood, 1955):

$$\frac{1}{K_f} = \frac{p_1}{K_{f_1}} + \frac{p_2}{K_{f_2}}. \tag{7.402}$$

It can be shown (e.g., Johnson, 2001) that $\mathcal{E}(\omega = 0)$ is equal to Gassmann's modulus (7.34) for a fluid whose modulus is K_f. On the other hand, at high frequencies, the pressure is not uniform but can be assumed to be constant within each phase. In such a situation Hill's theorem (Hill, 1964) gives the high-frequency limit $\mathcal{E}(\omega = \infty) = \mathcal{E}_0$. As an example, Figure 7.11 shows the phase velocity and dissipation factor as a function of frequency for a finely layered medium saturated with water and gas.

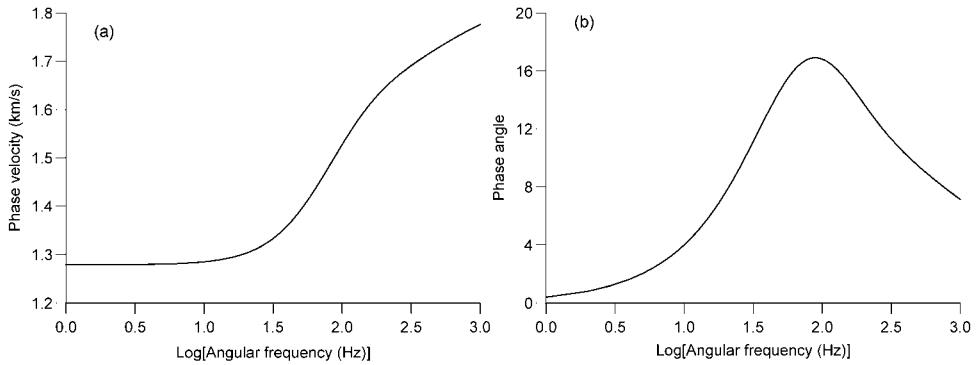

Figure 7.11: Phase velocity (a) and dissipation factor (b) as a function of frequency for a finely layered medium saturated with water and gas. The frame is the same for media 1 and 2, with $\phi = 0.3$, $K_m = 1.3$ GPa, $\mu_m = 1.4$ GPa and $\bar{\kappa} = 1$ Darcy; the grain properties are $K_s = 33.4$ GPa and $\rho_s = 2650$ Kg/m^3; the fluid properties are $K_{f_1} = 2.2$ GPa, $\rho_{f_1} = 975$ Kg/m^3, $\eta_1 = 1$ cP, $K_{f_2} = 0.0096$ GPa, $\rho_{f_2} = 70$ Kg/m^3 and $\eta_2 = 0.15$ cP. The gas saturation is $S_g = p_2 = 0.1$ and the period of the stratification is $d_1 + d_2 = 0.4$ m (White, Mikhaylova and Lyakhovitskiy, 1975).

The mesoscopic loss theory have been further refined by Norris (1993), Gurevich and Lopatnikov (1995), Gelinsky and Shapiro (1997), Johnson (2001), Pride, Berryman and Harris (2004) and Müller and Gurevich (2005). Johnson (2001) developed a generalization of White model for patches of arbitrary shape. This model has two geometrical parameters, besides the usual parameters of Biot's theory: the specific surface area and the size of the patches. Patchy saturation effects on acoustic properties have been observed by Murphy (1982), Knight and Nolen-Hoeksema (1990) and King, Marsden, and Dennis (2000). Cadoret, Marion and Zinszner (1995) investigated the phenomenon in the laboratory at the frequency range 1-500 kHz. Two different saturation methods result in different fluid distributions and give two different values of velocity for the same saturation. Imbibition by depressurization produces a very homogeneous saturation, while drainage by drying produces heterogeneous saturations at high water saturation levels. In the latter case, the experiments show considerably higher velocities, as predicted by White model.

Carcione, Helle and Pham (2003) performed numerical-modeling experiments based on Biot's equations of poroelasticity (Carcione and Helle, 1999) and White model of regularly distributed spherical gas inclusions. They showed that attenuation and velocity dispersion measurements can be explained by the combined effect of mesoscopic-scale inhomogeneities and energy transfer between wave modes. By using computerized tomography (CT) scans it is possible to visualize the fluid distribution and spatial heterogeneities in real rocks (Cadoret, Marion and Zinszner, 1995). Fractal models, such as the von Kármán correlation function, calibrated by the CT scans, were used by Helle, Pham and Carcione (2003) to model heterogeneous rock properties and perform numerical experiments based on Biot's equations of poroelasticity. These simulations show that Biot's theory gives correct attenuation levels when using heterogeneous models.

The mesoscopic loss mechanism indicates that information about the permeability of the rock – an important properties in hydrocarbon exploration –, is present in the seismic amplitudes (the diffusion length is proportional to $\sqrt{\bar{\kappa}}$). Therefore, measurements of the quality factor at low (seismic) frequencies may provide useful information about the structure of the host reservoir rock.

7.11 Green's function for poro-viscoacoustic media

Green's functions for poroelastic media are studied by several authors: Deresiewicz and Rice (1962), Burridge and Vargas (1979), Norris (1985, 1994), Boutin, Bonnet and Bard (1987), Pride and Haartsen (1996) and Sahay (1999). Boutin, Bonnet and Bard apply the theory of Auriault, Borne and Chambon (1985) and compute semi-analytical transient solutions in a stratified medium. Bonnet (1987) obtains a solution by applying the analogy between the poroelastic and thermoelastic equations (Norris, 1994), and Kazi-Aoual, Bonnet and Jouanna (1988) extend the solution of Boutin, Bonnet and Bard (1987) to the transversely isotropic case.

Here, we obtain an analytical transient solution for propagation of compressional waves in a homogeneous porous dissipative medium. The solution, based on a generalization of Biot's poroelastic equations, holds for the low- and high-frequency ranges, and includes viscoelastic phenomena of a general nature, besides Biot's relaxation mechanism. We consider the poroacoustic version of Biot's equations, i.e., with the rigidity of the matrix equal to zero[12]. These equations may describe wave motion in a colloid that can be considered either an emulsion or a gel. On one hand, it is an emulsion since shear waves do not propagate. On the other hand, since the "frame" modulus is different from zero, the "solid" component provides a sufficient structural framework for rigidity, and, therefore, can be considered as a gel.

7.11.1 Field equations

The poro-viscoacoustic model is dilatational, which implies no shear deformations. No shear deformations are obtained by setting $\mu_m = 0$ in equation (7.19). Moreover, using equations (7.22) and (7.32), we can write the stress-strain relations as

$$-p = H\vartheta_m - C\zeta, \tag{7.403}$$

[12]In principle, this medium is an idealization since the bulk modulus should also vanish in this case.

and

$$p_f = -\underline{C}\vartheta_m + M\zeta, \tag{7.404}$$

where $p = -\sigma_{ii}/3$ is the bulk pressure, $H = K + R + 2C$ and $\underline{C} = \alpha M$, with K, R and M defined in equations (7.16), (7.18) and (7.24), respectively. Equations (7.403) and (7.404) can be seen as the stress-strain relation in the frequency domain. Thus, invoking the correspondence principle (see Section 3.6), the stiffnesses become complex and depend on the angular frequency ω. Let us assume that H, $\underline{C}$ and M are appropriate complex moduli describing viscoelastic behavior, such that the expressions given in equations (7.16), (7.18) and (7.24) correspond to the high-frequency (lossless) limit

It is convenient to express equations (7.403) and (7.404) in matrix form as

$$\begin{pmatrix} p \\ p_f \end{pmatrix} = \begin{pmatrix} -H & \underline{C} \\ -\underline{C} & M \end{pmatrix} \cdot \begin{pmatrix} \vartheta_m \\ \zeta \end{pmatrix} \tag{7.405}$$

or, in compact notation,

$$\underline{\mathbf{p}} = \underline{\mathbf{P}} \cdot \underline{\mathbf{e}}, \tag{7.406}$$

where $\underline{\mathbf{P}}$ is the complex stiffness matrix.

The dynamical equations (7.210) and (7.213), restricted to the viscoacoustic case and considering a general viscodynamic operator Y, are

$$-\nabla(p - s_b) = \rho\partial_{tt}^2\mathbf{u}^{(m)} + \rho_f\partial_{tt}^2\mathbf{w} \tag{7.407}$$

and

$$-\nabla(p_f - s_f) = \rho_f\partial_{tt}^2\mathbf{u}^{(m)} + Y * \partial_t\mathbf{w}, \tag{7.408}$$

where $\mathbf{u}^{(m)}$ is the average displacement of the solid, and $\mathbf{w}$ is the average displacement of the fluid relative to the solid (7.172). The quantities s_b and s_f are body forces acting on the bulk material and on the fluid phase, respectively.

For harmonic oscillations, equations (7.407) and (7.408) can alternatively be written as

$$\nabla(\underline{\mathbf{p}} - \underline{\mathbf{s}}) = -\omega^2\underline{\mathbf{\Gamma}} \cdot \begin{pmatrix} \mathbf{u}^{(m)} \\ -\mathbf{w} \end{pmatrix}, \tag{7.409}$$

where

$$\underline{\mathbf{s}} = (s_b,\ s_f) \tag{7.410}$$

and

$$\underline{\mathbf{\Gamma}} \equiv \begin{pmatrix} -\rho & \rho_f \\ -\rho_f & \tilde{Y}/\mathrm{i}\omega \end{pmatrix} \tag{7.411}$$

is the viscodynamic matrix, and $\tilde{Y}$ is the Fourier transform of Y.

7.11.2 The solution

Taking the divergence in equation (7.409) and assuming a homogeneous medium, we can write

$$\Delta(\underline{\mathbf{p}} - \underline{\mathbf{s}}) = -\omega^2\underline{\mathbf{\Gamma}} \cdot \underline{\mathbf{e}}, \tag{7.412}$$

where

$$\underline{\mathbf{e}} = \begin{pmatrix} \vartheta_m \\ \zeta \end{pmatrix} = \mathrm{div} \begin{pmatrix} \mathbf{u}^{(m)} \\ -\mathbf{w} \end{pmatrix}, \tag{7.413}$$

and Δ is the Laplacian operator. Substituting the constitutive law (7.406), we have that equation (7.412) becomes

$$\Delta(\underline{\mathbf{p}} - \underline{\mathbf{s}}) + \omega^2 \underline{\mathbf{D}} \cdot \underline{\mathbf{p}} = \mathbf{0}, \tag{7.414}$$

where

$$\underline{\mathbf{D}} = \boldsymbol{\Gamma} \cdot \underline{\mathbf{P}}^{-1}. \tag{7.415}$$

Note that $\underline{\mathbf{D}}$ is a complex function of the frequency and does not depend on the position vector since the medium is homogeneous. This matrix may be decomposed as $\underline{\mathbf{D}} = \mathbf{A} \cdot \boldsymbol{\Lambda} \cdot \mathbf{A}^{-1}$, where $\boldsymbol{\Lambda}$ is the diagonal matrix of the eigenvalues, and $\mathbf{A}$ is a matrix whose columns are the right eigenvectors. Thus, substituting this decomposition into equation (7.414) and multiplying by $\mathbf{A}^{-1}$ from the left-hand side, we get

$$\Delta(\underline{\mathbf{v}} - \mathbf{f}) + \omega^2 \boldsymbol{\Lambda} \cdot \underline{\mathbf{v}} = \mathbf{0}, \tag{7.416}$$

where

$$\underline{\mathbf{v}} = (v_1, v_2) = \mathbf{A}^{-1} \cdot \underline{\mathbf{p}}, \tag{7.417}$$

and

$$\mathbf{f} = (f_1, f_2) = \mathbf{A}^{-1} \cdot \underline{\mathbf{s}}. \tag{7.418}$$

From (7.416), we get the following Helmholtz equations for the components of $\underline{\mathbf{v}}$:

$$(\Delta + \omega^2 \lambda_\nu) v_\nu = \Delta f_\nu, \quad \nu = 1, 2, \tag{7.419}$$

where λ_1 and λ_2 are the eigenvalues of $\underline{\mathbf{D}}$. They are related to the complex velocities of the fast and slow compressional waves. In fact, let us assume that a solution to equation (7.414) is of the form

$$\underline{\mathbf{p}} = \underline{\mathbf{p}}_0 \exp(-\mathrm{i}\mathbf{k} \cdot \mathbf{x}), \tag{7.420}$$

where $\mathbf{x}$ is the position vector and $\mathbf{k}$ is the complex wavevector. Putting this solution into equation (7.414) with zero body forces, and setting the determinant to zero, we obtain the dispersion relation

$$\det \left[\underline{\mathbf{D}} - \left(\frac{k}{\omega} \right)^2 \mathbf{I}_2 \right] = 0. \tag{7.421}$$

Since $\omega/k = v_c$ is the complex velocity, the eigenvalues of $\underline{\mathbf{D}}$ are $\lambda = 1/v_c^2$. Because $\underline{\mathbf{D}}$ is a second-rank matrix, two modes, corresponding to the fast and slow waves, propagate in the medium. A simplified expression for the eigenvalues is

$$\lambda_{1(2)} = \frac{1}{2 \det \underline{\mathbf{P}}} \left(U \pm \sqrt{U^2 - 4 \det \underline{\mathbf{P}} \det \boldsymbol{\Gamma}} \right), \tag{7.422}$$

where

$$U = 2\rho_f \underline{C} - \rho M - H(\tilde{Y}/\mathrm{i}\omega). \tag{7.423}$$

The phase velocities (7.288) calculated with the solutions (7.422) correspond to the solution of equations (7.287) with $\mu_m = 0$, and equation (7.290) if, in addition, $\eta = 0$.

Considering that the solution for the Green function (i.e., the right-hand side of (7.419)) is a space delta function at, say, the origin, both equations have the form

$$(\Delta + \omega^2 \lambda) g = -8\delta(\mathbf{x}), \tag{7.424}$$

where δ is Dirac's function. The 2-D solution (line source) of equation (7.424) is

$$g(r,\omega) = -2\mathrm{i}H_0^{(2)}\left[\omega r\sqrt{\lambda(\omega)}\right] \tag{7.425}$$

(Pilant, 1979, p. 55), where $H_0^{(2)}$ is the Hankel function of the second kind, and

$$r = \sqrt{x^2 + z^2}. \tag{7.426}$$

The 3-D solution (point source) of (7.424) is

$$g(r,\omega) = \frac{2}{\pi r}\exp\left[-\mathrm{i}\omega r\sqrt{\lambda(\omega)}\right] \tag{7.427}$$

(Pilant, 1979, p. 64), where

$$r = \sqrt{x^2 + y^2 + z^2}. \tag{7.428}$$

The solutions (7.425) and (7.427) as given by Pilant (1979) hold only for real arguments. However, by invoking the correspondence principle (Section 3.6), complex, frequency-dependent material properties can be considered. For instance, the poroelastic equations without the Biot mechanism (i.e, $\eta = 0$) have a real $\underline{\mathbf{D}}$ matrix, whose eigenvalues are also real – the velocities are real and frequency independent, without dispersion effects. The introduction of the Biot mechanism, via the correspondence principle, implies the substitution $m \to -\tilde{Y}(\omega)/\mathrm{i}\omega$. In the same way, viscoelastic phenomena of a more general nature can be modeled.

The solution of equation (7.419), with the band-limited sources f_1 and f_2, is then

$$v_\nu = \hat{f}_\nu \Delta g(\lambda_\nu) = \hat{f}_\nu G(\lambda_\nu), \tag{7.429}$$

where

$$G(\lambda_\nu) = -[\omega^2 \lambda_\nu g(\lambda_\nu) + 8\delta(\mathbf{x})], \tag{7.430}$$

and equation (7.424) has been used. In equation (7.429), we introduced the source vector

$$\hat{\mathbf{f}} = (\hat{f}_1, \hat{f}_2) = \mathbf{A}^{-1} \cdot \underline{\hat{\mathbf{s}}}\; h(\omega), \tag{7.431}$$

where

$$\underline{\hat{\mathbf{s}}} = (\hat{s}_b, \hat{s}_f) \tag{7.432}$$

is a constant vector and $h(\omega)$ is the frequency spectrum of the source.

The vector $\underline{\mathbf{p}}$ is obtained from equation (7.417) and written as

$$\underline{\mathbf{p}}(r,\omega) = \mathbf{A}(\omega)\underline{\mathbf{v}}(r,\omega). \tag{7.433}$$

From the form of v_1 and v_2 in equation (7.429) and using (7.431), we can explicitly write the solution as

$$\underline{\mathbf{p}} = \mathbf{A} \cdot \begin{pmatrix} G(\lambda_1) & 0 \\ 0 & G(\lambda_2) \end{pmatrix} \cdot \mathbf{A}^{-1}\underline{\hat{\mathbf{s}}}\; h. \tag{7.434}$$

Using $\underline{\mathbf{D}} = \mathbf{A} \cdot \mathbf{\Lambda} \cdot \mathbf{A}^{-1}$, and from the theory of functions of matrices (Lancaster and Tismenetsky, 1985, p. 311), equation (7.434) becomes

$$\underline{\mathbf{p}} = G(\underline{\mathbf{D}}) \cdot \underline{\hat{\mathbf{s}}} h, \tag{7.435}$$

where $G(\underline{\mathbf{D}})$ can be viewed as the evolution operator (or Green's function) of the system. An effective numerical implementation of the evolution operator is obtained by decomposing it into its Lagrange interpolator (Lancaster and Tismenetsky, 1985, p. 308). This yields

$$G(\underline{\mathbf{D}}) = \frac{1}{\lambda_1 - \lambda_2}\{[G(\lambda_1) - G(\lambda_2)]\underline{\mathbf{D}} + [\lambda_1 G(\lambda_2) - \lambda_2 G(\lambda_1)]\mathbf{I}_2\}. \tag{7.436}$$

This expression avoids the calculations of the eigenvectors of $\underline{\mathbf{D}}$ (i.e., of matrix $\mathbf{A}$). Using equation (7.430) and the complex velocities $v_{c\nu} = 1/\sqrt{\lambda_\nu}$, $\nu = 1, 2$, we note that equation (7.436) becomes

$$G(\underline{\mathbf{D}}) = \frac{\omega^2}{v_{c2}^2 - v_{c1}^2}\{[v_{c1}^2 g(v_{c2}) - v_{c2}^2 g(v_{c1})]\underline{\mathbf{D}} + [g(v_{c1}) - g(v_{c2}]\mathbf{I}_2\} - 8\delta(\mathbf{x})\mathbf{I}_2. \tag{7.437}$$

In the absence of viscoelastic dissipation and with the Biot mechanism deactivated (zero fluid viscosity), only the Green functions (7.425) and (7.427) are frequency dependent – the eigenvalues of $\underline{\mathbf{D}}$ are real. Let us denote the phase velocities of the fast and slow waves as $v_{\infty+}$ and $v_{\infty-}$, respectively (as in equation (7.290)). Then, the explicit frequency dependence of the evolution operator is

$$G(\underline{\mathbf{D}}, \omega) = \frac{G(v_{\infty+}, \omega)}{(v_{\infty-}/v_{\infty+})^2 - 1}(v_{\infty-}^2 \underline{\mathbf{D}} - \mathbf{I}_2) - \frac{G(v_{\infty-}, \omega)}{1 - (v_{\infty+}/v_{\infty-})^2}(v_{\infty+}^2 \underline{\mathbf{D}} - \mathbf{I}_2). \tag{7.438}$$

In this case, the solution can be obtained in closed form since the Green functions (7.425) and (7.427) can be Fourier transformed analytically to the time domain (Norris, 1985).

To ensure a time-domain real solution in the general viscoelastic case, we take

$$\underline{\mathbf{p}}(r, \omega) = \underline{\mathbf{p}}^*(r, -\omega), \tag{7.439}$$

for $\omega < 0$, where the superscript $*$ denotes the complex conjugate. Finally, the time domain solution is obtained by an inverse Fourier transform.

An example is shown in Figure 7.12 (see Carcione and Quiroga-Goode (1996) for details about the material properties and source characteristics). When the fluid is viscous enough, the slow wave appears as a quasi-static mode at the source location. This behavior is predicted by the analytical solution, where snapshots of the solid and fluid pressures due to a fluid volume injection are represented. The frequency band corresponds to the sonic range.

7.12 Green's function at a fluid/porous medium interface

The Rayleigh wave in a porous medium is composed of the fast P wave, the shear wave and the slow P wave. The physics has been studied by Deresiewicz (1962), who found that the Rayleigh wave is dissipative and dispersive due to losses by mode conversion to the slow wave (e.g., Bourbié, Coussy and Zinszner, 1987). Surface waves at liquid-porous media interfaces classify into three kinds. A true surface wave that travels slower than all the wave velocities (the generalization of the Scholte wave), a pseudo Scholte wave that travels

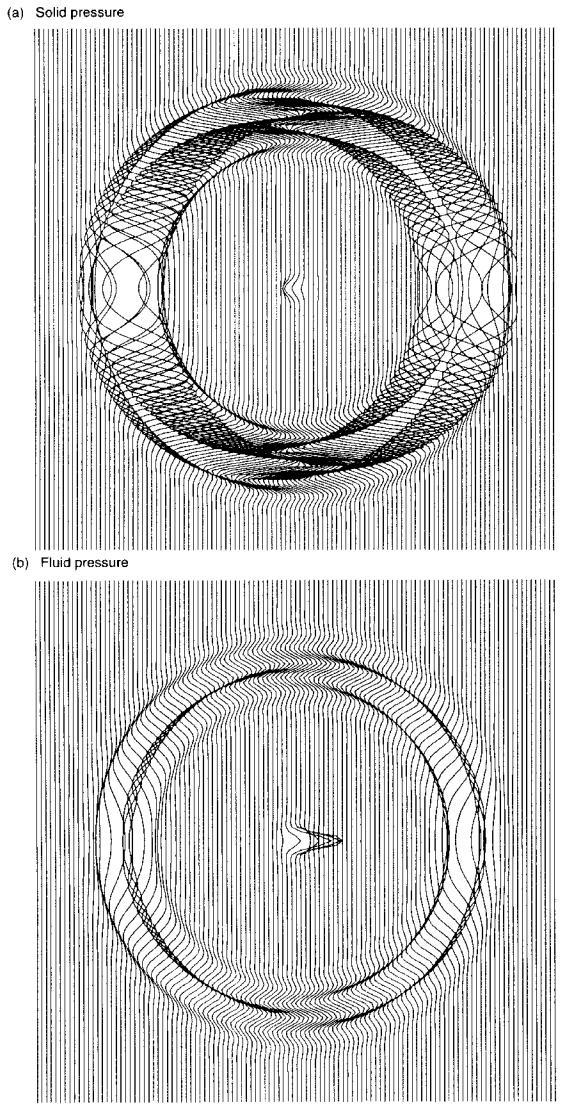

Figure 7.12: Snapshots of the solid pressure (a) and fluid pressure (b) for a porous medium saturated with a viscous fluid. The source dominant frequency is at the sonic range. The event at the source location is the slow "wave", which behaves as a quasi-static mode at those frequencies.

with a velocity between the shear-wave velocity and the slow-wave velocity (leaking energy to the slow wave), and a pseudo Rayleigh wave, which becomes the classical Rayleigh wave if the liquid density goes to zero (Feng and Johnson, 1982a,b; Holland, 1991; Edelman and Wilmanski, 2002). For sealed-pore conditions the true surface wave exists for all values of material parameters. Nagy (1992) and Adler and Nagy (1994) observed this surface wave in alcohol-saturated porous sintered glass and natural rocks. The conditions are a highly compressible fluid (e.g., air), a closed surface (sealed pores due to surface tension in Nagy's experiments) and negligible viscosity of the saturating fluid.

According to equation (7.375), the boundary conditions at an interface between a porous medium and a fluid are

$$\phi_1(v_3^{(f)(1)} - v_3^{(m)(1)}) = v_3^{(2)} - v_3^{(m)(1)}, \quad p_f^{(2)} - p_f^{(1)} = \frac{1}{\bar{\kappa}_s}\partial_t w_3, \quad \sigma_{33}^{(1)} = -p_f^{(2)}, \quad \sigma_{13}^{(1)} = \sigma_{23}^{(1)} = 0, \tag{7.440}$$

where we have considered the general case given by equation (7.367). The two limiting cases are equation (7.375) (open pores) and $\bar{\kappa}_s = 0$, which corresponds to sealed pores. In this case, there is no relative flow across the interface and the boundary conditions are

$$v_3^{(2)} = v_3^{(m)(1)}, \quad v_3^{(f)(1)} = v_3^{(m)(1)}, \quad \sigma_{33}^{(1)} = -p_f^{(2)}, \quad \sigma_{13}^{(1)} = \sigma_{23}^{(1)} = 0. \tag{7.441}$$

Feng and Johnson (1982b) obtained the high-frequency 2-D Green's function using the Cagniard-de Hoop technique. The source is a radial and uniform impulsive line source (a pressure source s_f in the fluid). If we assume that the upper medium is the fluid, the locations of the source and receiver are $(0, z_0)$ and (x, z) above the interface, in the overlying fluid half-space. The Green function is

$$G(x,z,t) = \begin{cases} 0, & -\infty < t < t_h, \\ \operatorname{Im}\left(\dfrac{R_f(s_h)}{2\pi\sqrt{t_b^2 - t^2}}\right), & t_h < t < t_b, \\ \operatorname{Re}\left(\dfrac{R_f(s_b)}{2\pi\sqrt{t^2 - t_b^2}}\right), & t > t_b, \end{cases} \tag{7.442}$$

where R_f is the reflection coefficient,

$$s_h(t) = \frac{xt - (z+z_0)\sqrt{t_b^2 - t^2}}{x^2 + (z+z_0)^2}, \tag{7.443}$$

$$s_b(t) = \frac{xt + \mathrm{i}(z+z_0)\sqrt{t^2 - t_b^2}}{x^2 + (z+z_0)^2}, \tag{7.444}$$

$$t_h = \frac{x}{v_{\infty+}} + (z+z_0)\sqrt{\frac{1}{v_f^2} - \frac{1}{v_{\infty+}^2}}, \tag{7.445}$$

and

$$t_b = \sqrt{x^2 + (z+z_0)^2}/v_f \tag{7.446}$$

(v_f is the wave-velocity of the fluid, $v_{\infty+}$ is the high-frequency fast P-wave velocity, a solution of equation (7.292), s_h and s_b are slownesses corresponding to the head and body wave, and t_h and t_b are the respective arrival times).

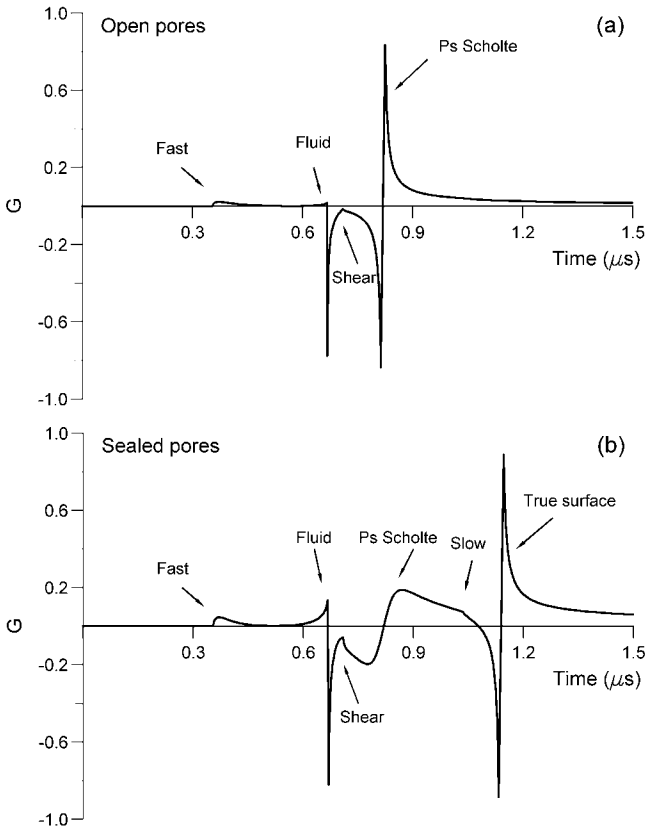

Figure 7.13: Calculated 2-D Green's functions for the water/water saturated fused glass beads planar interface system; the source and receivers are ideally located on the surface ($z = z_0 = 0$) and $x = 10$ cm. In (a) $\bar{\kappa}_s = \infty$, corresponding to open pores, and in (b) $\bar{\kappa}_s = 0$, corresponding to sealed pores. The medium properties are $K_s = 49.9$ GPa, $\rho_s = 2480$ kg/m^3, $K_m = 6.1$ GPa, $\mu_m = 3.4$ GPa, $\phi = 0.38$, $\mathcal{T} = 1.79$, $K_f = 2.25$ GPa, and $\rho_f = 1000$ kg/m^3. The labels indicate the fast P wave ("Fast"), the sound wave in the fluid ("Fluid"), the shear wave ("Shear"), the pseudo Scholte wave ("Ps Scholte"), the slow P wave ("Slow"), and the true surface wave ("True surface").

The expression of the reflection coefficient is

$$R_f(s) = \frac{\Delta_R(s)}{\Delta_0(s)}, \qquad \Delta_R = \det \mathbf{N}, \qquad \Delta_0 = \det \mathbf{D}, \tag{7.447}$$

and, using our notation, the components of matrix $\mathbf{D}(s)$ are[13]

$$\begin{aligned}
D_{11} &= 2\mu_m s^2 + (\alpha M F_+ - E_G)/v_{\infty+}^2 \\
D_{12} &= 2\mu_m s^2 + (\alpha M F_- - E_G)/v_{\infty-}^2 \\
D_{13} &= -2\mu_m s \gamma_S \\
D_{14} &= \rho_f \\
D_{21} &= \phi(\gamma_+/\bar{\kappa}_s + M/v_{\infty+}^2)F_+ - \phi\alpha M/v_{\infty+}^2 \\
D_{22} &= \phi(\gamma_-/\bar{\kappa}_s + M/v_{\infty-}^2)F_- - \phi\alpha M/v_{\infty-}^2 \\
D_{23} &= \phi^2 s/(\bar{\kappa}_s \mathcal{T}) \\
D_{24} &= \phi\rho_f \\
D_{31} &= (F_+ - 1)\gamma_+ \\
D_{32} &= (F_- - 1)\gamma_- \\
D_{33} &= -(1 - \phi/\mathcal{T})s \\
D_{34} &= -\gamma_f \\
D_{41} &= s\gamma_+ \\
D_{42} &= s\gamma_- \\
D_{43} &= s^2 - 1/(2v_S^2) \\
D_{44} &= 0,
\end{aligned} \tag{7.448}$$

where v_S is the high-frequency S-wave velocity (7.314), $v_{\infty-}$ is the high-frequency slow P-wave velocity, a solution of equation (7.292),

$$\gamma_j = \sqrt{1/v_j^2 - s^2}, \qquad (j = f,\ (\infty+),\ (\infty-),\ S), \tag{7.449}$$

$$F_+ = \phi - \frac{[(1-\phi)\rho_s + \phi\rho_f(\mathcal{T}-1)]v_{\infty+}^2 - E_m - (\alpha-\phi)^2 M}{\rho_f(\mathcal{T}-1)v_{\infty+}^2 + (\alpha-\phi)M} \tag{7.450}$$

and

$$F_- = \phi - \frac{[(1-\phi)\rho_s + \phi\rho_f(\mathcal{T}-1)]v_{\infty-}^2 - E_m - (\alpha-\phi)^2 M}{\rho_f(\mathcal{T}-1)v_{\infty-}^2 + (\alpha-\phi)M}. \tag{7.451}$$

The elements of $\mathbf{N}$ are the same of $\mathbf{D}$ except $N_{34} = \gamma_f$.

Figure 7.13 shows the Green functions for open (a) and sealed (b) pores. Note the presence of the slow surface wave, observed by Nagy (1992) at approximately 1.1 μs in the sealed-pore case.

7.13 Poro-viscoelasticity

Viscoelasticity can be introduced into Biot's poroelastic equations for modeling attenuation mechanisms related to the strain energy (stiffness dissipation) and the kinetic energy

[13] $D_{11} = 2\mu_m s^2 - (\alpha M F_+ - E_G)/v_{\infty+}^2$ in Feng and Johnson (1982b). Instead, the sign of the second term should be + (D. L. Johnson, personal communication).

(viscodynamic dissipation). In natural porous media such as sandstones, discrepancies between Biot's theory and measurements are due to complex pore shapes and the presence of clay. This complexity gives rise to a variety of relaxation mechanisms that contribute to the attenuation of the different wave modes. Stoll and Bryan (1970) show that attenuation is controlled by both the anelasticity of the skeleton (friction at grain contacts) and by viscodynamic causes. Stiffness dissipation is described in the stress-strain relation, and viscodynamic dissipation is a dynamic permeability effect due to the frequency-dependent interaction between the pore fluid and the solid matrix (Biot, 1956b; Johnson, Koplik and Dashen, 1987).

Let us consider, as an example, the 2-D stress-strain relations for an isotropic poroelastic medium in the (x,z)-plane. From equations (7.32) and (7.33), and using (7.22), we can rewrite the stress-strain relations as

$$\begin{aligned}
\partial_t\sigma_{11} &= E_m\partial_1 v_1^{(m)} + (E_m - 2\mu_m)\partial_3 v_3^{(m)} + \alpha M\epsilon + s_1\\
\partial_t\sigma_{33} &= (E_m - 2\mu_m)\partial_1 v_1^{(m)} + E_m\partial_3 v_3^{(m)} + \alpha M\epsilon + s_3\\
\partial_t\sigma_{13} &= \mu_m(\partial_3 v_1^{(m)} + \partial_1 v_3^{(m)}) + s_{13}\\
\partial_t p_f &= -M\epsilon + s_f\\
\epsilon &= \alpha(\partial_1 v_1^{(m)} + \partial_3 v_3^{(m)}) + \partial_1\dot{w}_1 + \partial_3\dot{w}_3,
\end{aligned} \tag{7.452}$$

where $v_i^{(m)}$ and $\dot{w}_i = \partial_t w_i$ are the components of the particle velocities of the solid and fluid relative to the solid (see equation (7.172)), s_1, s_3, s_{13} and s_f are external sources of stress for the solid and the fluid, respectively, and M, α and E_m are given in equations (7.24), (7.25) and (7.291).

The 2-D poroelastic equations of motion can be obtained from (7.210) and (7.211):

i) Biot-Euler's dynamical equations:

$$\begin{aligned}
\partial_1\sigma_{11} + \partial_3\sigma_{13} &= \rho\partial_t v_1^{(m)} + \rho_f\partial_t\dot{w}_1,\\
\partial_1\sigma_{13} + \partial_3\sigma_{33} &= \rho\partial_t v_3^{(m)} + \rho_f\partial_t\dot{w}_3.
\end{aligned} \tag{7.453}$$

ii) Dynamical Darcy's law:

$$\begin{aligned}
-\partial_1 p_f &= \rho_f\partial_t v_1^{(m)} + m\partial_t\dot{w}_1 + \bar{b} * \partial_t\dot{w}_1,\\
-\partial_3 p_f &= \rho_f\partial_t v_3^{(m)} + m\partial_t\dot{w}_3 + \bar{b} * \partial_t\dot{w}_3,
\end{aligned} \tag{7.454}$$

where $m = \mathcal{T}\rho_f/\phi$ (equation (7.212)), with $\mathcal{T}$ denoting the tortuosity, and $\bar{b}(t)$ a relaxation function. At low frequencies $\bar{b} = H(t)\eta/\bar{\kappa}$, where H is Heaviside's function, and we obtain (7.211) (Carcione, 1998, Arntsen and Carcione, 2001).

The stiffnesses E_m, μ_m and M are generalized to time-dependent relaxation functions, which we denote, in general, by $\psi(t)$. We assume that $\psi(0) = \psi_0$ equals the respective Biot modulus, i.e., we obtain Biot's poroelastic stress-strain relations at high frequencies. Assume, for example, that the relaxation functions are described by a single Zener model,

$$\psi(t) = \psi_0\left(\frac{\tau_\sigma}{\tau_\epsilon}\right)\left[1 + \left(\frac{\tau_\epsilon}{\tau_\sigma} - 1\right)\exp(-t/\tau_\sigma)\right]H(t), \tag{7.455}$$

where τ_ϵ and τ_σ are relaxation times (see Section 2.4.3).

We introduce viscoelasticity by replacing the products of the elastic moduli and field variables in equations (7.452) with time convolutions. For instance, in equations $(7.452)_1$

and $(7.452)_2$, these products are $E_m(\partial_1 v_1^{(m)} + \partial_3 v_3^{(m)})$, $\mu_m \partial_3 v_3^{(m)}$ and $M\epsilon$. We replace them with $\psi * \partial_t u$, where ψ denotes the relaxation function corresponding to E_m, μ_m or M, and u denotes $\partial_1 v_1^{(m)} + \partial_3 v_3^{(m)}$, $\mu_m v_3^{(m)}$ or ϵ. It is important to point out that this approach is purely phenomenological. As in the single-phase viscoelastic case (see Section 2.7), we introduce memory variables to avoid the time convolutions. Then, the terms $\psi * \partial_t u$ are substituted by $\psi_0 u + e$, where e is the memory variable. There are five stress memory variables related to the stress-strain relations, which satisfy the following differential equation:

$$\partial_t e = \psi_0 \left(\frac{1}{\tau_\epsilon} - \frac{1}{\tau_\sigma} \right) u - \frac{e}{\tau_\sigma}. \tag{7.456}$$

Two additional memory variables are introduced via viscodynamic dissipation, due to the time-dependent relaxation function $\bar{b}(t)$. Hence,

$$\bar{b}(t) = \frac{\eta}{\bar{\kappa}} \left[1 + \left(\frac{\tau_\epsilon}{\tau_\sigma} - 1 \right) \exp(-t/\tau_\sigma) \right] H(t), \tag{7.457}$$

the terms $\bar{b} * \partial_t u$ are replaced by $\bar{b}(0)u + e$, and the memory-variable equations have the form

$$\partial_t e = -\frac{1}{\tau_\sigma} \left[\frac{\eta}{\bar{\kappa}} \left(\frac{\tau_\epsilon}{\tau_\sigma} - 1 \right) u + e \right]. \tag{7.458}$$

In the frequency domain, the time convolution $\psi * u$ is replaced by $\tilde{\psi}\tilde{u}$. We obtain, from (7.455),

$$\tilde{\psi} = \psi_0 \left(\frac{\tau_\sigma}{\tau_\epsilon} \right) \left(\frac{1 + \mathrm{i}\omega\tau_\epsilon}{1 + \mathrm{i}\omega\tau_\sigma} \right), \tag{7.459}$$

and each complex modulus is denoted by $\tilde{E}_m$, $\tilde{\mu}_m$ and $\tilde{M}$.

Each set of relaxation times can be expressed in terms of a Q factor Q_0 and a reference frequency f_0 as

$$\begin{aligned} \tau_\epsilon &= (2\pi f_0 Q_0)^{-1} \left(\sqrt{Q_0^2 + 1} + 1 \right), \\ \tau_\sigma &= (2\pi f_0 Q_0)^{-1} \left(\sqrt{Q_0^2 + 1} - 1 \right). \end{aligned} \tag{7.460}$$

On the other hand, the frequency-domain viscodynamic operator has the form

$$\tilde{b} = \frac{\eta}{\bar{\kappa}} \left(\frac{1 + \mathrm{i}\omega\tau_\epsilon}{1 + \mathrm{i}\omega\tau_\sigma} \right). \tag{7.461}$$

The functional dependence of $\tilde{b}$ on ω is not that predicted by models of dynamic fluid flow. Appropriate dynamic permeability functions are given in Section 7.6.2. Here, we intend to model the viscodynamic operator in a narrow band about the central frequency of the source. The advantage of using equation (7.461) is the easy implementation in time-domain numerical modeling.

The results of a simulation with Biot's poroelastic theory are plotted in Figure 7.14b, and compared to the experimental microseismograms obtained by Kelder and Smeulders (1997), illustrated in Figure 7.14a. The discrepancies with the experimental results are due to the presence of non-Biot attenuation mechanisms. Figure 7.14c shows the poro-viscoelastic microseismograms. The relative amplitudes observed are in better agreement with the experiment than those predicted by Biot's theory without viscoelastic losses.

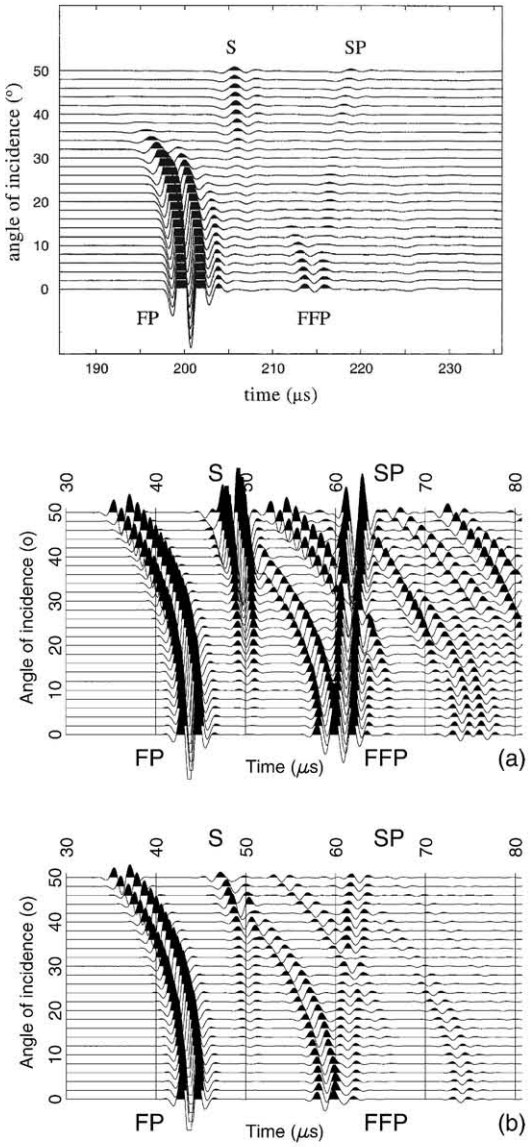

Figure 7.14: Microseismogram obtained by Kelder and Smeulders (1997) for Nivelsteiner sandstone as a function of the angle of incidence θ (top picture), and numerical microseismograms obtained from Biot's poroelastic theory (a) and Biot's poro-viscoelastic theory (b). The events are the fast compressional wave (FP), the shear wave (S), the first multiple reflection of the fast compressional wave (FFP) and the slow wave (SP).

In many cases, the results obtained with Biot (two-phase) modeling are equal to those obtained with single-phase elastic modeling, mainly at seismic frequencies (Gurevich, 1996). A correct equivalence is obtained with a viscoelastic rheology that requires one relaxation peak for each Biot (P and S) mechanism. The standard viscoelastic model, that is based on the generalization of the compressibility and shear modulus to relaxation functions, is not appropriate for modeling Biot complex moduli, since Biot's attenuation is of a kinetic nature – i.e, it is not related to bulk deformations. The problem can be solved by associating relaxation functions with each wave moduli. However, in a highly inhomogeneous medium, single-phase viscoelastic modeling is not, in principle, equivalent to porous-media modeling, due to substantial mode conversion from fast wave to quasi-static mode. For instance, if the fluid compressibility varies significantly from point to point, diffusion of pore fluid among different regions constitutes a mechanism that can be important at seismic frequencies (See Section 7.10).

7.14 Anisotropic poro-viscoelasticity

Anisotropic poroelasticity was introduced by Biot (1955, 1956) and Biot and Willis (1957) in terms of bulk parameters of total stress and strain. To our knowledge, Brown and Korringa (1975) were the first to obtain the material coefficients in terms of the properties of the grain, pore-fluid and frame (see Section 7.3.3). Later, Carroll (1980), Rudnicki (1985) and Thompson and Willis (1991) presented further micromechanical analysis of the stress-strain relations. Cheng (1997) related the Hookean constants to the engineering constants – obtained from laboratory measurements – including explicit relations for the orthorhombic and transverse isotropy material symmetries. Cheng's theory assumes that the solid constituent is isotropic and that anisotropy is due to the arrangements of the grains – i.e., the frame is anisotropic. Recently, Sahay, Spanos and de la Cruz (2000) used a volume-averaging method to obtain the stress-strain relations. Their approach include a differential equation for porosity, which describes the changes in porosity due to varying stress conditions.

Complete experimental data for anisotropic media is scarce. New propagation experiments on real rocks can be found in Lo, Coyner and Toksöz (1986) and Aoki, Tan and Bramford (1993). Wave propagation in anisotropic poroelastic rocks is investigated by Norris (1993), Ben-Menahem and Gibson (1993), Parra (1997), and Gelinsky and Shapiro (1997) and Gelinsky, Shapiro, Müller and Gurevich (1998), who study plane layered systems and the effects of anisotropic permeability. Numerical simulations of wave propagation for the transversely isotropic case – in rocks and synthetic materials – are given in Carcione (1996b), and a complete analysis in terms of energy is given by Carcione (2001a). The developments in this section follow the last reference (i.e., Carcione, 2001a).

We have shown in Section 4.3.1 that in single-phase anisotropic viscoelastic media, the phase velocity is the projection of the energy-velocity vector onto the propagation direction. We have also generalized other similar relations valid in the isotropic viscoelastic case. Here, those relations are further extended for anisotropic poro-viscoelastic media for the following reasons. Firstly, they provide a simple and useful means for evaluating the time-averaged kinetic-, strain- and dissipated-energy densities from the wavenumber, attenuation and energy-flow vectors. Secondly, they can be used to verify the kinematic and dynamic properties – in terms of energy – of complex porous materials. For instance,

the above relation between phase and energy velocities has immediate implications for ultrasonic experiments. If a pulse of acoustic energy is radiated by a plane-wave transducer, the wave front travels along the wavenumber direction, which is normal to the transducer surface, but the wave packet modulation envelope travels in the direction of the energy velocity. This means that the receiving transducer must be offset in order to intercept the acoustic pulse, and the corresponding angle is the angle between the wavenumber and energy-velocity vectors. Although that relation between the velocities is well known for anisotropic lossless media (e.g., Auld, 1990a, p. 222; equation (1.114)), it is not immediately evident that it holds for poro-viscoelastic and anisotropic media.

In our example later in this chapter, we consider wave propagation in one of the planes of mirror symmetry of an orthorhombic material (human femoral bone). Bulk viscoelasticity is modeled by using the concept of eigenstrain (see Section 4.1) and the low-frequency viscodynamic operator is used to model Biot-type dissipation.

7.14.1 Stress-strain relations

The stress-strain relations (7.131) and (7.133) can be rewritten in matrix form as

$$\boldsymbol{\sigma} = \mathbf{C}^u \cdot \mathbf{e}, \tag{7.462}$$

where

$$\boldsymbol{\sigma} = (\sigma_{11}, \sigma_{22}, \sigma_{33}, \sigma_{23}, \sigma_{13}, \sigma_{12}, -p_f)^\top, \tag{7.463}$$

is the stress array,

$$\mathbf{e} = (e_1^{(m)}, e_2^{(m)}, e_3^{(m)}, e_4^{(m)}, e_5^{(m)}, e_6^{(m)}, -\zeta)^\top, \tag{7.464}$$

is the strain array, with $e_I^{(m)}$ denoting the strain components of the porous frame and ζ the variation of fluid content,

$$\mathbf{C}^u = \begin{pmatrix} c_{11}^u & c_{12}^u & c_{13}^u & c_{14}^u & c_{15}^u & c_{16}^u & M\alpha_1 \\ c_{12}^u & c_{22}^u & c_{23}^u & c_{24}^u & c_{25}^u & c_{26}^u & M\alpha_2 \\ c_{13}^u & c_{23}^u & c_{33}^u & c_{34}^u & c_{35}^u & c_{36}^u & M\alpha_3 \\ c_{14}^u & c_{24}^u & c_{34}^u & c_{44}^u & c_{45}^u & c_{46}^u & M\alpha_4 \\ c_{15}^u & c_{25}^u & c_{35}^u & c_{45}^u & c_{55}^u & c_{56}^u & M\alpha_5 \\ c_{16}^u & c_{26}^u & c_{36}^u & c_{46}^u & c_{56}^u & c_{66}^u & M\alpha_6 \\ M\alpha_1 & M\alpha_2 & M\alpha_3 & M\alpha_4 & M\alpha_5 & M\alpha_6 & M \end{pmatrix}, \tag{7.465}$$

where c_{IJ}^u are the components of the elasticity matrix of the undrained porous medium (7.136).

The time rate of the strain can be written as

$$\partial_t \mathbf{e} = \boldsymbol{\nabla}^\top \cdot \underline{\mathbf{v}}, \tag{7.466}$$

where

$$\underline{\mathbf{v}} \equiv (v_1^{(m)}, v_2^{(m)}, v_3^{(m)}, w_1, w_2, w_3)^\top \tag{7.467}$$

and

$$\boldsymbol{\nabla} = \begin{pmatrix} \partial_1 & 0 & 0 & 0 & \partial_3 & \partial_2 & 0 \\ 0 & \partial_2 & 0 & \partial_3 & 0 & \partial_1 & 0 \\ 0 & 0 & \partial_3 & \partial_2 & \partial_1 & 0 & 0 \\ 0 & 0 & 0 & 0 & 0 & 0 & \partial_1 \\ 0 & 0 & 0 & 0 & 0 & 0 & \partial_2 \\ 0 & 0 & 0 & 0 & 0 & 0 & \partial_3 \end{pmatrix}. \tag{7.468}$$

The form (7.466), relating the particle velocities to the strain components, as well as the differential operator (7.468) are generalizations of those used by Auld (1990a).

Biot (1956c) developed a generalization of the stress-strain relations to the viscoelastic case by invoking the correspondence principle and using relaxation functions based on mechanical models of viscoelastic behavior. Dissipation is due to a variety of anelastic mechanisms. An important mechanism is mesoscopic loss discussed in Section 7.10. Another mechanism is the squirt-flow (Biot, 1962; Dvorkin, Nolen-Hoeksema and Nur, 1994) by which a force applied to the area of contact between two grains produces a displacement of the surrounding fluid in and out of this area. Since the fluid is viscous, the motion is not instantaneous and energy dissipation occurs. Other important attenuation mechanisms are discussed by Biot (1962). Using the correspondence principle (see Section 3.6), we generalize to relaxation functions the elements of matrix $\mathbf{C}^u$, and equation (7.462) becomes

$$\boldsymbol{\sigma} = \boldsymbol{\Psi} * \partial_t \mathbf{e}, \tag{7.469}$$

where $\boldsymbol{\Psi}$ is the relaxation matrix. Matrix $\mathbf{C}^u$ is obtained from $\boldsymbol{\Psi}$ when $t \to 0$ if we consider that Biot's poroelastic theory corresponds to the unrelaxed state.

7.14.2 Biot-Euler's equation

In matrix form, equations (7.255) and (7.258) can be written as

$$\nabla \cdot \boldsymbol{\sigma} = \mathbf{R} \cdot \partial_t \underline{\mathbf{v}} + \mathbf{f}, \tag{7.470}$$

where

$$\mathbf{f} \equiv (f_1, f_2, f_3, 0, 0, 0, 0)^\top \tag{7.471}$$

is a body force array, and

$$\mathbf{R} = \begin{pmatrix} \rho & 0 & 0 & \rho_f & 0 & 0 \\ 0 & \rho & 0 & 0 & \rho_f & 0 \\ 0 & 0 & \rho & 0 & 0 & \rho_f \\ \rho_f & 0 & 0 & \psi_1 * & 0 & 0 \\ 0 & \rho_f & 0 & 0 & \psi_2 * & 0 \\ 0 & 0 & \rho_f & 0 & 0 & \psi_3 * \end{pmatrix} \tag{7.472}$$

is the density matrix operator. We refer to (7.470) as Biot-Euler's equation.

7.14.3 Time-harmonic fields

Let us consider a time-harmonic field $\exp(\mathrm{i}\omega t)$, where ω is the angular frequency. The stress-strain relation (7.469) becomes

$$\boldsymbol{\sigma} = \mathbf{P} \cdot \mathbf{e}, \qquad \mathbf{P} = \mathcal{F}(\partial_t \boldsymbol{\Psi}), \tag{7.473}$$

where $\mathbf{P}$ is the complex and frequency-dependent stiffness matrix, and the operator $\mathcal{F}$ denotes time Fourier transform. Equation (7.466) becomes

$$\mathrm{i}\omega \mathbf{e} = \nabla^\top \cdot \underline{\mathbf{v}}. \tag{7.474}$$

Substituting equation (7.474) into (7.473), we obtain

$$\mathrm{i}\omega\boldsymbol{\sigma} = \mathbf{P}\cdot(\nabla^{\top}\cdot\underline{\mathbf{v}}). \tag{7.475}$$

For time-harmonic fields, Biot-Euler's equation (7.470) becomes

$$\nabla\cdot\boldsymbol{\sigma} = \mathrm{i}\omega\mathbf{R}\cdot\underline{\mathbf{v}} + \mathbf{f}, \tag{7.476}$$

where

$$\mathbf{R} = \begin{pmatrix} \rho & 0 & 0 & \rho_f & 0 & 0 \\ 0 & \rho & 0 & 0 & \rho_f & 0 \\ 0 & 0 & \rho & 0 & 0 & \rho_f \\ \rho_f & 0 & 0 & \bar{Y}_1/(\mathrm{i}\omega) & 0 & 0 \\ 0 & \rho_f & 0 & 0 & \bar{Y}_2/(\mathrm{i}\omega) & 0 \\ 0 & 0 & \rho_f & 0 & 0 & \bar{Y}_3/(\mathrm{i}\omega) \end{pmatrix}, \tag{7.477}$$

and $\bar{Y}_i$ are given in equation (7.238), provided that the correction (7.241) is used for high frequencies, or the specific operator is obtained by experimental measurements.

The derivation of the energy-balance equation is straightforward when using complex notation. The procedure given in Section 4.3.1 for single-phase media is used here. The dot product of the complex conjugate of equation (7.474) with $-\boldsymbol{\sigma}^{\top}$ gives

$$-\boldsymbol{\sigma}^{\top}\cdot\nabla^{\top}\cdot\underline{\mathbf{v}}^{*} = \mathrm{i}\omega\boldsymbol{\sigma}^{\top}\cdot\mathbf{e}^{*}, \tag{7.478}$$

On the other hand, the dot product of $-\underline{\mathbf{v}}^{*\top}$ with equation (7.476) is

$$-\underline{\mathbf{v}}^{*\top}\cdot\nabla\cdot\boldsymbol{\sigma} = -\mathrm{i}\omega\underline{\mathbf{v}}^{*\top}\cdot\mathbf{R}\cdot\underline{\mathbf{v}} - \underline{\mathbf{v}}^{*\top}\cdot\mathbf{f}. \tag{7.479}$$

Adding equations (7.478) and (7.479), we get

$$-\boldsymbol{\sigma}^{\top}\cdot\nabla^{\top}\cdot\underline{\mathbf{v}}^{*} - \underline{\mathbf{v}}^{*\top}\cdot\nabla\cdot\boldsymbol{\sigma} = \mathrm{i}\omega\boldsymbol{\sigma}^{\top}\cdot\mathbf{e}^{*} - \mathrm{i}\omega\underline{\mathbf{v}}^{*\top}\cdot\mathbf{R}\cdot\underline{\mathbf{v}} - \underline{\mathbf{v}}^{*\top}\cdot\mathbf{f}. \tag{7.480}$$

The left-hand side is simply

$$-\boldsymbol{\sigma}^{\top}\cdot\nabla^{\top}\cdot\underline{\mathbf{v}}^{*} - \underline{\mathbf{v}}^{*\top}\cdot\nabla\cdot\boldsymbol{\sigma} = 2\ \mathrm{div}\ \mathbf{p}, \tag{7.481}$$

where

$$\mathbf{p} = -\frac{1}{2}\begin{pmatrix} \sigma_{11} & \sigma_{12} & \sigma_{13} & -p_f & 0 & 0 \\ \sigma_{12} & \sigma_{22} & \sigma_{23} & 0 & -p_f & 0 \\ \sigma_{13} & \sigma_{23} & \sigma_{33} & 0 & 0 & -p_f \end{pmatrix}\cdot\underline{\mathbf{v}}^{*} \tag{7.482}$$

is the complex Umov-Poynting vector. Using (7.481) and the stress-strain relation (7.473), we find that equation (7.480) gives

$$2\ \mathrm{div}\ \mathbf{p} = \mathrm{i}\omega\mathbf{e}^{\top}\cdot\mathbf{P}\cdot\mathbf{e}^{*} - \mathrm{i}\omega\underline{\mathbf{v}}^{*\top}\cdot\mathbf{R}\cdot\underline{\mathbf{v}} - \underline{\mathbf{v}}^{*\top}\cdot\mathbf{f}, \tag{7.483}$$

where we used the fact that $\mathbf{P}$ is a symmetric matrix. Equation (7.483) can be rewritten as

$$\begin{aligned}\mathrm{div}\ \mathbf{p} = 2\mathrm{i}\omega&\left[\frac{1}{4}\mathrm{Re}(\mathbf{e}^{\top}\cdot\mathbf{P}\cdot\mathbf{e}^{*}) - \frac{1}{4}\mathrm{Re}(\underline{\mathbf{v}}^{*\top}\cdot\mathbf{R}\cdot\underline{\mathbf{v}})\right] \\ +2\omega&\left[-\frac{1}{4}\mathrm{Im}(\mathbf{e}^{\top}\cdot\mathbf{P}\cdot\mathbf{e}^{*}) + \frac{1}{4}\mathrm{Im}(\underline{\mathbf{v}}^{*\top}\cdot\mathbf{R}\cdot\underline{\mathbf{v}})\right] - \frac{1}{2}\underline{\mathbf{v}}^{*\top}\cdot\mathbf{f}.\end{aligned} \tag{7.484}$$

The significance of this equation becomes clear when we recognize that each of its terms has a precise physical meaning on a time average basis. When using complex notation for plane waves, the field variables are obtained as the real part of the corresponding complex fields.

In the following derivation, we use the properties (1.105) and (1.106). Using these relations, we identify

$$\frac{1}{4}\mathrm{Re}(\mathbf{e}^{\top}\cdot\mathbf{P}\cdot\mathbf{e}^{*}) = \frac{1}{2}\langle \mathrm{Re}(\mathbf{e}^{\top})\cdot\mathrm{Re}(\mathbf{P})\cdot\mathrm{Re}(\mathbf{e})\rangle \equiv \langle V\rangle \tag{7.485}$$

as the strain-energy density,

$$\frac{1}{4}\mathrm{Re}(\underline{\mathbf{v}}^{*\top}\cdot\mathbf{R}\cdot\underline{\mathbf{v}}) = \frac{1}{2}\langle \mathrm{Re}(\underline{\mathbf{v}}^{*\top})\cdot\mathrm{Re}(\mathbf{R})\cdot\mathrm{Re}(\underline{\mathbf{v}}\,)\rangle \equiv \langle T\rangle \tag{7.486}$$

as the kinetic-energy density,

$$-\frac{1}{2}\omega\ \mathrm{Im}(\mathbf{e}^{\top}\cdot\mathbf{P}\cdot\mathbf{e}^{*}) + \frac{1}{2}\omega\ \mathrm{Im}(\underline{\mathbf{v}}^{*\top}\cdot\mathbf{R}\cdot\underline{\mathbf{v}}) =$$

$$-\omega\langle \mathrm{Re}(\mathbf{e}^{\top})\cdot\mathrm{Im}(\mathbf{P})\cdot\mathrm{Re}(\mathbf{e})\rangle + \omega\langle \mathrm{Re}(\underline{\mathbf{v}}^{\top})\cdot\mathrm{Im}(\mathbf{R})\cdot\mathrm{Re}(\underline{\mathbf{v}}\,)\rangle \equiv -\langle \dot{D}_V\rangle - \langle \dot{D}_T\rangle \tag{7.487}$$

as minus the rate of dissipated strain-energy density ($-\langle \dot{D}_V\rangle$, the first term) minus the rate of dissipated kinetic-energy density ($-\langle \dot{D}_T\rangle$, the second term), and

$$-\frac{1}{2}\underline{\mathbf{v}}^{*\top}\cdot\mathbf{f} \equiv P_s \tag{7.488}$$

as the complex power per unit volume supplied by the body forces.

We may define the corresponding time-averaged energy densities $\langle D_V\rangle$ and $\langle D_T\rangle$ by the relations

$$\langle \dot{D}_V\rangle = \omega\langle D_V\rangle \quad \text{and} \quad \langle \dot{D}_T\rangle = \omega\langle D_T\rangle. \tag{7.489}$$

Substituting the preceding expressions into equation (7.484), we obtain the energy-balance equation,

$$\mathrm{div}\ \mathbf{p} - 2\mathrm{i}\omega(\langle V\rangle - \langle T\rangle) + \omega\langle D\rangle = P_s, \tag{7.490}$$

where

$$\langle D\rangle = \langle D_V\rangle + \langle D_T\rangle \tag{7.491}$$

is the total time-averaged dissipated-energy density.

The total stored energy density is

$$\langle E\rangle = \langle V\rangle + \langle T\rangle. \tag{7.492}$$

If there is no dissipation ($\langle D\rangle = 0$) and, since in the absence of sources ($P_s = 0$) the net energy flow into or out of a given closed surface must vanish, $\mathrm{div}\ \mathbf{p} = 0$. Thus, the average kinetic energy equals the average strain energy. As a consequence, the stored energy is twice the strain energy.

7.14.4 Inhomogeneous plane waves

A general plane-wave solution for the particle velocity (7.467) is

$$\underline{\mathbf{v}} = \underline{\mathbf{v}}_0 \exp[\mathrm{i}(\omega t - \mathbf{k} \cdot \mathbf{x})], \tag{7.493}$$

where $\underline{\mathbf{v}}_0$ represents a constant complex vector and $\mathbf{k}$ is the wavevector. This is, in general, complex and can be written as

$$\mathbf{k} \equiv \boldsymbol{\kappa} - \mathrm{i}\boldsymbol{\alpha} = (k_1, k_2, k_3), \tag{7.494}$$

where $\boldsymbol{\kappa}$ and $\boldsymbol{\alpha}$ are the real wavevector and attenuation vector, respectively. They indicate the directions and magnitudes of propagation and attenuation. In general, these directions differ and the plane wave is called inhomogeneous. For inhomogeneous viscoelastic plane waves, the operator (7.468) takes the form

$$\nabla \rightarrow -\mathrm{i}\mathbf{K}, \tag{7.495}$$

where

$$\mathbf{K} = \begin{pmatrix} k_1 & 0 & 0 & 0 & k_3 & k_2 & 0 \\ 0 & k_2 & 0 & k_3 & 0 & k_1 & 0 \\ 0 & 0 & k_3 & k_2 & k_1 & 0 & 0 \\ 0 & 0 & 0 & 0 & 0 & 0 & k_1 \\ 0 & 0 & 0 & 0 & 0 & 0 & k_2 \\ 0 & 0 & 0 & 0 & 0 & 0 & k_3 \end{pmatrix}. \tag{7.496}$$

When the operator is applied to a conjugated field, ∇ should be replaced by $\mathrm{i}\mathbf{K}^*$.

Substituting the differential operator into equations (7.478) and (7.479) and assuming zero body forces, we get

$$-\boldsymbol{\sigma}^{\top} \cdot \mathbf{K}^{*\top} \cdot \underline{\mathbf{v}}^* = \omega \boldsymbol{\sigma}^{\top} \cdot \mathbf{e}^* \tag{7.497}$$

and

$$-\underline{\mathbf{v}}^{*\top} \cdot \mathbf{K} \cdot \boldsymbol{\sigma} = \omega \underline{\mathbf{v}}^{*\top} \cdot \mathbf{R} \cdot \underline{\mathbf{v}}, \tag{7.498}$$

respectively. The left-hand sides of equations (7.497) and (7.498) contain the complex Umov-Poynting vector (7.482). In fact, by virtue of equation (7.494), equations (7.497) and (7.498) become

$$2\mathbf{k}^* \cdot \mathbf{p} = \omega \boldsymbol{\sigma}^{\top} \cdot \mathbf{e}^* \tag{7.499}$$

and

$$2\mathbf{k} \cdot \mathbf{p} = \omega \underline{\mathbf{v}}^{*\top} \cdot \mathbf{R} \cdot \underline{\mathbf{v}}, \tag{7.500}$$

respectively. Adding (7.499) and (7.500), and using equation (7.494) ($\mathbf{k}^* + \mathbf{k} = 2\boldsymbol{\kappa}$), we obtain

$$4\boldsymbol{\kappa} \cdot \mathbf{p} = \omega \left(\boldsymbol{\sigma}^{\top} \cdot \mathbf{e}^* + \underline{\mathbf{v}}^{*\top} \cdot \mathbf{R} \cdot \underline{\mathbf{v}} \right). \tag{7.501}$$

Using equation (1.105), the time average of the real Umov-Poynting vector (7.482)

$$-\mathrm{Re} \begin{pmatrix} \sigma_{11} & \sigma_{12} & \sigma_{13} & -p_f & 0 & 0 \\ \sigma_{12} & \sigma_{22} & \sigma_{23} & 0 & -p_f & 0 \\ \sigma_{13} & \sigma_{23} & \sigma_{33} & 0 & 0 & -p_f \end{pmatrix} \cdot \mathrm{Re}(\underline{\mathbf{v}}), \tag{7.502}$$

is

$$\langle \mathbf{p} \rangle = \mathrm{Re}(\mathbf{p}), \tag{7.503}$$

which gives the average power flow.

As in the previous section, the time average of the strain-energy density

$$\langle V \rangle = \frac{1}{2}\mathrm{Re}(\boldsymbol{\sigma}^{\top}) \cdot \mathrm{Re}(\mathbf{e}) \tag{7.504}$$

is

$$\langle V \rangle = \frac{1}{4}\mathrm{Re}(\boldsymbol{\sigma}^{\top} \cdot \mathbf{e}^{*}) = \frac{1}{4}\mathrm{Re}(\mathbf{e}^{*\top} \cdot \mathbf{P} \cdot \mathbf{e}). \tag{7.505}$$

Similarly, the time-averaged kinetic-energy density is

$$\langle T \rangle = \frac{1}{4}\mathrm{Re}\left(\underline{\mathbf{v}}^{*\top} \cdot \mathbf{R} \cdot \underline{\mathbf{v}}\right), \tag{7.506}$$

and the time-averaged strain and kinetic dissipated-energy densities are

$$\langle D_V \rangle = \frac{1}{2}\mathrm{Im}(\mathbf{e}^{*\top} \cdot \mathbf{P} \cdot \mathbf{e}), \tag{7.507}$$

and

$$\langle D_T \rangle = -\frac{1}{2}\mathrm{Im}\left(\underline{\mathbf{v}}^{*\top} \cdot \mathbf{R} \cdot \underline{\mathbf{v}}\right), \tag{7.508}$$

respectively. The last two quantities represent the energy loss per unit volume due to viscoelastic and viscodynamic effects, respectively. The minus sign in equation (7.508) is due to the fact that $\mathrm{Im}(\bar{Y}_I/\mathrm{i}\omega) < 0$ (see equation (7.477)). It can be shown that the dissipated energies should be defined with the opposite sign if an $\exp(-\mathrm{i}\omega t)$ kernel is used. This is the case for the dissipated kinetic energy in the work of Carcione (1996b).

Substituting equations (7.503), (7.505) and (7.506) into the real part of equation (7.501), we obtain

$$\boldsymbol{\kappa} \cdot \langle \mathbf{p} \rangle = \omega(\langle V \rangle + \langle T \rangle) = \omega \langle E \rangle, \tag{7.509}$$

where $\langle E \rangle$ is the stored energy density (7.492). Furthermore, the imaginary part of equation (7.501) gives

$$2\,\boldsymbol{\kappa} \cdot \mathrm{Im}\ \mathbf{p} = \omega(\langle D_V \rangle - \langle D_T \rangle). \tag{7.510}$$

The wave surface is the locus of the end of the energy-velocity vector multiplied by one unit of propagation time, with the energy velocity defined as the ratio of the average power-flow density $\langle \mathbf{p} \rangle$ to the total energy density $\langle E \rangle$. Since this is equal to the sum of the average kinetic- and strain-energy densities $\langle K \rangle$ and $\langle V \rangle$, the energy velocity is

$$\mathbf{v}_e = \frac{\langle \mathbf{p} \rangle}{\langle T + V \rangle}. \tag{7.511}$$

Dissipation is quantified by the quality factor, which can be defined as

$$Q = \frac{2\langle V \rangle}{\langle D \rangle}. \tag{7.512}$$

Using the definition of the energy velocity and equation (7.509), we obtain

$$\hat{\boldsymbol{\kappa}} \cdot \mathbf{v}_e = v_p, \qquad (\mathbf{s}_R \cdot \mathbf{v}_e = 1), \tag{7.513}$$

where $v_p = \omega/\kappa$ is the phase velocity, and $\mathbf{s}_R = \hat{\boldsymbol{\kappa}}/v_p$ is the slowness vector. Relation (7.513), as in a single-phase medium (see equation (4.78)), means that the phase velocity is simply the projection of the energy velocity onto the propagation direction.

Finally, subtracting equation (7.499) from (7.500) and using (7.494) yields the energy-balance equation

$$-2\boldsymbol{\alpha} \cdot \mathbf{p} = 2\mathrm{i}\omega(\langle V \rangle - \langle T \rangle) - \omega\langle D \rangle. \tag{7.514}$$

Taking the real part of (7.514), we get

$$2\boldsymbol{\alpha} \cdot \langle \mathbf{p} \rangle = \omega\langle D \rangle. \tag{7.515}$$

This equation is the generalization of equation (4.83) for viscoelastic single-phase media, stating that the time-averaged dissipated energy can be obtained as the projection of the average power-flow density onto the attenuation direction.

7.14.5 Homogeneous plane waves

For homogeneous waves, the propagation and attenuation directions coincide and the wavevector can be written as

$$\mathbf{k} = (\kappa - \mathrm{i}\alpha)\hat{\boldsymbol{\kappa}} \equiv k\hat{\boldsymbol{\kappa}}, \tag{7.516}$$

where

$$\hat{\boldsymbol{\kappa}} = (l_1, l_2, l_3) \tag{7.517}$$

defines the propagation direction through the directions cosines l_1, l_2 and l_3. For homogeneous waves

$$\mathbf{K} \to k\mathbf{L} = k \begin{pmatrix} l_1 & 0 & 0 & 0 & l_3 & l_2 & 0 \\ 0 & l_2 & 0 & l_3 & 0 & l_1 & 0 \\ 0 & 0 & l_3 & l_2 & l_1 & 0 & 0 \\ 0 & 0 & 0 & 0 & 0 & 0 & l_1 \\ 0 & 0 & 0 & 0 & 0 & 0 & l_2 \\ 0 & 0 & 0 & 0 & 0 & 0 & l_3 \end{pmatrix}, \tag{7.518}$$

where k is the complex wavenumber. Using (7.495), we see that equations (7.475) and (7.476) give

$$\left(\mathbf{R}^{-1} \cdot \boldsymbol{\Gamma} - v_c^2 \mathbf{I}_6\right) \cdot \underline{\mathbf{v}} = 0, \tag{7.519}$$

where

$$\boldsymbol{\Gamma} = \mathbf{L} \cdot \mathbf{P} \cdot \mathbf{L}^{\top} \tag{7.520}$$

is the Kelvin-Christoffel matrix, and

$$v_c = \frac{\omega}{k} \tag{7.521}$$

is the complex velocity.

Making zero the determinant, equation (7.519) gives the following dispersion relation:

$$\det(\mathbf{R}^{-1} \cdot \boldsymbol{\Gamma} - v_c^2 \mathbf{I}_6) = 0. \tag{7.522}$$

The eigensystem formed by equations (7.519) and (7.522) gives six eigenvalues and the corresponding eigenvectors. Four of them correspond to the wave modes, and the others

equal zero, since it can be shown that two rows of the system matrix are linearly dependent. These modes correspond to the fast and slow quasi-compressional waves, and the two quasi-shear waves.

The slowness and attenuation vectors for homogeneous waves can be expressed in terms of the complex velocity as

$$\mathbf{s}_R = \mathrm{Re}\left(\frac{1}{v_c}\right)\hat{\boldsymbol{\kappa}} \tag{7.523}$$

and

$$\boldsymbol{\alpha} = -\omega \mathrm{Im}\left(\frac{1}{v_c}\right)\hat{\boldsymbol{\kappa}}, \tag{7.524}$$

respectively. (Note that $(1/v_c)$ is the reciprocal of the phase velocity.)

The average strain-energy density (7.505) can be written, using equations (7.474), (7.495) and (7.518)-(7.521), in terms of the density as matrix $\mathbf{R}$

$$\langle V \rangle = \frac{1}{4}|v_c|^{-2}\mathrm{Re}(v_c^2 \underline{\mathbf{v}}^\top \cdot \mathbf{R} \cdot \underline{\mathbf{v}}^*), \tag{7.525}$$

where we used the fact that $\mathbf{R}$ and $\boldsymbol{\Gamma}$ are symmetric matrices.

Equation (7.525) is formally similar to the strain-energy density in anisotropic viscoelastic media, where $\langle V \rangle = \frac{1}{4}\rho_s|v_c|^{-2}\mathrm{Re}(v_c^2)|\mathbf{v}|^2$ (see Section 4.3.1). In a single-phase medium, every particle-velocity component is equally weighted by the density. Note that, when the medium is lossless, v_c is real and the average strain-energy density equals the average kinetic energy (7.506).

From equations (7.505) and (7.506) and using the property $\underline{\mathbf{v}}^\top \cdot \mathbf{R} \cdot \underline{\mathbf{v}}^* = \underline{\mathbf{v}}^{*\top} \cdot \mathbf{R} \cdot \underline{\mathbf{v}}$ (because $\mathbf{R}$ is symmetric), we note that the stored energy density (7.492) becomes

$$\langle E \rangle = \frac{1}{4}\mathrm{Re}\left[\left(1 + \frac{v_c^2}{|v_c|^2}\right)\underline{\mathbf{v}}^\top \cdot \mathbf{R} \cdot \underline{\mathbf{v}}^*\right]. \tag{7.526}$$

When the medium is lossless, v_c and $\mathbf{R}$ are real, and $\langle E \rangle$ is equal to twice the average kinetic energy (7.506).

For calculation purposes, the Umov-Poynting vector (7.482) can be expressed in terms of the eigenvector $\underline{\mathbf{v}}$ and complex velocity v_c. The average power flow (7.503) can be written as

$$\langle \mathbf{p} \rangle = -\frac{1}{2}\mathrm{Re}\left[\hat{\mathbf{e}}_i(\mathbf{U}^i \cdot \boldsymbol{\sigma}^\top) \cdot \underline{\mathbf{v}}^*\right], \tag{7.527}$$

where $\hat{\mathbf{e}}_i$ is the unit Cartesion vector and the Einstein convention for repeated indices is used; $\mathbf{U}^i$ are 6×7 matrices with most of their elements equal to zero, except U^1_{11}, U^1_{26}, U^1_{35}, U^1_{47}, U^2_{16}, U^2_{22}, U^2_{34}, U^2_{57}, U^3_{15}, U^3_{24}, U^3_{33} and U^3_{67}, which are equal to 1. Substitution of the stress-strain relation (7.473) into (7.527) and the use of equations (7.474), (7.495) and (7.518)-(7.521) yields the desired expression

$$\langle \mathbf{p} \rangle = \frac{1}{2}\mathrm{Re}\left[v_c^{-1}\underline{\mathbf{v}}^\top \cdot \mathbf{L} \cdot \mathbf{P} \cdot (\hat{\mathbf{e}}_i \mathbf{U}^{i\top}) \cdot \underline{\mathbf{v}}^*\right]. \tag{7.528}$$

To obtain the quality factor (7.512), we follow the same steps that led to equation (7.525) and note that the dissipated energy (7.491) can be written as

$$\langle D \rangle = \frac{1}{2}\mathrm{Im}\left[\left(\frac{v_c^2}{|v_c|^2} - 1\right)\underline{\mathbf{v}}^\top \cdot \mathbf{R} \cdot \underline{\mathbf{v}}^*\right]. \tag{7.529}$$

Using equation (7.525), we obtain

$$Q = \frac{2\langle V \rangle}{\langle D \rangle} = \frac{\mathrm{Re}(v_c^2 \underline{\mathbf{v}}^\top \cdot \mathbf{R} \cdot \underline{\mathbf{v}}^*)}{2\ \mathrm{Im}(v_c)\mathrm{Re}(v_c \underline{\mathbf{v}}^\top \cdot \mathbf{R} \cdot \underline{\mathbf{v}}^*)}. \tag{7.530}$$

If there are no losses due to viscosity effects ($\mathbf{R}$ is real and $\langle D_T \rangle = 0$), $\underline{\mathbf{v}}^\top \cdot \mathbf{R} \cdot \underline{\mathbf{v}}^*$ is real and

$$Q = \frac{\mathrm{Re}(v_c^2)}{\mathrm{Im}(v_c^2)}, \tag{7.531}$$

as in the single-phase case (see Section 4.3.1).

7.14.6 Wave propagation in femoral bone

Let us consider propagation of homogeneous plane waves in human femoral bone (orthorhombic symmetry), investigated by Carcione, Cavallini and Helbig (1998) using a single-phase theory for anisotropic viscoelastic media. (See Cowin (1999) for a survey of the application of poroelasticity in bone mechanics.). A similar application for rocks is given by Carcione, Helbig and Helle (2003), where the effects of pore pressure and fluid saturation are also investigated.

To introduce viscoelastic attenuation, we use a stress-strain relation based on model 2 of Section 4.1. Each eigenvector (or eigenstrain) of the stiffness matrix defines a fundamental deformation state of the medium. The six eigenvalues (or eigenstiffnesses) represent the genuine elastic parameters. In the elastic case, the strain energy is uniquely parameterized by the six eigenstiffnesses. These ideas date back to the middle of the 19th century when Lord Kelvin introduced the concept of "principal strain" (eigenstrain in modern terminology) to describe the deformation state of a medium (Kelvin, 1856).

We assume that the bone is saturated with water of bulk modulus $K_f = 2.5$ GPa, density $\rho_f = 1000$ kg/m^3 and viscosity $\eta = 1$ cP; the grain bulk modulus is $K_s = 28$ GPa, the grain density is $\rho_s = 1815$ kg/m^3, the porosity is $\phi = 0.4$, the tortuosities are $\mathcal{T}_1 = 2$, $\mathcal{T}_2 = 3$ and $\mathcal{T}_3 = 3.6$, and the matrix permeabilities are $\bar{\kappa}_1 = 1.2 \times 10^{-12}$ m^2, $\bar{\kappa}_2 = 0.8 \times 10^{-12}$ m^2 and $\bar{\kappa}_3 = 0.7 \times 10^{-12}$ m^2. The stiffness matrix of the drained porous medium in Voigt's notation (c_{IJ}, see Section 7.3) is

$$\begin{pmatrix} 18 & 9.98 & 10.1 & 0 & 0 & 0 \\ 9.98 & 20.2 & 10.7 & 0 & 0 & 0 \\ 10.1 & 10.7 & 27.6 & 0 & 0 & 0 \\ 0 & 0 & 0 & 6.23 & 0 & 0 \\ 0 & 0 & 0 & 0 & 5.61 & 0 \\ 0 & 0 & 0 & 0 & 0 & 4.01 \end{pmatrix},$$

in GPa. The components of this matrix serve to calculate the elements of matrix $\mathbf{C}^u$ by using equation (7.136). This matrix corresponds to the high-frequency (unrelaxed) limit,

whose components are

$$\mathbf{C}^u = \begin{pmatrix} 19.8 & 11.7 & 11.5 & 0 & 0 & 0 & 3.35 \\ 11.7 & 21.8 & 12.03 & 0 & 0 & 0 & 3.14 \\ 11.5 & 12.03 & 28.7 & 0 & 0 & 0 & 2.59 \\ 0 & 0 & 0 & 6.23 & 0 & 0 & 0 \\ 0 & 0 & 0 & 0 & 5.61 & 0 & 0 \\ 0 & 0 & 0 & 0 & 0 & 4.01 & 0 \\ 3.35 & 3.14 & 2.59 & 0 & 0 & 0 & 6.12 \end{pmatrix},$$

in GPa. In order to apply Kelvin's formulation, Hooke's law has to be written in tensorial form. This implies multiplying the (44), (55) and (66) elements of matrix $\mathbf{C}^u$ by a factor 2 (see equation (4.8)) and taking the leading principal submatrix of order 6 (the upper-left 6×6 matrix). This can be done for the undrained medium, for which the variation of fluid content ζ is equal to zero (closed system) (Carcione, Helbig and Helle, 2003). Let us call this new matrix (tensor) $\bar{\mathbf{C}}^u$. This matrix can be diagonalized to obtain

$$\bar{\mathbf{C}}^u = \mathbf{Q} \cdot \mathbf{\Lambda} \cdot \mathbf{Q}^\top, \tag{7.532}$$

where $\mathbf{\Lambda} = \mathrm{diag}(\Lambda_1, \Lambda_2, \Lambda_3, \Lambda_4, \Lambda_5, \Lambda_6)^\top$ is the eigenvalue matrix, and $\mathbf{Q}$ is the matrix formed with the eigenvectors of $\bar{\mathbf{C}}^u$, or more precisely, with the columns of the right (orthonormal) eigenvectors. (Note that the symmetry of $\bar{\mathbf{C}}^u$ implies $\mathbf{Q}^{-1} = \mathbf{Q}^\top$.) Hence, in accordance with the correspondence principle and its application to equation (7.532), we introduce the viscoelastic stiffness tensor

$$\bar{\mathbf{C}} = \mathbf{Q} \cdot \mathbf{\Lambda}^{(v)} \cdot \mathbf{Q}^\top, \tag{7.533}$$

where $\mathbf{\Lambda}^{(v)}$ is a diagonal matrix with entries

$$\Lambda_i^{(v)}(\omega) = \Lambda_I M_I(\omega). \qquad I = 1, \ldots, 6. \tag{7.534}$$

The quantities M_I are complex and frequency-dependent dimensionless moduli. We describe each of them by a Zener model, whose relaxation frequency is equal to ω (see equation (4.6)). In this case, we have

$$M_I = \frac{\sqrt{Q_I^2 + 1} - 1 + \mathrm{i}Q_I}{\sqrt{Q_I^2 + 1} + 1 + \mathrm{i}Q_I}, \tag{7.535}$$

where Q_I is the quality factor associated with each modulus. (We note here that if an $\exp(-\mathrm{i}\omega t)$ kernel is used, $\mathrm{i}Q_I$ should be replaced by $-\mathrm{i}Q_I$, and the dissipated strain energy should be defined with the opposite sign.) To recover the Voigt's notation, we should divide the (44), (55) and (66) elements of matrix $\bar{\mathbf{C}}$ by a factor 2. This gives the complex matrix $\mathbf{P}$.

In orthorhombic porous media, there are six distinct eigenvalues, and, therefore, six complex moduli. We assume that the dimensionless quality factors are defined as $Q_I = (\Lambda_I/\Lambda_6)Q_6$, $I = 1, \ldots, 6$, with $Q_6 = 30$. This choice implies that the higher the stiffness, the higher the quality factor (i.e., the harder the medium, the lower the attenuation). Matrix $\mathbf{P}$ is then given by

$$\mathbf{P} = \begin{pmatrix} 19.6 + \mathrm{i}0.26 & 11.7 + \mathrm{i}0.002 & 11.5 + \mathrm{i}0.001 \\ 11.7 + \mathrm{i}0.002 & 21.5 + \mathrm{i}0.26 & 12.0 + \mathrm{i}0.001 \\ 11.5 + \mathrm{i}0.001 & 12.0 + \mathrm{i}0.001 & 28.4 + \mathrm{i}0.26 \\ 0 & 0 & 0 \\ 0 & 0 & 0 \\ 0 & 0 & 0 \\ 3.35 & 3.14 & 2.59 \end{pmatrix}$$

$$\begin{pmatrix} 0 & 0 & 0 & 3.35 \\ 0 & 0 & 0 & 3.14 \\ 0 & 0 & 0 & 2.59 \\ 6.1 + \mathrm{i}0.13 & 0 & 0 & 0 \\ 0 & 5.48 + \mathrm{i}0.13 & 0 & 0 \\ 0 & 0 & 3.88 + \mathrm{i}0.13 & 0 \\ 0 & 0 & 0 & 6.12 \end{pmatrix},$$

in GPa.

Polar representations of the attenuation factors (7.524) and energy velocities (7.511) are shown in Figure 7.15 and 7.16, respectively, for the (x, z) principal plane of the medium ($l_2 = 0$). Only one quarter of the curves are displayed because of symmetry considerations. The Cartesian planes of an orthorhombic medium are planes of symmetry, and, therefore, one of the shear waves, denoted by S, is a pure cross-plane mode. The tickmarks in Figure 7.16 indicate the polarization directions $(v_1, 0, v_3)$, with the points uniformly sampled as a function of the phase angle. The curves are plotted for a frequency of $f = \omega/(2\pi)$ = 10 kHz, smaller than the characteristic frequency $f_c = \eta\phi/(\mathcal{T}_3\rho_f\bar{\kappa}_3)$ = 15 kHz, which determines the upper limit of the low-frequency theory.

The strong dissipation of the slow qP wave is due to the Biot mechanism, i.e, the viscodynamic effect. On the other hand, it can be shown that $\langle D_V \rangle$ and $\langle D_T \rangle$ are comparable for the qP, qS and S waves. Anisotropic permeability affects the attenuation of the slow qP wave. According to Biot's theory, the lower the permeability, the higher the attenuation. In fact, the vertical attenuation factor is higher than the horizontal attenuation factor. Anisotropic tortuosity mainly affects the velocity of the slow qP wave. This is (approximately) inversely proportional to the square root of the tortuosity. Hence, the vertical velocity is smaller than the horizontal velocity.

The three faster waves propagating in the (x, z)-plane of a single-phase orthorhombic medium have the following velocities along the coordinate axes:

$$\begin{aligned} &v_{qS}(0) = v_{qS}(90) = \sqrt{p_{55}/\rho} \\ &v_{qP}(0) = \sqrt{p_{33}/\rho}, \qquad v_{qP}(90) = \sqrt{p_{11}/\rho} \\ &v_S(0) = \sqrt{p_{44}/\rho}, \qquad v_S(90) = \sqrt{p_{66}/\rho}, \end{aligned} \tag{7.536}$$

where 0 corresponds to the z-axis and 90 to the x-axis, and c_{IJ} are the complex stiffnesses. The velocities (7.536) do not correspond exactly to the velocities in the porous case, since here the density is a matrix, not a scalar quantity. For instance, the densities corresponding to the S and qS waves along the z-axis are $\rho - \rho_f^2/\mathbf{R}_{55}$ and $\rho - \rho_f^2/\mathbf{R}_{44}$, where $\mathbf{R}_{44}$ and $\mathbf{R}_{55}$ are components of matrix $\mathbf{R}$ defined in equation (7.477). However, the

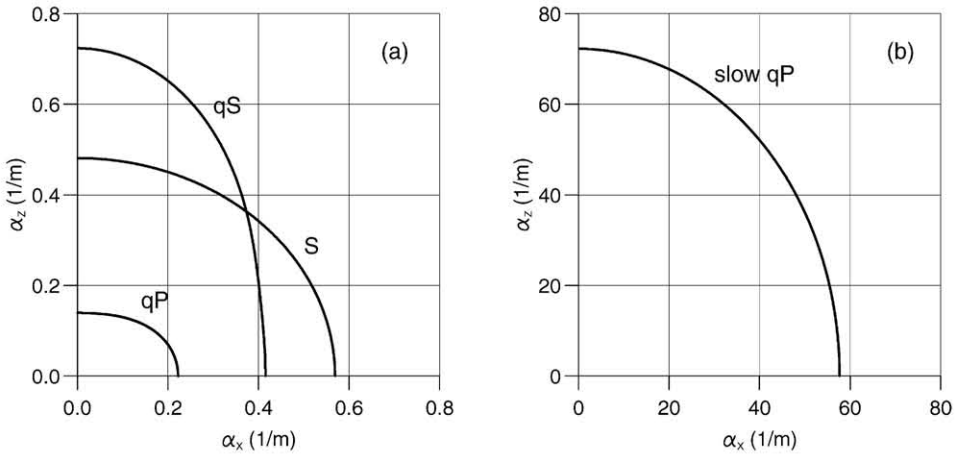

Figure 7.15: Polar representation of the attenuation factors in one of the planes of mirror symmetry of human femoral bone saturated with water, where (a) illustrates the fast quasi-compressional wave qP, the quasi-shear wave qS, and the pure cross-plane shear wave S, and (b) shows the slow quasi-compressional wave. The frequency is 10 kHz.

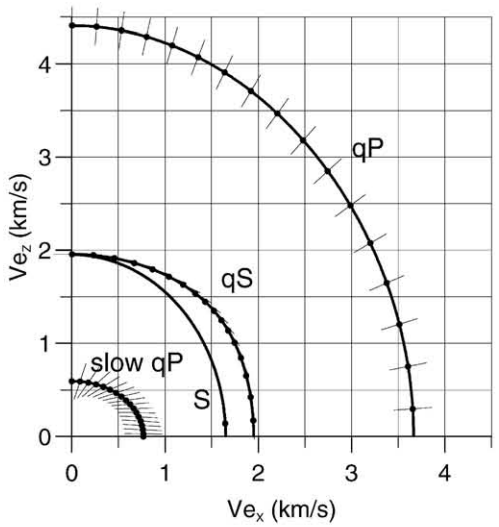

Figure 7.16: Polar representation of the energy velocities in one of the planes of mirror symmetry of human femoral bone saturated with water, where qP is the fast quasi-compressional wave, qS is the quasi-shear wave, S is the pure cross-plane shear wave, and slow qP is the slow quasi-compressional wave. The tickmarks indicate the polarization directions $(v_1, 0, v_3)$ for the qP, slow qP and qS waves, while the polarization of the S wave is (0,1,0). The curves correspond to a frequency of 10 kHz.

velocities (7.536) can be used to qualitatively verify the behavior of the energy-velocity curves. On the basis of these equations, Figure 7.16 is in agreement with the values indicated above for matrix **P**.